# Functional Genomic Analysis of the Periodic Transcriptome in the Developing *Drosophila* Wing

## Thesis

UNRESTRICTED.

# Functional genomic analysis of the periodic transcriptome in the developing *Drosophila* wing

Liang Liang, B.Sc.

A thesis submitted in fulfillment of the
requirements of the Open University
for the Degree of Doctor of Philosophy

The Stowers Institute for Medical Research
Kansas City, Missouri, USA
an Affiliated Research Center of the
Open University, UK

30th, November, 2013

Date of Submission: 26 November 2013
Date of Award: 29 April 2014



ProQuest LLC.
789 East Eisenhower Parkway
P.O. Box 1346
Ann Arbor, MI 48106 – 1346

# Dedication

To my Grandparents, Wensheng Liang and Fenghua Zhang

for their unwavering love.

# Acknowledgements

I would first especially like to thank my supervisor Matt Gibson for his continuous support, advice, and encouragement during the past five years in the lab. I also would like to thank my committee members and mentors: Rong Li, Robb Krumlauf, Scott Hawley, and Leanne Wiedemann for their constant help and suggestions all the way through my pre-doctoral training.

Additionally, my thesis project has been helped by many people in different departments of the Stowers Institute. Thanks to Jeff Haug, Jungeun Park and Ruihong Zhu for flow cytometry assistance; Christopher Seidel for microarray and RNA sequencing data analysis; Guangbo Chen, Alex Garrett, Arcady Mushegian, Hua Li, and Jim Vallandingham for other computational assistance; Christopher Wood for technical assistance in website construction; Karin Zueckert-Gaudenz, Allison Peak, Anoja Perera, Kendra Walton, Kate Malanowski, William McDowell, and Brian Fleharty for help with microarray, RNA-seq and qPCR validation; Fengli Guo for help with TEM; Sean McKinney, Amanda Kroesen, and Zulin Yu for live imaging assistance; Macie Walker for her advice on *in situ* hybridization; Emily Meyer, Usha Nagarajan, and Yiran Xie for technical assistance; all other Gibson lab members for discussion; and Lynnette Gutchewsky and Shelly Hornbuckle for administrative assistance.

I am also especially grateful to my third-party monitor Susan Abmayr for her constant help, Jennifer Gerton and Daniel St. Johnston for being my examiners, as well as Paul Trainor for serving as examination chair.

I would also like to thank Dorothy Stanley, Jennifer Knapp, Lisa Sandell, Takuya Akiyama, Aissam Ikmi, Man Mohan, Tamara Potapova, and other friends for their suggestions and support during my manuscript preparation and thesis writing.

Finally, I would like to thank my parents and my in-laws, who came overseas to help during my manuscript preparation and thesis writing. I especially thank my father-in-law, who has walked every day between home and the Institute over one hundred times, bringing my baby for a daytime 'snack.'

This work was funded by the Stowers Institute and Burroughs Wellcome Fund for Medical Research (to M.G.).

# Abstract

The eukaryotic cell cycle is the central molecular oscillator underlying tissue growth. Although previous studies have analyzed global cell cycle-associated transcription using unicellular systems, precisely how cell cycle-dependent processes are integrated in multicellular development *in vivo* remains unclear. One multicellular context-specific cell cycle event is the Interkinetic Nuclear Migration (IKNM), a conserved process by which proliferating nuclei translocate to the apical epithelial surface of the epithelium to execute mitosis. How cell cycle progression is linked with IKNM remains poorly understood.

Here, I report the global cell cycle-associated transcriptomes of *Drosophila* wing disc epithelial cells (multicellular system) and cultured S2 cells (unicellular system). With an integrative FACS-microarray technique, we identified over 600 genes with periodic expression profiles in each context. Intriguingly, despite the common periodic genes identified, we also identified 200 genes periodically expressed only in the wing disc cells, including many core cell cycle components. I further explored the function of those wing disc periodic genes by tissue-specific RNAi knockdown. Combining flow cytometry and confocal imaging, I defined 107 periodic genes that control wing growth, wherein 35 periodic genes control cell cycle progression in the developing wing but not in S2 cells (compared with results from S2 RNAi screens).

In addition to several novel regulators of mitotic cell size and chromosome segregation, I also identified two novel wing disc-specific periodic genes, knockdown of which disrupt IKNM. Strikingly, in both cases, disconnecting nuclei positioning with mitosis does not disrupt cell cycle progression *per se*. One of the IKNM genes is a potential lincRNA, which may regulate the expression of kinesin-like protein, Klp54D, and is required for normal centriole function. Taken together, my study provided a global functional perspective on cell cycle regulation *in vivo*, and identified numerous novel periodic genes that control growth, cell proliferation and IKNM in the epithelial context.

# Abbreviations

| | |
|---|---|
| WD | Wing Disc |
| S2 cell | *Drosophila* Schneider 2 Cells |
| G1 phase | Gap 1 Phase |
| S phase | Synthesis Phase |
| G2 phase | Gap 2 Phase |
| M phase | Mitotic Phase |
| HH | Hedgehog |
| DPP | Decapentaplegic |
| RB | Retinoblastoma protein |
| MAPs | Microtubule-associated proteins |
| CDK | Cyclin-dependent kinase |
| M-CDK | Mitotic cyclin-dependent kinase |
| DDK | Dbf4-dependent kinase Cdc7–Dbf4 |
| MCM | Mini-chromosome maintenance |
| ARS | Autonomously replicating sequence |
| ORC | Origin replication complex |
| SAC | Spindle assembly checkpoint |
| pre-RC | Pre-replication complex |
| MF | Morphogenetic furrow |
| APC | Anaphase-promoting complex |
| HOAP | HP1/ORC-associated protein |
| NEBD | Nuclear envelope break down |
| GO | Gene Ontology |
| MEME | Multiple EM for Motif Elicitation |
| KEGG | Kyoto Encyclopedia of Genes and Genomes |

| | |
|---|---|
| PPI | Protein-protein Interaction |
| lincRNA | Long Intergenic Non-coding RNA |
| lncRNA | Long Non-coding RNA |
| IKNM | Interkinetic Nuclear Migration |
| PH3 | Phospho-Histone H3 |
| F-Actin | Filamentous-actin |
| PE | Peripodial Epithelium |
| CE | Columnar Epithelium |
| MT | Microtubule |
| MTOC | Microtubule-organizing Center |
| FACS | Fluorescence Activated Cell Sorting |
| TEM | Transmission Electron Microscopy |
| SEM | Scanning Electron Microscope |
| PFA | Paraformaldehyde |
| p-MRLC | phospho-myosin regulatory light chain II |
| HMSD | Hexamethyldisilazane |
| PBS | Phosphate buffered saline |
| TBS | Tris-buffered saline |
| SSC | Saline-sodium citrate |
| 7AAD | 7-Aminoactinomycin D |
| MEOH | Methanol |
| DEPC | Diethyl pyrocarbonate |
| DTT | Dithiothreitol |
| FBS | Fetal bovine serum |
| PE | Phycoerythrin |
| SPIM | Single Plane Illumination Microscopy |

| | |
|---|---|
| RT | Room Temperature |
| SNT | Supernatant |
| ND | Not Done |
| DGC | *Drosophila* gene collection |
| VDRC | Vienna *Drosophila* RNAi Center |
| DGRC | *Drosophila* Genomics Resource Center |

# Table of Contents

# Table of Figures

# Table of Tables

# Introduction

## 1.1 Overview

Cell division is one of the fundamental processes that drive tissue growth. Decades of study using unicellular models have uncovered the regulation of key processes of core cell cycle machinery, such as cell cycle-associated periodic transcription (Cho *et al.*, 1998; Cho *et al.*, 2001; Laub *et al.*, 2000; Menges *et al.*, 2003; Oliva *et al.*, 2005; Rustici *et al.*, 2004; Spellman *et al.*, 1998; Whitfield *et al.*, 2002). Unlike single-cell systems, however, cell division in a developing tissue has to be coordinated with the developmental control of growth, patterning, and morphogenesis. In the vertebrate neural tube, for example, nuclei migrate during cell cycle progression such that mitotic events are confined to the apical epithelial surface (Sauer, 1935). This process, interkinetic nuclear migration (IKNM), is proposed to be important for determining the cell fate of neural progenitors in vertebrates (Cappello *et al.*, 2006; Del Bene *et al.*, 2008; Murciano *et al.*, 2002; Xie *et al.*, 2007). Outside of the vertebrate nervous system, IKNM is a deeply conserved process, taking place in a broad spectrum of pseudostratified epithelia (Meyer et al., 2011). Nevertheless, despite the ubiquity of this conserved mitotic cell behavior, mechanisms linking nuclear cell cycle progression to IKNM remain unclear, and the potential contributions of periodically expressed genes to the regulation of IKNM and other tissue-specific processes have received little direct attention.

In this thesis, using an integrative FACS-microarray method, I functionally analyze global cell cycle-associated transcription in the developing wing of *Drosophila melanogaster*. In order to gain insight into global aspects of cell cycle-associated transcription as well as the role of periodic genes in wing development, I profiled gene expression in G1 and G2/M-phase wing disc cells isolated using a novel dissociation-Fluorescent-Activated Cell Sorting (FACS) protocol. By directly comparing the cell cycle-associated transcriptome of wing disc cells with that of cultured S2 cells, we identified both common and con-

text-dependent periodic genes. These genes were further tested for their function in tissue development, cell proliferation, cell cycle phasing, and mitosis in the developing wing. The vast majority of genes identified using this approach were not revealed in a previous S2 RNAi screen *in vitro* (Bjorklund *et al.*, 2006). Notably, I also implicate two novel periodic genes in the control of mitotic nuclear position during IKNM, highlighting the importance of understanding the regulation of cell cycle progression in a context-dependent manner.

## 1.2 Cell cycle regulation in eukaryotic cells

Cell cycle progression is controlled by a combination of transcriptional and post-translational regulatory events (Morgan, 2006). At the transcriptional level, oscillations in the expression of cell cycle phase-specific cyclins regulate cyclin-CDK complex activity, which promotes cell cycle progression (Figure 1-1). Here, I briefly introduce the major aspects of the core cell cycle machinery and the transcriptional regulation of the cell division.

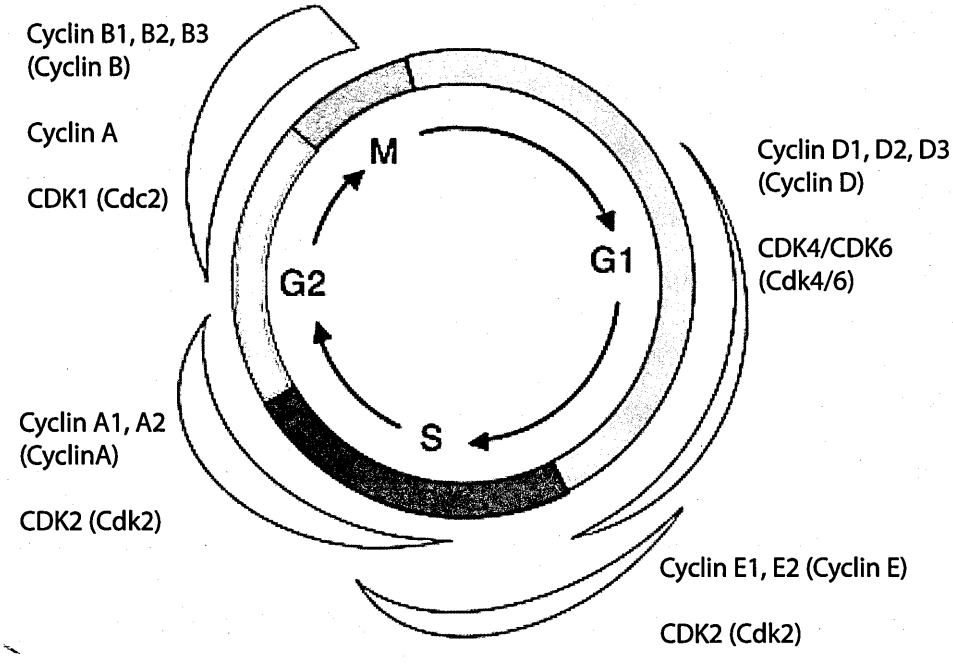


**Figure 1-1 A typical mitotic cell cycle and the approximate timing of activity for different complexes of cyclins and CDKs, based on published mammalian studies.** *Drosophila* family members are indicated between brackets. Shapes outside the cycle indicate the oscillation of corresponding cyclin-CDK complex activity (Adapted from van den Heuvel, 2005).

### 1.2.1 The core cell cycle machinery

The eukaryotic cell cycle has been intensively investigated for the past decades. For a cell to reproduce, the core machinery typically drives two fundamental tasks: the faithful duplication and the accurate segregation of the genomic information. Thus, core cell cycle regulation is primarily centered on accomplishing DNA replication in S phase and cell division in M phase, notwithstanding the variation in the details of cell cycle progression between different organisms and tissues (Alberts, 2002; Budirahardja and Gonczy, 2009). Here, I review the universal characteristics of cell-cycle control systems in eukaryotic cells, with a focus on DNA replication, mitosis, and checkpoints.

#### 1.2.1.1 DNA replication

DNA replication is a highly conserved process consisting of initiation, elongation, and termination. Among these, replication initiation process involves sequential dynamic steps including origin recognition, licensing, unwinding (activation of the helicase), and elongative assembly (replisome loading) (reviewed in Bell and Dutta, 2002). Origins are discrete sites along each chromosome where replication begins. The origins are identified as A/T-rich ARS consensus sequence (ACS) around 100bp in *Saccharomyces cerevisiae* (Leatherwood, 1998), whereas they are not defined DNA sequences and probably are determined by epigenetic mechanisms in metazoans (Aggarwal and Calvi, 2004; Danis *et al.*, 2004). In an ATP-dependent manner, the Origin Replication Complex (ORC) binds to replication origins through the cell cycle (Bell and Stillman, 1992; Gossen *et al.*, 1995). In G1 phase, DNA-bound ORC interacts with Cdc6 and Cdt1, which bring the hexameric MCM helicase complex, and form the licensed prereplication (pre-RC) initiative complexes (Aparicio *et al.*, 1997; Feger, 1999; Tanaka *et al.*, 1997). After the MCM helicase becomes activated, the scaffold protein CDC45 helps load the replisome, which contains DNA polymerases and the GINS complex (Moyer *et al.*, 2006; Wohlschlegel *et al.*, 2002; Zou and Stillman, 1998). This process is dependent on the activity of CDK (cyclin-dependent ki-

nase) and DDK (Dbf4-dependent kinase) in the beginning of S phase (Masumoto *et al.*, 2002; Tanaka *et al.*, 2007; Yabuuchi *et al.*, 2006; Zegerman and Diffley, 2007). In S phase, bidirectional replication forks are activated, subsequent DNA replication starts, and CDK activity ensures no new pre-RC assembly in S (reviewed in Sclafani and Holzen, 2007). This is achieved by elevated activity of CDK, which phosphorylates pre-RC components, such as ORC, Cdc6, and the MCMs. The phosphorylation of pre-RC controls their release from the chromatin, degradation, and nuclear export, which prevent re-replication (Bell and Dutta, 2002; Dahmann *et al.*, 1995). In addition, the level of geminin, an inhibitor of pre-RC formation by preventing Cdt1 function and MCM loading, increases as S phase proceeds till it is degraded by APC in late M phase (Wohlschlegel *et al.*, 2000). Thus, both CDK activity and geminin contribute to the prevention of re-replication.

#### 1.2.1.2 Mitosis

The mitotic phase is the most dynamic phase of the cell cycle at cellular level, including the major events of the G2 to M transition, chromosome segregation, and cytokinesis. The G2 to M transition commits cells to mitosis, and is positively regulated by the activation of CDK1 (M-Cdk) through Plk1 (Barr *et al.*, 2004; Pomerening *et al.*, 2003). In metazoan cells, mitosis consists of the sequential stages: prophase, prometaphase, metaphase, anaphase, telophase, and cytokinesis (Alberts, 2002). In prophase, centrioles segregate and chromatin condenses into chromosomes, where sister chromatids are bound tightly together by the cohesin protein complex, which is established during DNA replication (Toth *et al.*, 1999). In prometaphase, the nuclear envelope breaks down (NEBD), and kinetochores complete their assembly at centromeres and attach to MT spindle fibers (Chan *et al.*, 2005). Next, the mitotic spindle aligns the chromosomes at the metaphase plate in metaphase. Anaphase starts once cells trigger the irreversible metaphase-anaphase transition through the activity of the ubiquitin ligase anaphase-promoting complex (APC), which inactivates M-Cdk and triggers sister chromatid separation by the proteolytic disso-

lution of cohesin (reviewed in Ciosk *et al.*, 1998; Funabiki *et al.*, 1996; Xiong and Gerton, 2010). Separated sister chromatids then move to opposite poles of the cell. In telophase, the nuclear envelope reforms around daughter nuclei, chromosomes decondense, and spindle fibers disperse. During cytokinesis, the cleavage furrow separates the cytoplasm by the actomyosin contractile ring to complete mitosis (Gulyas, 1973; Pardo and Nurse, 2003; Pelham and Chang, 2002).

#### 1.2.1.3 Checkpoints

Checkpoints are critical mechanisms to prevent errors by blocking cell cycle progression during cell division. Thus, checkpoint mechanisms are applied at multiple stages of the cell cycle to maintain genomic integrity after replication stress, DNA damage, spindle assembly errors, or chromosome segregation defects. For the replication checkpoint, the pathway consists of sensors (e.g., RPA, PCNA), amplifying mediators (e.g., Mrc1), transducers (e.g., Mec1, Chk1, Chk2, ATM, and ATR) and effector targets (e.g., CDK, CDC45, MCM, p53, and BRCA1). Consequently, the activation of this checkpoint transduction pathway translates the signal into the response of cell cycle arrest and DNA repair (Reviewed in Nyberg *et al.*, 2002). However, the effects on the cell cycle (transient delay in G1, S or G2, or prolonged arrest in G1 or G2) depend on the stage of the cell cycle relative to the restriction point controlled by RB/E2F, passing through which commits a cell to division (Bartek *et al.*, 1997; Sherr and McCormick, 2002) and the activated checkpoint pathways will arrest the cells at G2/M.

In mitosis, the spindle assembly checkpoint senses the alignment of chromosomes at metaphase. By monitoring kinetochore tension (Khodjakov and Pines, 2010), it prevents Securin and Cyclin B degradation, thus inhibiting chromosome separation when sister chromatid pairs lack attachment with spindle fibers (a failure of bi-oriented attachment) (Li and Nicklas, 1995; Musacchio and Salmon, 2007; Rieder *et al.*, 1995). The spindle assembly checkpoint can be triggered by a single unattached kinetochore, which inhibits all

APC-Cdc20 activity through the mitotic checkpoint proteins Mad1, Bub1, Mad2, Mad3/BubR1, and BubR3 (Musacchio and Salmon, 2007; reviewed in Rhind and Russell, 2012). When all kinetochores are attached with MTs, the inhibition of APC is relieved and the cell enters anaphase.

Perturbing checkpoint genes is generally detrimental to cells. Checkpoint mutants in budding yeast do not stop mitosis with stresses, leading to chromosome instability and cell death (Hartwell and Weinert, 1989; Weinert and Hartwell, 1988; Weinert *et al.*, 1994). Defects in checkpoint proteins, such as Chk2, ATM, and p53 lead to human cancer (Kastan and Bartek, 2004).

### 1.2.2 Transcriptional regulation of the cell cycle

#### 1.2.2.1 The transcriptional regulatory network in G1 phase

Transcriptionally, the pRB/E2F pathway directly regulates expression of cyclin E and other target genes to drive the G1/S transition (Duronio and O'Farrell, 1995; Duronio and Xiong, 2013; Dyson, 1998; Geng *et al.*, 1996; Ohtani *et al.*, 1995). In this regard, temporal regulation of transcription downstream of E2F ensures coordinated expression of factors required for G1/S progression and cellular growth (Datar *et al.*, 2000; Duronio and Xiong, 2013; Dyson, 1998). In quiescent mammalian cells, overexpression of E2F can induce S phase entry (Johnson *et al.*, 1993), and in *Drosophila*, ectopic E2F can accelerate cell cycle progression (Neufeld *et al.*, 1998). Similarly, overexpression of G1 cyclins results in truncated G1 phases (Johnson *et al.*, 1993; Ohtsubo and Roberts, 1993; Resnitzky *et al.*, 1994) and is reported to induce mammary gland tumors in mice (Smith *et al.*, 2006; Wang *et al.*, 1994). These studies collectively demonstrate the importance of proper cell cycle-associated transcription and thus raise a critical question: How much of the genome is periodically transcribed in a cell cycle-associated manner?

#### 1.2.2.2 The global analysis of the periodic transcriptome in single-cell systems

A paradigm for understanding global cell cycle-associated transcription has emerged from studies of synchronized cells in humans (Cho *et al.*, 2001; Whitfield *et al.*, 2002), budding yeast (Cho *et al.*, 1998; Spellman *et al.*, 1998), fission yeast (Oliva *et al.*, 2005; Rustici *et al.*, 2004), bacteria (Laub *et al.*, 2000) and plant cell culture (Menges *et al.*, 2003). Collectively, these studies have identified hundreds of periodic genes, a large number of which are involved in cell cycle-specific processes and expressed at peak levels when their functions are required. However, to date, global analyses of periodic transcription have focused on single-cell systems, and the potential intricacies of the periodic transcriptome in complex multicellular tissues remain poorly understood.

#### 1.2.2.3 Periodic genes in normal development and diseases

Although the periodic transcriptomes of complex tissues have not been studied globally, individual periodic genes have been identified that play a role in coupling cell cycle progression to developmental events and disease processes. *Drosophila cdc25* (*string*) represents a classic example of transcriptional control of early zygotically driven cell divisions. Its dynamic expression controls the temporal and spatial control of patched-synchronized cell divisions in the early *Drosophila* embryo (Edgar and O'Farrell, 1989; Foe, 1989). String level is regulated by Tribbles through protein degradation (Mata *et al.*, 2000). During early gastrulation, blocking cell division through inhibition of String by Tribbles in the mesoderm is essential for the morphogenetic process (Seher and Leptin, 2000). In addition to the dynamic regulation of *string* and *tribbles*, *humpty dumpty* (*hd*) is a conserved gene whose expression peaks at G1/S in both humans (Whitfield *et al.*, 2002) and in *Drosophila* (Bandura *et al.*, 2005). In *Drosophila* imaginal discs and brain tissue, *hd* is required for cell proliferation and developmental DNA amplification. Another interesting example is the Inhibitor of Apoptosis Protein (IAP), Survivin (*Deterin* in *Drosophila*), which functions at the interface between cell proliferation and cell survival in human

cancer cells (Li *et al.*, 1998). Survivin is believed to counteract a default induction of apoptosis in G2/M through G2/M phase-specific expression (Li *et al.*, 1998). The overexpression of Survivin in cancer may help transformed cells go through mitosis by inhibiting apoptosis (Li *et al.*, 1998). Thus, beginning with the characterization of periodically expressed genes, previous studies have identified essential factors directly functioning in the cell cycle, or involved in cell cycle-related processes. This suggests that defining periodic genes *in vivo* may provide a pool of important candidates to better understand cell proliferation and its related processes in the developmental context.

## 1.3 Control mitotic division in development

Although the core cell cycle machinery has been thoroughly investigated in representative single-cell systems, it is only more recently that light has been shed on the molecular mechanisms that integrate cell division with the metazoan development *in vivo*. Despite the conservation of molecular mechanisms controlling the central processes of cell division (e.g., DNA replication), many context-specific facets of mitosis have been identified within *in vivo* systems. Here, I focused on general and context-specific insights of two questions related to the process of mitotic division: mitotic cell rounding, and mitotic spindle length.

### 1.3.1 Control of cell morphology during mitosis

When dividing into two cells from one, cells go through active changes in morphology. Besides the dynamic process of cytokinesis, metazoan cells go through another conserved process during mitosis with a drastic change in their morphology, which is mitotic rounding (Cramer and Mitchison, 1997; Meyer et al., 2011, b; Thery and Bornens, 2008). Mitotic rounding occurs in prophase immediately after cyclin B1-Cdk1 activation and can be reversed by a Cdk inhibitor (Gavet and Pines, 2010b). This cell morphology change precedes NEBD as it requires only a low level of Cyclin B1-Cdks activity (Gavet and Pines, 2010b). In addition to Cdk complex activity, both cytoskeletal and environmen-

tal mechanisms have been studied, from which RhoA, actomyosin cortex, and hydrostatic pressure have been found to drive cell rounding in mitosis *in vitro* and *in vivo* (Maddox and Burridge, 2003; Meyer et al., 2011, b; Stewart *et al.*, 2011). Functionally, recent studies have suggested mitotic rounding is essential for normal mitotic spindle assembly in HeLa cells (Lancaster *et al.*, 2013). At the tissue level, mitotic cell rounding accelerates the process of epithelial invagination in the *Drosophila* tracheal placode (Kondo and Hayashi, 2013). Within the context of epithelia, mitotic rounding is observed to associate with apical translocation of mitotic nuclei (the process of IKNM discussed in section 1.4) (Kondo and Hayashi, 2013; Meyer et al., 2011, b). However, whether the apical mitotic cell rounding is required for IKNM is unclear.

### 1.3.2 Control of mitotic spindle length

The mitotic spindle is the dynamic subcellular apparatus that mediates mitotic chromosome segregation through MT-based force (Inoue and Salmon, 1995). Thus, the assembly of the mitotic spindle is critical to ensure the faithful separation of duplicated genomic information to daughter cells. In addition to MTs, the spindle is assembled by MT-associated proteins (MAPs) and MT motor proteins (i.e., kinesins, dyneins). In metaphase, the spindle maintains a steady state, with pairs of sister chromatids aligned at the spindle equator. However, after the sudden transition from metaphase to anaphase, the spindle elongates with pole-pole spacing increased to separate chromosomes through dynamic MTs and its motor proteins (reviewed in Goshima and Scholey, 2010).

For the accurate segregation of chromatids, in general, the size of the spindle is critical for not only aligning the sister chromatids in the middle of the cells but placing chromosomes at the center of each daughter cell. Thus, spindle length often scales with cell size. In *Xenopus laevis*, spindle length shows approximately linear increase with cell length under 200 μm (Wuhr *et al.*, 2008). This scaling could be a consequence of cell surface boundary that restricts the pulling force from astral MT. For the mitotic spindles having

centrosomes and astral MTs, the growing astral MTs develop a pushing force once they hit the cell cortex. This force generated via a polymer ratchet mechanism, then give an inward force to centrosomes, which limits the spindle length (centrosome-to-centrosome distance) (Dogterom and Yurke, 1997; Mogilner and Oster, 2003). However, this scaling rule has an upper limit, as in the case of *Xenopus laevis*, the spindle length never exceeds 60 μm, which may be controlled by intrinsic mechanisms (Brown *et al.*, 2007; Wuhr *et al.*, 2008).

Although mitotic spindle length generally scales with mitotic cell size, there are many significant exceptions. For example, the syncytial *Drosophila* early embryo (around 500 μm long) contains hundreds of mitotic spindles (11.8 μm at cycle 11) (Brust-Mascher *et al.*, 2009), the length of which may be controlled intrinsically or by the cleavage furrows around the spindles (Sullivan and Theurkauf, 1995). Additionally, in mitosis and meiosis that result in asymmetric segregation of daughter cells, spindle length is also not adapted to position segregated chromosomes in the daughter cells (Ellefson and McNally, 2009; Siller and Doe, 2009). The potential intrinsic mechanisms include centrosome size (Greenan *et al.*, 2010), kinetochore-MT interactions and chromosome structure (reviewed in Dumont and Mitchison, 2009; Goshima *et al.*, 2007; Neurohr *et al.*, 2011).

## 1.4 Interkinetic nuclear migration (IKNM)

Interkinetic nuclear migration is one of the best representations of cell cycle regulation in the developmental context of the epithelium. The unique aspects of apical-basal polarity and junctions in the epithelium interact with the morphogenesis of an epithelial tissue (St Johnston and Sanson, 2011). In a growing pseudostratified columnar epithelium, elongated epithelial cell shapes and apical-basal polarization provide an additional layer of complexity and dynamics to mitotic division at the spatial level. Interphase nuclei are positioned at relatively basal parts of the cell layer (in most part of the thesis, especially in the results, "basal" means below the septate junction-delimited mitotic zone (MZ)), while the rounded mitotic cells are only observed at very apical locations. This IKNM phenomenon

was first described in pig neural tube (Sauer, 1935) and was later discovered to be a universal feature of pseudostratified epithelium, even in sea anemone (Meyer et al., 2011). However, the molecular mechanisms and functions of IKNM remain still unclear. There are at least three major questions in the field.

### 1.4.1 Both actomyosin and MT function may be involved in IKNM

What drives IKNM? Studies from different systems have concluded that IKNM is driven by actomyosin contractility (Meyer et al., 2011; Norden *et al.*, 2009; Schenk *et al.*, 2009), or MTs and their associated motor proteins (Del Bene *et al.*, 2008; Hu *et al.*, 2013; Kosodo *et al.*, 2011; Tsai *et al.*, 2010). Specifically, both the Actin depolymerizing drug Cytochalasin B/D and the non-muscle myosin inhibitor Blebbistatin have a long history used in IKNM studies for perturbing apical localization of mitotic nuclei (Messier and Auclair, 1974; Meyer et al., 2011; Murciano *et al.*, 2002; Norden *et al.*, 2009; Webster and Langman, 1978). Besides inhibiting actomyosin activity, perturbing the MT motor protein dynein and its regulators, including dynactin, Lis1, NudC, have also been suggested to affect the apical localization of mitotic nuclei in zebrafish retina (Del Bene *et al.*, 2008) and mouse cerebral cortex (Gambello *et al.*, 2003; Hu *et al.*, 2013; Tsai *et al.*, 2007; Tsai *et al.*, 2010). However, because most of the IKNM studies mark the localization of mitotic events using anti-Phospho-Histone H3 (anti-PH3), whose signal starts to accumulate on chromosomes during G2 (Gurley *et al.*, 1978; Hans and Dimitrov, 2001; Hendzel *et al.*, 1997), few evidences have suggested basal cell division (e.g. cytokinesis) after perturbation, it is possible that some basal anti-PH3+ nuclei observed were in G2 phase but not mitosis.

### 1.4.2 The nuclear migration is tightly correlated with cell cycle progression

How is mitotic nuclear position linked with cell cycle progression? The most intriguing aspect of IKNM is the tight correlation of nuclear position with mitotic timing. Blocking the cell cycle at mitotic phase resulted in arrested mitotic nuclei only at the apical surface (Langman *et al.*, 1966; Sauer and Chittenden, 1959; Sauer and Walker, 1959).

Consistently, slowing down the cell cycle of retinal neuroepithelia results in a proportional delay of the nuclear migration (Pearson *et al.*, 2005; Willer *et al.*, 2005). Further, IKNM stopped with completely inhibited cell division by pharmacological manipulations in neuroepithelia (reviewed in Baye and Link, 2008; Ueno *et al.*, 2006). Despite the observation of association, it is still unknown if nuclear translocation is only simply correlated with mitosis, or if a global regulator of the core cell machinery (such as CDK) also controls nuclear migration.

### 1.4.3 The significance of IKNM

What is the function of IKNM in the epithelium? Though IKNM was implicated in cell fate determination of neural progenitors (Murciano *et al.*, 2002; Xie *et al.*, 2007), a more fundamental function of IKNM has been proposed accommodating the ubiquity of its conservation. Based on the fact that the centrosomes were accumulated at the apical surface of the epithelia (Chenn *et al.*, 1998; Nakajima *et al.*, 2013; Tamai *et al.*, 2007), one of the hypotheses is that nuclei must reach the apical surface to meet the centrosomes and organize mitotic spindles (Baye and Link, 2008; Chenn *et al.*, 1998). Indeed, silencing centrosomal protein Cep120 and its interacting partner TACCs impairs both IKNM and neural progenitor self-renewal (Xie *et al.*, 2007). Interestingly, recent studies have shown that besides nuclear translocation, IKNM may also involve active centrosome movement. Instead of sitting statically on the apical side before mitosis, more dynamic centrosome hopping behavior was observed, in which centrosomes could leave the apical side to bring basal mitotic nuclei to the apical surface in chicken neural tube, mouse cortical slides, as well as rat brain (Hu *et al.*, 2013; Spear and Erickson, 2012). Together, these data suggest that bringing mitotic nuclei and centrosomes together at the apical epithelial surface may be a general feature and a highly regulated process. These highlight the need to obtain mutants that only disrupt mitotic nuclear position while maintaining other essential aspects of cell division, in order to investigate the function of IKNM.

In sum, despite the ubiquity of this conserved IKNM phenomenon, its fundamental function and the molecular mechanisms linking nuclear migration to cell cycle progression remain unclear.

## 1.5 The developmental system of *Drosophila* wing imaginal disc

### 1.5.1 Overview of the *Drosophila* model system

*Drosophila* melanogaster represents an ideal model system to study conserved developmental processes. *Drosophila* is easy to maintain and breed, having a relatively short life cycle. In about 10 days (at 25 °C), an individual *Drosophila* develops from a fertilized embryo to an adult fly through embryogenesis, larval development (molting twice), and a pupal stage. In addition, *Drosophila* carries only four chromosomes with a sequenced genome, and more importantly, it allows advanced genetic manipulation to identify and characterize the function of novel genes and RNA (Gilbert, 2010). Over a century of genetic study and intensive systematic genetic screens have discovered numerous mutants and their related genes which define many conserved developmental processes, such as the spatial patterning of body structures (Nusslein-Volhard and Wieschaus, 1980).

In additional to traditional mutagenesis screens, RNAi techniques permit genome-wide cell cycle screens in cultured *Drosophila* S2 cells (Bettencourt-Dias and Goshima, 2009; Bjorklund *et al.*, 2006; Boutros *et al.*, 2004; Rogers and Rogers, 2008). Recently, increasing numbers of *in vivo* RNAi screens have been reported (Cronin *et al.*, 2009; Dietzl *et al.*, 2007; Mummery-Widmer *et al.*, 2009; Neumuller *et al.*, 2011; Ni *et al.*, 2009; Pospisilik *et al.*, 2010; Saj *et al.*, 2010), with access to fly RNAi resources from the VDRC, DGRC, TRiP and NIG stock centers. However, to the best of our knowledge, no RNAi screens have been reported that investigate growth and cell cycle progression in the developing *Drosophila* wing.

### 1.5.2 Development of the wing imaginal disc

In *Drosophila*, the adult wings and other appendage structures are derived from imaginal discs, monolayer epithelial sacs that undergo rapid and continuous proliferation during larval development (Cohen, 1993). The *Drosophila* wing imaginal disc, composed mainly of a single layer of columnar epithelial cells, gives rise to the adult wing. This structure has been used extensively to investigate pattern formation, growth, and cell cycle regulation (Cruz *et al.*, 2009; Martin-Castellanos and Edgar, 2002; Neufeld *et al.*, 1998).

During wing disc development, positional information arises that separate disc into anterior/posterior (expressing the homeodomain gene *apterous* in the dorsal side, and *engrailed* in the posterior (Lawrence and Morata, 1976); Figure1-2) and dorsal/ventral compartments (expressing homeodomain gene apterous in the dorsal side,Garcia-Bellido *et al.*, 1976). These compartment boundaries are defined by mitotic clonal analysis, which prohibit mixing of cells from different subregions (Garcia-Bellido *et al.*, 1976). Besides lineage restrictions, the wing disc is also extensively patterned (reviewed inBryant, 1974; Whittle, 1990). By analyzing cuticle structures formed by fragmented disc (Bryant, 1975) and wing cuticle mutants (Lindsley and Zimm, 1992), detailed cell fates have been mapped and genes specifically required for wing formation and patterning were discovered. These include components of signaling pathways that direct the growth and patterning of the wing disc, such as DPP/BMP, WG/WNT, VN/EGF, Notch, and Hh pathways. Indeed, an ectopic expression of Dpp and Wingless can induce duplication of wing regions (Capdevila and Guerrero, 1994; Diaz-Benjumea and Cohen, 1995).

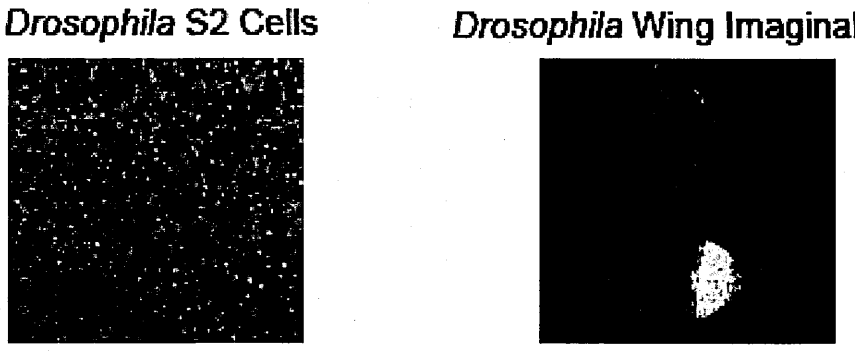


**Figure 1-2 The two *Drosophila* systems used in this thesis study.**
*Drosophila* S2 cells are the most commonly used culture system for genome-wide RNAi screens (image from internet). They are actively dividing with the length of the cell cycle around 24 hours. In contrast to the floating-cultured single-cell system, cells in a developing *Drosophila* wing imaginal disc are also actively dividing (with a cell cycle timing of roughly 12 hours at third instar) but also received positional information that distinguishes them into compartments. This staining image shows posterior compartment (*green, en-GAL4; UAS-GFP*) and anterior compartment (*red, Ci*; protein level is higher next to the A/P compartment boundary) (Motzny and Holmgren, 1995).

### 1.5.3 Growth and cell division in the wing imaginal disc

As a developing epithelial tissue with well-defined patterning mechanisms, the wing imaginal disc is an ideal model to understand growth and cell cycle regulation in a tissue context (Serrano and O'Farrell, 1997). The wing disc originates from an embryonic primordium, comprising about 50 cells at the time of embryo hatching, and developing into the third instar stage with about 50,000 cells (Garcia-Bellido and Merriam, 1971). Although wing growth is directed by patterning signals (Schwank and Basler, 2010), active cell division occurs ubiquitously without an obvious spatial pattern until late in development (Garcia-Bellido and Merriam, 1971; Johnston and Edgar, 1998). There is active investigation into how this uniform growth is controlled by morphogen gradients, including Dpp and Wingless (Campbell and Tomlinson, 1999; Hamaratoglu *et al.*, 2011; Lander *et al.*, 2011; Moreno *et al.*, 2002; Schwank *et al.*, 2012; Wartlick *et al.*, 2011a; Wartlick *et al.*, 2011b; Zhang *et al.*, 2013). In addition to the active role in promoting cell proliferation, later in wing disc development, Wingless and Notch signalings induce cell cycle arrest in a zone of non-proliferating cells (ZNC) at the dorsal/ventral boundary (Johnston and Edgar, 1998; O'Brochta and Bryant, 1985).

Cell proliferation, cell growth, and tissue compartment growth are highly coordinated in disc cells (Neufeld *et al.*, 1998; Resino and Garcia-Bellido, 2004; Thompson, 2010). During active division, cell size is approximately constant in the disc proper, and apoptosis events are few and sporadic (Milan *et al.*, 1997). Overexpression of *CycE* and *String*, which are the key molecules regulating the G1/S and G2/M transitions, result in a corresponding shortening of G1 and G2 phases but little changes in the overall cell doubling time or wing size. When cell death is inhibited, overexpression of the upstream regulator of *CycE* and *String*, E2F and its repressor RBP, results in shortening or extension of both G1 and G2 phases. However, though total cell number changes in the manipulated compartment, cell size also changes inversely and the relative size of that subdomain is not altered (Neufeld *et al.*, 1998).

In addition to having sophisticated genetic tool kits and well-studied developmental process, the *Drosophila* wing disc also provides a number of established methods for cell cycle analysis, such as mosaic clonal analysis (Xu and Rubin, 1993) and flow cytometry (Neufeld *et al.*, 1998). Thus, the wing disc offers us an epithelial context to extend our knowledge from single-cell systems and to dissect important questions of cell division *in vivo*.

## 1.6 Aims of this thesis

In this thesis project, I address three specific questions:

1. What is the global periodic transcriptome in the developing *Drosophila* wing imaginal disc, and how does it compare with the global periodic transcriptome from the unicellular system of S2 cells?
2. What are the developmental functions of the periodically expressed genes?
3. Do periodic genes of the wing disc function in cell cycle progression or other cell cycle-related processes, such as IKNM?

# Methods

## 2.1 Wing disc dissociation, Fluorescent-Activated Cell Sorting (FACS), and live cell cycle analysis of wing disc and S2 cells

### 2.1.1 Wing disc dissociation

For live wing disc cell FACS assays, *Drosophila* larvae were raised at 25°C at low density until the 3rd instar wandering stage, washed and dissected in PBS (pH 7.4). Forty wing discs were transferred into 300 µl 25°C 0.25% Trypsin-EDTA (Sigma, T4049), drawn through an 18G11/2 gauge needle ten times and then incubated for 15 minutes at 25°C. 150 µl heat inactivated FBS (hi-FBS; GIBCO, 10438) was added to stop the enzymatic reaction and samples were again drawn through the 18G11/2 needle ten times. After a brief low speed centrifuge (1,600rpm for 5min), cells were washed and resuspended in culture solution (Schneider's *Drosophila* Medium (GIBCO, 11720034), containing 2% hi-FBS (GIBCO, 10438) or staining solution (see next).

Please refer to a step-by-step protocol in 2.12 for details.

### 2.1.2 Wing disc cell staining, FACS, and live cell cycle analysis

Dissociated wing disc cells were kept in staining solution (Schneider's *Drosophila* Medium (GIBCO, 11720034), containing 2% hi-FBS (GIBCO, 10438), and 1 µg/ml Hoechst 33342 (Invitrogen, H1399) for 20 minutes at 25°C. The sample were then transferred for sorting or cell cycle analysis using an Influx Flow Cytometer (BD Biosciences). 7AAD (7-Aminoactinomycin D; Invitrogen, A1310; 1 µg/ml) was added five minutes before cell cycle analysis to labeling dying cells.

Please refer to a step-by-step protocol in 2.12 for details.

### 2.1.3 S2 cell staining and FACS, and live cell cycle analysis

For S2 cell FACS, low-passage cells (less than 30 passages) were used to count and check for viability using a Vi-Cell XR Cell Viability Analyzer (Beckman Coulter) before

experiments. Cells were collected by a brief low speed centrifugation, washed using PBS (pH 7.2), and treated with 0.25% Trypsin-EDTA for 1 minute. Hi-FBS was then added, followed by centrifugation. Cells were then washed and resuspended in staining solution (Schneider's *Drosophila* Medium, containing 2% hi-FBS and 2 μg/ml Hoechst 33342) for 20 minutes at 25°C before sorting using the Influx flow cytometer.

Please refer to a step-by-step protocol in 2.12 for details.

### 2.1.4 Flow cytometry data analysis

Flow cytometry data were analyzed using FlowJo (Tree Star) and Modfit (Verity Software House) software. FlowJo was used for primary data viewing and analysis. Modfit was used for cell cycle phasing analysis.

## 2.2 RNA extraction

### 2.2.1 Total RNA extraction from FACS sorted wing disc and S2 cells

For the FACS/microarray experiment, wing disc and S2 cells were subject to cytometric analysis and partitioned into G1 and G2/M populations. Robust gating was applied based on 2N and 4N peak positions. Cells were sorted directly into RNAprotect Cell Reagent (QIAGEN, 76526) and total RNA was extracted (QIAGEN RNeasy Plus Micro Kit, 74034) in triplicate for S2 and *OreR* wing disc cells, and in duplicate for $w^{1118}$ wing disc cells.

### 2.2.2 Total RNA extraction for RNA-sequencing

For RNA-seq, 30 third instar wing discs of each genotype were dissected in Ringer's solution; nota were removed to isolate the knockdown domain of *Bx-GAL4*. Dissected material was immediately frozen in liquid nitrogen for total RNA extraction in triplicate (QIAGEN RNeasy Mini Kit). Three biological replicates were used for each condition.

### 2.2.3 Total RNA extraction for qPCR assays

Total RNA was extracted from the third instar wing discs of each genotype with nota removed to isolate the knockdown domain of *Bx-GAL4.* . Dissected material was immediately frozen in liquid nitrogen for total RNA extraction in triplicate (QIAGEN RNeasy Mini Kit). At least three biological replicates were used for each condition.

## 2.3 Gene expression analysis

### 2.3.1 Microarray analysis

Biotinylated cRNA was prepared from total RNA (Ambion, MessageAmp III RNA Amplification kit, AM1793), labeled, and hybridized to Affymetrix GeneChip *Drosophila* Genome 2.0 arrays consisting of probe sets representing over 18,500 transcripts based on Flybase version 3.1. Data was analyzed using the R statistical environment. CEL files were processed and normalized using RMA (Irizarry *et al.*, 2003).

The linear modeling package Limma (Smyth, 2004), which calculates a moderated t-statistic, was used to derive gene expression coefficients using cell type and cell cycle phase as factors to identify differentially expressed genes. A function called decideTests () was used to generate the microarray venn diagram in the Figure 3-3. It examines a matrix of t-statistics and classifies them as up, down, or not significant with a Benjamini-Hochberg adjusted p-value of 0.05 (default). The result is a matrix of columns for each comparison, rows for each gene, and values of 1, -1, or 0 to denote significant up, down, or insignificant change respectively.

### 2.3.2 RNA sequencing

Poly-A selected, strand-specific RNA-Seq libraries were made using the Illumina TruSeq Stranded RNA kit (Illumina). The resulting libraries were purified using Agencourt AMPure XP system (Backman Coulter), and then quantified using a Bioanalyzer (Agilent Technologies) and a Qubit Fluorometer (Life Technologies). All libraries were pooled, re-quantified and run as high output mode on 50 bp single-end lanes on an Illumina HiSeq

2500 instrument, using HiSeq Control Software 2.0.5 and Real-Time Analysis (RTA) version 1.17.20.0. The Illumina Secondary Analysis Package (CASAVA-1.8.2) was run to demultiplex reads and to generate FASTQ files. The resulting single-end sequence reads were aligned to the *Drosophila* genome, version dm3 from UCSC, using TopHat version 2.0.8 allowing only unique alignments. Genes with a sum of less than 3 reads per million across all 12 data sets were filtered out. Fold changes in gene expression and p-values between samples were quantified in the R environment using the edgeR library (Robinson *et al.*, 2010) from Bioconductor. Microarray and RNA-seq data were deposited at GEO (GSE54928).

### 2.3.3 Quantitative PCR (qPCR) assays

qPCR was performed with Taqman assay on 7900HT Fast Real-Time PCR System (Applied Biosystems) and analyzed with qBasePLUS software (Biogazelle).

## 2.4 RNA *in situ* hybridization

### 2.4.1 Synthesis of RNA probe

Linearized templates were generated from freshly purified and enzyme-digested plasmid or PCR products carrying the target gene sequence and a T7, SP6, or T3 promoter. *In vitro* transcription (25 µl) were performed at 37 °C for 2-12 hours. Checked the synthesized probe by running 1 µl on a 1% agarose TAE gel. Stopped the reaction by adding 2 µl of RQ1 RNase-Free DNase and incubate the reaction at 37 °C for 15 minutes. Finally, precipitated the RNA probe by adding 50 µl DEPC-H2O, 25 µl 10M ammonium acetate and 200 µl 100% ethanol (-20°C) on dry ice for 30 minutes, or at -80 °C overnight. Centrifuge the tube at 13,000rpm at 4°C for 20min, and then remove the supernatant carefully to leave the pellet. Washed the pellet using 1ml 70% ethanol (-20°C). Brief air dried, dissolved the pellet in 1ml prehybe solution, and stored it at -20°C. Used 25 to 50 µl for 1ml prehybe solution in an *in situ* experiment.

Please refer to a step-by-step protocol in 2.12 for details.

### 2.4.2 *In situ* hybridization

I adapted the protocol from an *in situ* hybridization protocol of zebrafish embryo

(learned from Macie Walker during my rotation at Paul Trainor Lab in 2009).

Please refer to a step-by-step protocol in 2.12 for details.

## 2.5 Bioinformatics

### 2.5.1 Gene ontology analysis

Gene Ontology (GO) analysis was done using Bioconductor GeneAnswers Package.

### 2.5.2 Heatmap

Heatmaps were generated using MultiExperiment Viewer (MeV, v4.8; Saeed *et al.*, 2006).

### 2.5.3 Motif analysis

The consensus sequences motif enriched in the upstream regions of gene classes were identified using motif discovery tool Multiple EM for Motif Elicitation (MEME; Bailey and Elkan, 1994), and the motif comparison tool TOMTOM (Gupta *et al.*, 2007). The results of MEME, TOMTOM, and other motif analyses can be accessed at: http://wiki.stowers-institute.org/research/AlexanderGarrett/Projects/cell-cycle.

### 2.5.4 Gene interaction network

Protein interaction data, including both physical and predicted interactions were extracted from GeneMANIA (Warde-Farley *et al.*, 2010). The networks were then constructed using Cytoscape (Cline *et al.*, 2007).

## 2.6 Fly strains, RNAi Screens, and periodic gene function website

### 2.6.1 Fly strains

The following fly strains were used: *OreR*, $w^{1118}$, *yw; UAS-mCD8-GFP* (Bloomington 5137), $w^{1118}$, *Bx-GAL4*; *UAS-dicer2* (*Bx-GAL4* also known as *MS1096-GAL4*, Bloomington 25706; for RNAi adult wing screen and RNA-seq), *UAS-dicer2,* $w^{1118}$; *engrailed-GAL4, UAS-EGFP* (Bloomington 25752; for flow cytometry analysis), *UAS-dicer2,* $w^{1118}$;

*nubbin-GAL4* (Bloomington 25754), *A9-GAL4, UASp-GFP-Cnn; Sp/Cyo* (made from Bloomington 8761and 7255), and *A9-GAL4, UASp-GFP-Cnn; His2Av-mRFP* (made from Bloomington 8761, 7255 and 23651 respectively; for live imaging and SPIM). RNAi lines for screens were ordered from the Vienna *Drosophila* RNAi Center (VDRC) P-Element RNAi Library (GD library). *CR32027* was identified from the screen using *CR32027-IR1* (26860, VDRC, GD library), while *CR32027-IR2* (103512, VDRC, KK library) was used for confirmation. Additional RNAi lines used: *Klp54D-IR1* (36577, TRiP), *Klp54D-IR2* (100140, VDRC, KK library), *Cyp6a17-IR* (33887, TRiP).

### 2.6.2 RNA screens

Males from *UAS-IR* lines were crossed with *GAL4* line virgin females. RNAi screens and all crosses were all conducted at 25°C, except a few lines at 18°C and 29°C as noted. Phenotypes were scored blindly for both male and female progeny. For most of the imaging analysis, only male larvae were used.

### 2.6.3 Periodic gene function website

Representative RNAi screen phenotypic results can be accessed at: http://odr.stowers.org/FlyCycle. The ortholog information used in the website and in Table S8 was extracted from BDGP5 and GRCh37.p12 of Ensembl Genes 73.

## 2.7 Wing disc ex vivo culture for drug experiments and live imaging

### 2.7.1 Wing disc ex vivo culture for drug experiments

For drug experiments, third instar larvae were washed in PBS and dissected in Shields and Sang M3 Insect media (Sigma) with 2% FBS (Gibco), Penicillin (100 units/ml) -Streptomycin (100 µg/mL streptomycin; Sigma) and BPYE (2.5 g/L Bacto-peptone, 1 g/L yeast extract, and 0.5 g/L KHCO3). Anterior-half carcasses, including wing imaginal discs, were immediately transferred into 75µl of culture media in the center wells of an uncoated

2x 9 μ-Slide (Ibidi). Corner wells of the slide were filled with 100μl sterile water and heated by a light beam to generate a humid chamber. For inhibitor experiments, we used Cytochalasin D (Sigma; 100 μM), Taxol/Paclitaxel (EMD; 250 μM), and nocodazole (Sigma; 500 μM). After a 30-minute incubation at room temperature with low-speed agitation, carcasses were fixed and stained as above.

### 2.7.2 Wing disc ex vivo culture for live imaging

For live imaging, the culture solution above was mixed 1:1 with Ringer's solution (130 mM NaCl, 5 mM KCl, 1.5 mM MgCl2) to reduce autofluorescence. Live discs were mounted between two pieces of Scotch double-sided tape (3M) in a 35mm glass bottom culture dish (MatTek) and covered by a round 5mm coverslip (Fisher Scientific; for Spinning Disk) at room temperature, or in 1% agarose in the Ringer's solution (for SPIM) at 30°C.

## 2.8 Adult wing cuticle preparation for imaging

### 2.8.1 Preparation of Hoyer's medium

Prepare under a fume hood. Add 15 g of gum arabic to 25 mL of H2O in a glass beaker. Heat to 60°C, and stir overnight on a magnetic stirrer. Successively add 100 g of chloral hydrate. After the chloral hydrate has dissolved, add 10 g of glycerol. Centrifuge the solution for 30 min at 10,000g and filter the solution through glass wool. Store the solution at room temperature in a tightly sealed flask. Shortly before use, centrifuge Hoyer's medium in a tabletop centrifuge for at least 15 min to pellet undissolved particles (the recipe is from Cold Spring Harbor Protocols).

### 2.8.2 Adult wing sample preparation

Adult flies were collected in 1 ml of 70% ethanol (can be stored at 4°C), and put them on low-speed nutator for 30 minutes at RT. Flies were then rehydrated through a graded series of ethanol to pure water. Dissected the fly wings with forceps in water under

a dissection scope. Centrifuge Hoyer's medium in a tabletop centrifuge for 20 minutes on high speed. Carefully transferred and mounted the wings in a drop of 15 µl Hoyer's medium (use clear liquid) on a slide. Put the cover slip (avoid making air bubbles). Finally, placed the slide on a 65°C heat block for 1 hour before imaging. The slide could be stored at RT permanently.

## 2.9 Immunofluorescence Analysis

### 2.9.1 Information of primary antibodies

Primary antibodies used were: Rabbit anti-phospho-Histone 3 (Upstate; 1:1000), Mouse anti-Dlg (DSHB; 1:500), Mouse anti-α-Tubulin (Sigma; 1:5000), Rabbit anti-phospho-light chain of myosin II (p-MRLC, Cell Signaling; 1:50), and Rabbit anti-cleaved Caspase 3 (Cell Signaling; 1:500).

### 2.9.2 Sample preparation and staining procedure

Wandering third instar larvae were dissected and fixed in 4% paraformaldehyde (PBS, pH 7.4) for 25 minutes. Carcasses were washed in PBT (PBS with 0.1% Triton X100) three times for 20 minutes, and then stained in primary antibodies overnight at 4°C. Samples were washed in PBT for three 20-minute washes and incubated with secondary antibodies (1:1000 in PBS) and Alexa Phalloidin 546 (Invitrogen, A22283; 1:250 in PBS) for 4h at RT. Nuclei were stained with 5 µg/ml Hoechst 34580 (Invitrogen, H21486) for 30 minutes at RT.

## 2.10 Confocal and live imaging

### 2.10.1 Confocal imaging of wing disc

Confocal images were captured using a Leica SP5 confocal microscope, and analyzed using ImageJ and Fiji.

### 2.10.2Live imaging of apical mitosis in wing disc

A Zeiss PerkinElmer Ultraview Spinning Disk system was used for live imaging of mitotic cell division. Spinning disk images were taken and viewed using Volocity, and de-convolution was performed with Huygens software (Scientific Volume Imaging).

### 2.10.3Single Plane Illumination Microscopy (SPIM) of IKNM

The IKNM time lapses were taken using a SPIM system built in the Stowers Institute Imaging Core. All images were analyzed using ImageJ (Schneider *et al.*, 2012). For quantification of the distance of anti-PH3+ nuclei from the apical epithelial surface, nuclei from the strong knockdown regions (wing pouch for nub-GAL4 and dorsal wing pouch for A9-GAL4) were used.

## 2.11 Electron Microscopy (EM)

### 2.11.1Transmission Electron Microscopy (TEM)

Dissected third instar wing imaginal discs were fixed for two hours with 2.5% paraformaldehyde and 2% glutaraldehyde in PBS at room temperature. The samples were then rinsed in PBS and post-fixed with 1% osmium tetroxide containing 0.1% potassium ferricyanide for one hour at room temperature. The samples were then dehydrated through a graded series of ethanol to 100%, infiltrated and embedded in EPON resin. The resin was then polymerized at 60 °C for 48 hrs. Sections (80-100nm) were cut on a Leica ultramicrotome using a diamond knife. These sections were then stained with 2% uranyl acetate and lead citrate for ten minutes and six minutes respectively and visualized using a FEI Tecnai transmission electron microscope.

### 2.11.2Scanning Electron Microscope (SEM)

Adult flies were fixed in with 2.5% paraformaldehyde and 2% glutaraldehyde in PBS overnight. The samples were then rinsed in water for three times and post-fixed with 1% osmium tetroxide for one hour at room temperature. After three time water rinses, the

samples were then dehydrated through a graded series of ethanol (30%, 50%, 70%, 80%, 95%, and 100%) each for 10 minutes. The samples were then treated with hexamethyldisilazane (HMSD) twice for 15 minutes. The flies were then transferred carefully into a petri dish with a filter paper at the bottom, and let air dry overnight prior to imaging. The adult fly eyes were visualized using a Hitachi TM-1000 Scanning Electron Microscope.

## 2.12 Step-by-step protocols and notes for FACS and *in situ*

In addition to the method in previous section, I attached my step-by-step protocols and some critical notes for both experiments here, in order to provide more details on flow cytometry and *in situ* hybridization for future reference.

### 2.12.1LIA Protocol: *Drosophila* wing imaginal disc cell disassociation and Hoechst 33342 staining (optional) for live cell cycle analysis using Flow Cytometry

#### 2.12.1.1 Notes

I optimized this protocol from the old wing disc cell dissociation and staining protocol (Neufeld *et al.*, 1998) during the two-month rotation in Gibson lab at the end of 2008. Introducing syringe-based mechanical disruption to the old wing disc dissociation protocol largely improved the dissociation efficiency. More importantly, adding a step to stop the enzymatic reaction and subsequently removing the enzyme from the dissociated cell system enhanced the yield of live cells. As a result, compared with the old 2-4 hour-long enzymatic protocol for imaginal disc dissociation, the new method recovered approximately three times more live cells (about 11,000 isolated live cells per wing disc, based on the negative trypan blue-staining signal) within a shorter time (20 minutes compared with 120 minutes, also see Results).

The idea of needle and syringe first came to me from searching and reading classical papers about establishing *in vitro* cultures of imaginal disc cells, which mention a step with 'vigorous pipetting'. I took it further into practice after a personal communication

with Dennis Ridenour at Kulesa lab, who was experienced with chick embryo dissociation. Ruihong Zhu and Jeff Haug also provided me with enormous help during this process for running my numerous samples and giving comments on the dissociation quality.

If you have never done tissue dissociation or flow cytometry, I recommend to perform a couple of pilot experiments using this protocol before you start a "real" cell sorting or flow cytometry experiment.

Finally, good luck for whatever you are planning to do now!

#### 2.12.1.2 Materials

Microcentrifuge tubes

18 gauge needles

1 ml syringes

Foil

4-Channel Timer

#### 2.12.1.3 Reagents

dH2O

0.25% Trypsin-EDTA (Sigma T4049, others may also work.)

1X PBS

Schneider's *Drosophila* Medium

Fetal bovine serum (FBS, Heat inactivated), store in 4C

Hoechst 33342

7AAD

#### 2.12.1.4 Estimated time

Preparation: 5 min

Dissociation: 15 min

Staining: 25 min

Other sample processing steps: 5-10 min

Total: around 50 min

#### 2.12.1.5 Procedures

1) Prepare good larvae for the experiment ahead of time.
2) Briefly thaw 0.25% Trypsin-EDTA in 25C water bath. Before dissection, transfer it into 1.5ml tubes (500µl/for 40discs, this volume can be adjusted for more or less discs).
3) Warm Schneider's *Drosophila* Medium in 25C water bath.
4) Prepare Schneider's *Drosophila* Medium with 2% FBS. Warm in 25C water bath.
5) Mark 1ml syringes with 18 gauge needles, one FBS-, one FBS+ (for multiple samples of the same genotype); or mark the syringe for each sample of individual genotype.
6) Transfer larvae from vial/bottle with forceps or brushes into a Petri dish or glass crystallization dish. Use 3 rinses of $dH_2O$ to remove food and yeast, rinse briefly with 70% EtOH, and follow with 2 rinses in $dH_2O$, and 1 rinse in PBS. Note: after final rinse, leave enough PBS to hold larvae without submerging them.
7) Place three drops of PBS onto a siliconized glass slide. In one drop dissect the washed larvae. Invert the anterior half and strip of fat body and gut. Transfer the anterior half to the second drop, using forceps, to dissect away the wing imaginal discs, excluding other tissues e.g. other discs, trachea. Finally, transfer the discs to the third drop to wash them of residual media (yeast) and larval tissues
8) Transfer the discs into a tube with 0.25% Trypsin-EDTA via a 20ul micropipettor which has been coated with protein and fat from the dissected

larvae by pipetting up and down the liquid from the first drop. Note: Pipette the minimum possible liquid when transferring the discs in case of significant change to medium concentration.

9) As soon as all the discs are collected and transferred into the tube with 0.25% Trypsin-EDTA, draw samples through a FBS- 18 gauge needle around10 times.
10) Incubate the sample in 25C water bath for 15min.
11) Stop reaction by adding FBS ½ volume of the typsin (250ul FBS for 500ul trypsin).
12) Gently dissociate cells in each tube by drawing sample through a FBS+ 18 gauge needle around 15 times.
13) Centrifuge cells at 1600 rpm for 5 minutes at RT.
14) Two options here: If the cells are from transgenic flies and/or don't need to be stained by other dye, remove SNT and resuspend cells in 500 ul Schneider's *Drosophila* Medium with 2% FBS. And the sample is ready to run the flow cytometry (the sample may be stable at RT. for about 1h, but run the sample the sooner the better). If the sample needs to be stained by Hoechst33342, remove SNT and resuspend cells in 750 ul Schneider's *Drosophila* Medium, and go on with the following steps.
15) Centrifuge at 1600 rpm for 5 mins at RT.
16) Remove SNT and resuspend cells in 500 ul Schneider's *Drosophila* Medium. Add Hoechst33342 to a final concentration of 1ug/ml.
17) Incubate at 25C water bath for 20 minutes. Add 7AAD to a final concentration of 1ug/ml for 5min.
18) Run the sample on the flow cytometry as soon as possible.

### 2.12.2LIA Protocol: *Drosophila* S2 cell Hoechst 33342 staining for live cell cycle analysis using Flow Cytometry

#### 2.12.2.1 Notes

Get a great DNA profile on a flow cytometer is not an easy task as it appears, while it is a game of trying different conditions of each experimental step. Although no dissociation is needed for culture cells, staining conditions becomes essential. I optimized and consolidated this S2 staining protocol for cell cycle live analysis after testing over 80 different staining conditions (reagent concentration, pH, DNA dye, etal.) based upon my established wing disc cell staining protocol (listed above) during the experiments in 2009.

Additionally, for cell sorting, it is critical to add the detergent pluronic F68 (originally suggested by Jeff Haug) to the running solution (usually PBS) in the cytometer to avoid cell bursting when dropping into the collecting solution.

#### 2.12.2.2 Materials

Microcentrifuge tubes

Foil

25C water bath

Mini-centrifuge

50ml tube shelf

4-Channel Timer

#### 2.12.2.3 Reagents

dd$H_2O$

0.25% Trypsin-EDTA (Sigma T4049, others may also work.)

1X PBS, 7.2

Schneider's *Drosophila* Medium

Fetal bovine serum (FBS, Heat inactivated), store in 4C

Hoechst 33342

7AAD

#### 2.12.2.4 Estimated time

Preparation: 5 min

Processing cells: 5 min

Staining: 25 min

Total: 35 min

#### 2.12.2.5 Procedures

1) Turn on water bath.
2) Prepare Schneider's *Drosophila* Medium with 2% FBS. Warm it up. Also warm up 0.25% Trypsin-EDTA, and FBS to 25C.
3) Prepare 100x Hoechst 33342 working solution using ddH2O.
4) Prepare Schneider's *Drosophila* Medium+ 2% FBS, with Hoechst 33342 2ug/ml, as staining solution for post-sort and wash the Cytometer tube.
5) Transfer 1ml fresh S2 cells into a microcentrifuge tube.
6) Mini-centrifuge for 1min, and discard the SNT.
7) Wash the cells by resuspending them into 1.5ml PBS 7.2.
8) Centrifuge again, discard SNT and resuspend in 1ml Trypsin-EDTA for 1min.
9) Add 0.5ml FBS. Mix the solution.
10) Centrifuge for 1min.
11) Discard the SNT. Resuspend the cells in Schneider's *Drosophila* Medium+ 2% FBS. Add Hoechst 33342 to a final concentration of 2ug/ml.
12) Incubate at 25C water bath for 20 minutes. Add 7AAD to a final concentration of 1ug/ml for 5min.
13) Run the sample on the flow cytometry as soon as possible.

### 2.12.3LIA Notes: FACS and live cell cycle analysis using an Influx Flow Cytometer (BD Biosciences)

#### 2.12.3.1 Aims for this notes

1. To consistently perform experiments using the established protocol for cell cycle profile and cell size analysis using wing disc cells;

2. To compare cell cycle profile and cell size in wing discs with/between GFP- (internal control), GFP+ (RNAi) cells, and between samples running on Influx cytometer on different days.

#### 2.12.3.2 Machine setting

For FACS live cell sorting, use 12psi/100tip, which seems to be better than using higher psi and bigger tips.

For live cell cycle analysis, use 45psi/70tip.

For setting of each cytometer parameter, such as scale of FSC and SSC, use the setting of sample 10cy041-514 as example

#### 2.12.3.3 During sample running on a flow cytometer

1. Run size beads to do the size alignment and correction curve.

2. Run the sample as soon as possible, preventing it from sitting on the bench and keep the sample with Hoechst stained away from light.

3. For the whole process, no additional fluid, no vortex (sample could be shaken by hands but avoid vortexing), and no on ice;

4. Run through each sample to collect as many cells as possible, since GFP+ cells may be less in RNAi cells;

5. Record the sample running starting time, ending time, G1 and G2 peak position in Hoechst Blue Int. channel. (Liang will bring the sheet before the experiment);

6. Check the alignment multiple times during the running, to get tight CVs;

7. Collect Int data for both Red and Blue, adjust two signal channels to be comparable (use sample 10cy041-514 experiment settings);

8. Try to fixed G1 peak position between samples, to get consistent profile for comparison (use sample 10cy041-514 experiment settings);

9. Try to move cell apart from debris in the FSC/SSC window (use sample 10cy041-514 experiment settings);

10. Adjust the window to make sure the data from bigger cells and smaller cells are all collected, since the RNAi cells could have different size compared with wild type (use sample 10cy041-514 experiment settings).

11. Run a few wild type samples to see the consistency between samples.

12. Run the same sample multiple time through the day to check.

13. For live cell sorting, check the machine performance by post-sort two or three times in a one day sorting.

### 2.12.4LIA Protocol: RNA Probe synthesis for *in situ* hybridization to *Drosophila* imaginal discs

#### 2.12.4.1 Notes

I adapted this probe synthesis protocol from an *in situ* hybridization protocol of zebrafish embryo (learned from Macie Walker during my rotation at Paul Trainor Lab in 2009) and a published protocol of high-throughput RNA *in situ* hybridization to whole-mount *Drosophila* embryos (Weiszmann *et al.*, 2009).

#### 2.12.4.2 Procedures

1) Templates were obtained by PCR from cDNA clones of *Drosophila* gene collection (DGC) following a published protocol (Weiszmann *et al.*, 2009), or by directly digesting 5ug plasmid to linearize in a sealed tube, usually in

37C water bath, 2h (Check enzyme product information for details). Checked on a 1% TAE agrose gel till completely linearized.

2) Clean up the PCR product or linearized plasmid using Qiagen PCR purification kit, eluted in 30ul DEPC water.

3) *In vitro* transcription:

Mix the following in the order indicated, at RT.

**Table 2-1 *In vitro* transcription for RNA probe synthesis.**

| Reagents | Amount |
|---|---|
| 5x transcription buffer | 5ul |
| 100mM DTT | 1.5ul |
| DIG 10x nucleotide mix (on ice) | 2.5ul |
| Fresh linearized plasmid (or PCR product) | 1ug (use less for PCR product) |
| DEPC-H2O | Up to the 23ul |
| Rnasin ribonuclease inhibitor(on ice) | 1ul |
| T7 polymerase(on ice) | 1ul |
| Total | 25ul |

4) Seal the tube and short spin; incubate at 37C waterbath, 2h.

5) Short spin, remove 1ul aliquot and run on 1% TAE gel to check synthesis. Expect to see RNA band 10 folds more intense than plasmid band, suggesting 10-15 ug probe synthesized.

6) Add 2 ul of RQ1 RNase-Free DNase I, seal the tube and short spin; incubate at 37C waterbath for 15min.

7) Add 50 ul DEPC-H2O, 25 ul 10M ammonium acetate and 200 ul 100% ethanol (-20C).

8) Mix and leave on dry ice for 30min, or at -80C overnight.

9) 13-15000rpm spin at 4C, 20min. Remove the supernatant carefully, leave the pellet.

10) Wash the pellet by adding 1ml 70% ethanol (-20C); 13-15000rpm spin at 4C, 5min. Remove the supernatant carefully, 13-15000rpm spin at 4C, 1min. Record the rough size for the pellet.

11) Use 10 ul tip to remove all the ethanol. Air dry pellet for about 5min until obvious traces of ethanol have evaporated. Do not over dry the pellet (don't let the pellet turn from white to transparent).

12) Re-dissolve pellet in 1 ml prehybe solution and store at -20C. Use 25-50 ul for *in situ* 1 ml prehybe solution.

### 2.12.5LIA Protocol: RNA *in situ* hybridization to *Drosophila* imaginal discs

#### 2.12.5.1 Notes

I adapted this *in situ* hybridization protocol from an *in situ* hybridization protocol of zebrafish embryo (learned from Macie Walker during my rotation at Paul Trainor Lab in 2009).

#### 2.12.5.2 Reagents

**Table 2-2 Prehybe solution recipe.**

| **Prehybe solution** | **100ml** |
|---|---|
| 50% formamide | 50ml of 100% |
| 5 x SSC | 25ml of 20 x |
| 1% SDS | 10ml of 10% |
| tRNA | 2ml of 12.5mg/ml |
| 50ug/ml heparin | 50ul of 50mg/ml |
| Citric acid to pH 5.5 | Around 5ml |
| DEPC water to final 100ml | |

Store at -20°C.

**Table 2-3 Hybe wash solution recipe.**

| Hybe wash | 100ml |
|---|---|
| 50% formamide | 50ml of 100% |
| 2 x SSC | 10ml of 20 x |
| 0.1% tween20 | 100ul of tween20 |
| Citric acid to pH 5.5 | Around 2ml |
| DEPC water to final 100ml | |

Store at -20°C.

**Table 2-4 NTMT development solution recipe.**

| NTMT | 50ml |
|---|---|
| 100mM NaCl | 5ml of 1M NaCl |
| 100mM Tris pH9.5 | 5ml of 1M Tris pH9.5 |
| 1% tween20 | 0.5ml of tween20 |
| 50mM $MgCl_2$(add at the last) | 5ml of 0.5M MgCl2 |
| DEPC water to final 50ml | |

Use freshly made solution each time. For a short period of time, store the solution at RT.

PBT and TBT have 1% Tween 20, prepare using 10x PBS or TBS.

Probes: Place 20ul dig probe rxn in 1ml prehybe solution and store @ -20C. Use 25-50ul of this diluted probe per 1ml prehyb for *in situ*.

### 2.12.5.3 Procedures

**Dissect, fix and store samples in methanol:**

1) Wandering third instar larvae were dissected in PBS (pH 7.4). Carcasses were quickly washed in PBS and then fixed in 2%PFA/PBS without rocking, 4C overnight.
2) Wash using PBS for 5min x 2 at RT, rocking.
3) Dehydrate samples through MEOH/PBT, RT:

4) 25%MEOH/PBT, 50%MEOH/PBT, 75%MEOH/PBT, 100%MEOH/PBT, 100%MEOH/PBT, 5min each, rocking, finally in100%MEOH/PBT, samples can be stored at -20C.

**First Day**

**Rehydrate samples and *in situ* hybridization (~5h):**

1) Prepare 37C water bath.(Turn it off after use)
2) Rehydrate samples through MEOH/PBT, RT:
3) 75%MEOH/PBT, 50%MEOH/PBT, 25%MEOH/PBT, PBT, 5min each, rocking.
4) PBT 5min x 2, rocking.
5) Postfix with 4%PFA/0.2%GA, 10min, RT, rocking.
6) PBT 5min x 3, rocking.
7) Equilibrate samples with 1:1 prehybe solution/PBT @ 37C, 5min.
8) Equilibrate samples with prehybe solution @ 37C, 5min.
9) Place samples in hyb oven and prehyb, 2h @ 65C, rocking.
10) Place probe in new tube with 1ml prehybe solution. Heat at 80C waterbath for 5min before adding. Hyb overnight @65C, rocking.

**Second Day**

**Wash and antibody incubation (~5h):**

1) Heatup the desire amount washing solution @ 65C and keep them there.
2) Wash using prehybe solution, 30min x 2 @65C, rocking.
3) Wash using hybe wash, 30min x 3 @65C, rocking.
4) Wash using TBT, 5min x 3 @ RT, rocking.
5) Block with 10% hi-LS/TBT, 2h @RT, rocking.
6) Incubate samples with antibody (anti dig-antibody 1:5000/block solution) @ 4C, overnight, rocking.

**Third Day**

**Wash and development (~1d):**

1) Wash using TBT, 30min x 8 @RT, rocking.
2) Remove the last TBT wash as much as possible, wash samples with fresh made NTMT, 5min x 2.
3) This step is light sensitive. Develop with NBT/BCIP in NTMT @ RT until desired color intensity (can be a few mins to overnight). 50ul NBT and 25ul BCIP per 10ml NTMT. (Can stop half earlier, the other half later.)
4) Quick rinse with ddH2O, then PBT.
5) 4% PFA/PBS, 1h @ RT or 4C overnight.
6) When ready to take pictures, wash samples in PBT, 5min x 3 @ RT, rocking.
7) Put samples in glycerol gradient: 25%, 50%, 75% @RT, rocking.
8) Mount samples in 75% glycerol and take pictures on slide with or without spacer.

# Results

## 3.1 Global analysis of cell cycle-associated transcription

### 3.1.1 FACS-microarray analysis of wing discs and S2 cells

To define the global cell cycle-associated transcriptional profile in the developing wing, I first developed a physical and enzymatic disruption protocol to more rapidly dissociate whole discs into a suspension of single cells. Introducing physical disruption to the conventional enzymatic protocol for wing disc dissociation (Neufeld *et al.*, 1998) largely improved the dissociation efficiency. More importantly, adding a step to stop the enzymatic reaction and subsequently removing the enzyme from the dissociated cell system enhanced the yield of live cells. As a result, compared with the conventional 2-4 hour-long enzymatic protocol, the new method recovered approximately three times more live cells (about 11,000 isolated live cells per wing disc, based on the negative trypan blue-staining signal) within a shorter time (20 minutes compared with 120 minutes).

Using this approach, dissociated live wing disc cells were stained for DNA content and then sorted into G1 and G2/M populations by FACS using a robust gating strategy (Figure 3-1). To compare cell cycle-associated transcription in the wing epithelium with that observed in cell culture, I performed a parallel series of FACS experiments in cultured *Drosophila* S2 cells (Figure 3-1). Based on an assumption that cells in both G1 and G2/M phases are normally distributed, I made a simple cell cycle distribution model for each cell type. Robust gating was applied each time based on the cell cycle models. Technically, before each sorting, people who run the cytometer (Jeff Haug, Ruihong Zhu and I) start with running a small amount of the sample to get the peak positions of G1 and G2/M populations. Next, peak position values from the Hoechst Blue Int. channel were put into excel tables that I made based on the cell cycle models. Finally, gating positions for both G1 and G2/M were auto-calculated in the excel sheet and used for setting up the gates for cell sorting.

More specifically, if we set G1 peak to x and G2 peak position to y, we used:

for wing disc cells, G1 gate ended at position: $x + \frac{1}{5}(y - x)$;

G2 gate started at position: $y - \frac{9}{20}(y - x)$

for S2 cells, G1 gate ended at position: $x + \frac{1}{6}(y - x)$;

G2 gate started at position: $y - \frac{58}{147}(y - x)$.

To validate the gating strategy and the system stability, post-sorts were performed before and after the cell sorting for all the FACS experiments. As a result, we consistently observed a clear separation of the G1 and G2/M populations, confirming my technical approach. Indeed, by comparing the sorted cells from different cell cycle phases, we also observed increased forward scatter and side scatter in the G2/M population compared with G1. Forward scatter is roughly correlated with cell size and cell structure or composition, and it has been used as a measurement of cell size (Neufeld *et al.*, 1998). This result confirmed that for both wing disc and S2 cells, there is a continuous cell growth in average size corresponding with cell cycle progression (Figure 3-1).

From the sorted G1 and G2/M populations, I extracted total RNA, followed by a bioanalyzer analysis to examine RNA quality and quantity. RNA samples were then subjected to SIMR molecular biology core facility for microarray analysis. Three biological replicates were examined for each condition, and evaluated using a moderated t-statistic (Smyth, 2004) (done by Chris Seidel) to define the most significant periodic genes in both wing discs and S2 cells (Figure 3-2, adjusted p value $< 0.05$).

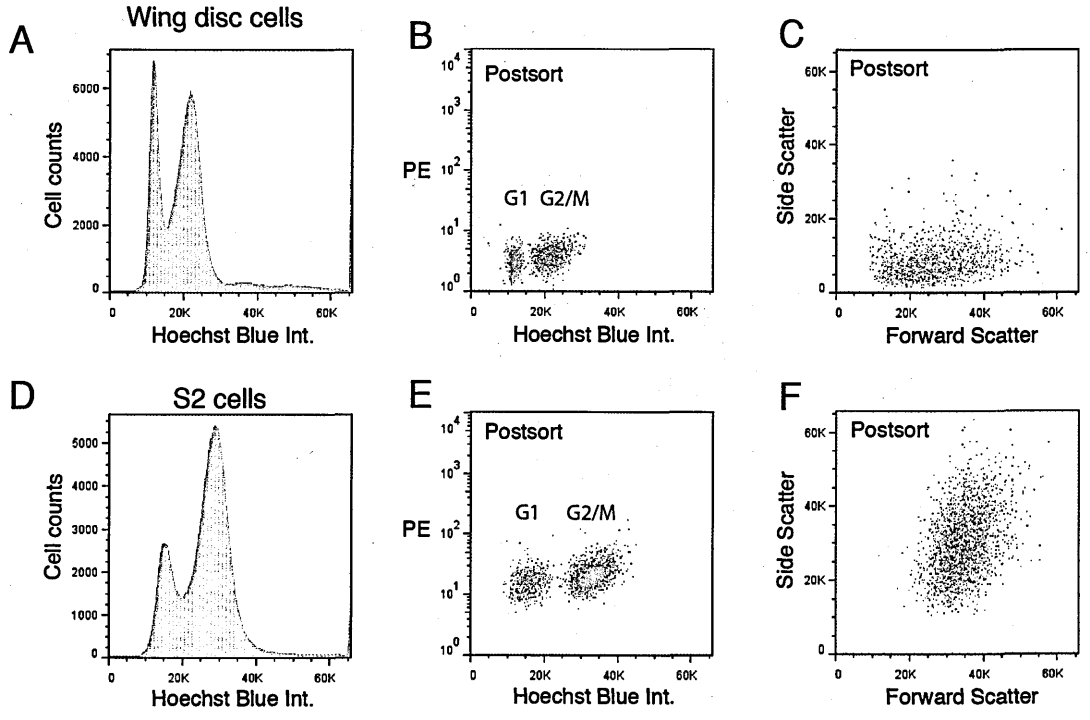


**Figure 3-1 Fluorescent-Activated Cell Sorting (FACS) of *Drosophila* wing disc cells and S2 cells.**

(A) Cell cycle profile from flow cytometry data of dissociated wing disc cells. (B-C) Postsort of wing disc cells.

(B) The cell cycle phases of sorted wing disc cells were confirmed by postsort, showing a clear separation of the sorted G1 (green) and G2/M (red) cell populations from the Hoechst Blue Integral (Int.) channel. Signal of PE (Phycoerythrin) channel is recorded from a detector with a 585 nm band-pass filter.

(C) We observed increased forward scatter and side scatter in the G2/M population, corresponding to an increased average cell size.

(D) Cell cycle profile from flow cytometry data of S2 cells. Note that S2 cells have a relatively longer G2/M phase compared with wing disc cells.

(E-F) Postsort of S2 cells. Sorted G1 and G2/M populations had a clear separation and G2/M cells also had a larger average cell size.

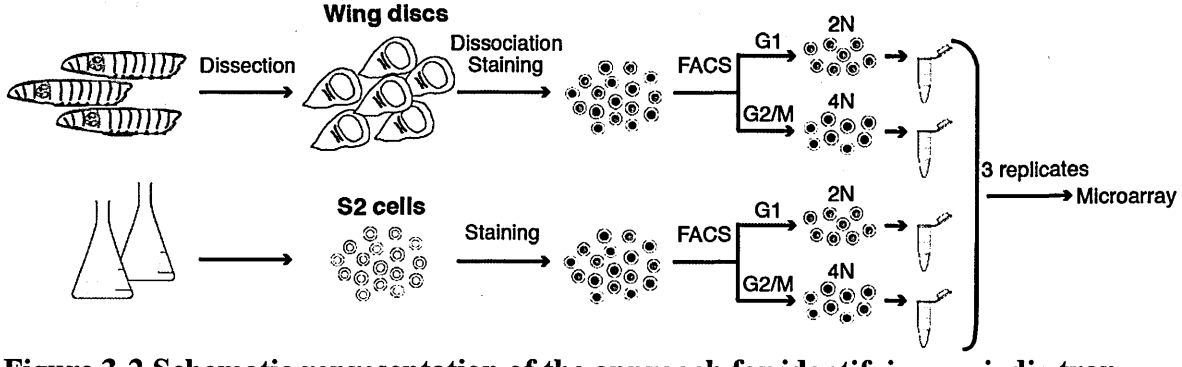


**Figure 3-2 Schematic representation of the approach for identifying periodic transcriptome in *Drosophila* wing disc epithelial cells and S2 cells.**

Integrative FACS-microarray analysis was performed for identifying cell-cycle phase dependent transcription in wing disc epithelial cells and S2 cells.

### 3.1.2 Classification of periodic genes in wing discs and S2 cells

Based on the statistical analysis described above, we identified over 700 cell cycle-associated genes in wing discs and over 600 in S2 cells (Figure 3-3).

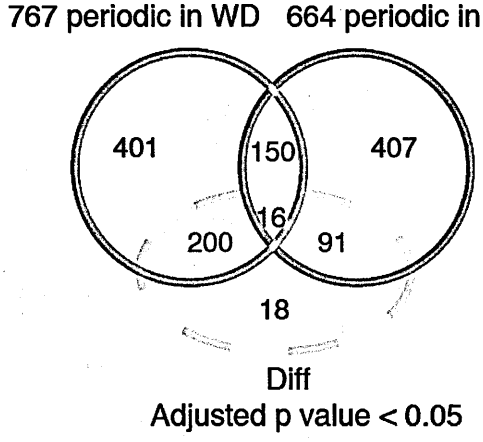


**Figure 3-3 Periodic transcripts identified by microarray.**
Venn diagram illustrating sets of periodic transcripts in wing discs (WD) and S2 cells (S2), as well as the most differentially expressed genes (Diff) based on t-statistics with a Benjamini-Hochberg adjusted p value of 0.05. These sets included 200 genes (WD specific) that were periodic exclusively in the wing disc cells and 91 (S2 specific) that were periodic only in S2 cells. The intersection of the WD and S2 sets included 150 genes with similar patterns of periodic expression in both cell types (Common), as well as 16 genes displaying opposite periodic behaviors (Opposite). For simplicity, the Opposite gene group was manually segregated from the Common category.

The intersection of these sets included 150 genes with similar patterns of periodic expression in both cell types (defined as Common genes in Figure 3-3, 3-4, 3-5, and Table S1).

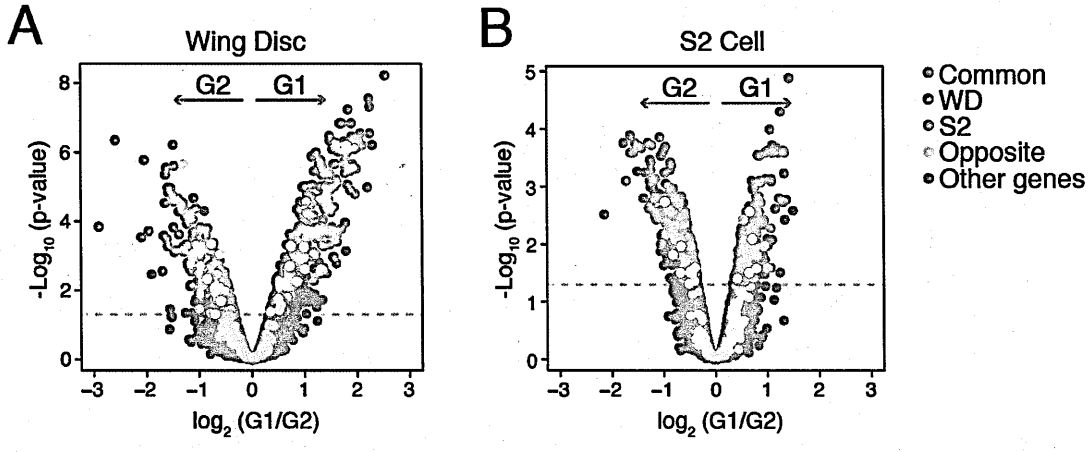


**Figure 3-4 Volcano plots of gene expression analysis for OreR wing disc cells and S2 cells.**
The dashed grey line indicates the adjusted p-value cutoff of 0.05 used to define significant gene sets. Genes with specific behaviors across data sets are divided into classes and highlighted in color.

Intriguingly, 200 genes were periodic exclusively in wing disc cells, and 91 were periodic only in S2 cells (defined as Wing Disc Specific and S2 Specific in Figure 3-3, 3-4, 3-5, and Table S1). Furthermore, 16 genes displayed opposing periodic behavior between the two cell types (defined as Opposite; Figure 3-3, 3-4, 3-5, and Table S1).

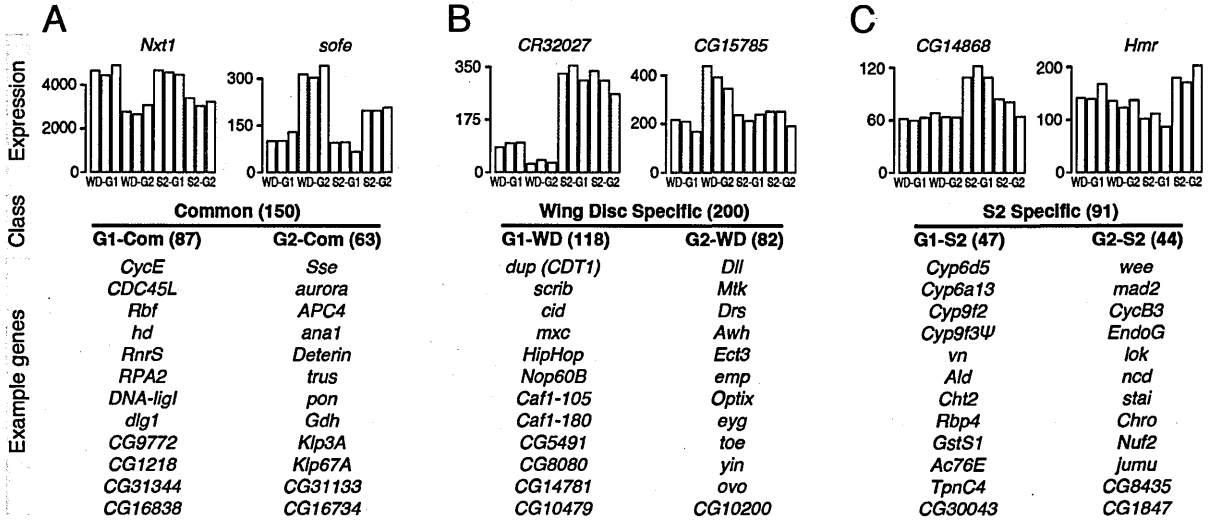


**Figure 3-5 Categorization of periodic transcripts into six main classes.**
Representative expression data and example genes are shown for the G1 and G2 Common (A), Wing Disc Specific (B), and S2 Specific classes (C). The numbers of transcripts in each class are listed in parentheses.

The observed variability between periodic transcription in wing discs and S2 cells is not likely to represent experimental noise, since we found a strong correlation in global periodic gene expression between control wing disc samples from two different laboratory strains, *OreR* and $w^{1118}$ (Figure 3-6; Pearson Correlation = 0.909). In this case, only 19 probe sets (among 18,952 analyzed) exhibited a significant difference in periodic expression between the two strains (Table S2).

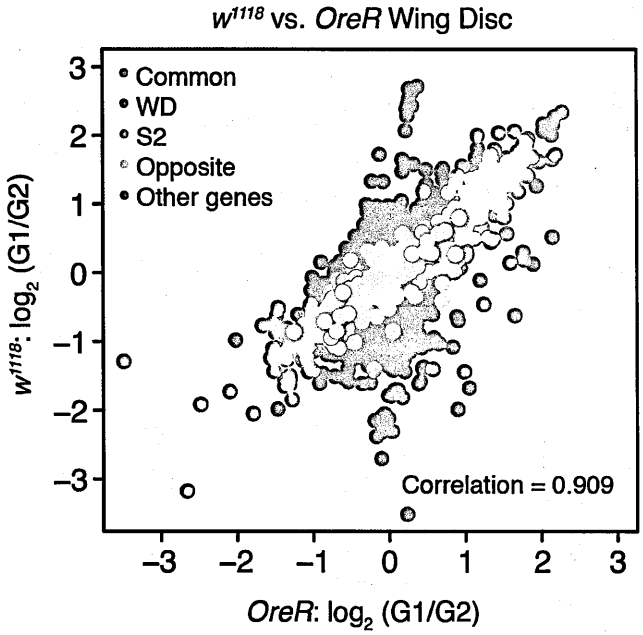


**Figure 3-6 Comparison between periodic gene expression in two different genetic backgrounds: OreR and $w^{1118}$.**
The periodic genes identified in OreR wing discs and S2 cells are highlighted in color. The Pearson correlation for the colored genes between the two experiments was measured at 0.909 as indicated.

### 3.1.3 Validation of periodic expression *in vivo*

To validate periodic expression *in vivo*, I selected a set of 24 genes that included both cell cycle genes (e.g., *pcna*, *Cdc6*, and *Borr*), as well as novel periodic genes (e.g., *CG1218* and *CG10200*) and examined their expression in the eye imaginal disc. I utilized the spatial pattern of the cell cycle regulation in the eye imaginal disc to validate the periodic expression *in vivo*. In the late third instar larva stage, the eye disc includes a morphogenetic furrow (MF, Figure 3-26) that sweeps from posterior to anterior of the eye discs, producing a stripe of disc cells arrested in G1. Posterior to the MF, a group of cells reenter the cell cycle in a second mitotic wave, which leads to stripes of cells in distinct cell cycle phases of S and M (Baker, 2001). By examining the RNA expression pattern in the eye disc using *in situ* hybridization, 22/24 genes exhibited cell-cycle associated expression (Figure 3-7 and Figure 3-8) relative to the stripe of G1 arrested cells in the morphogenetic furrow.

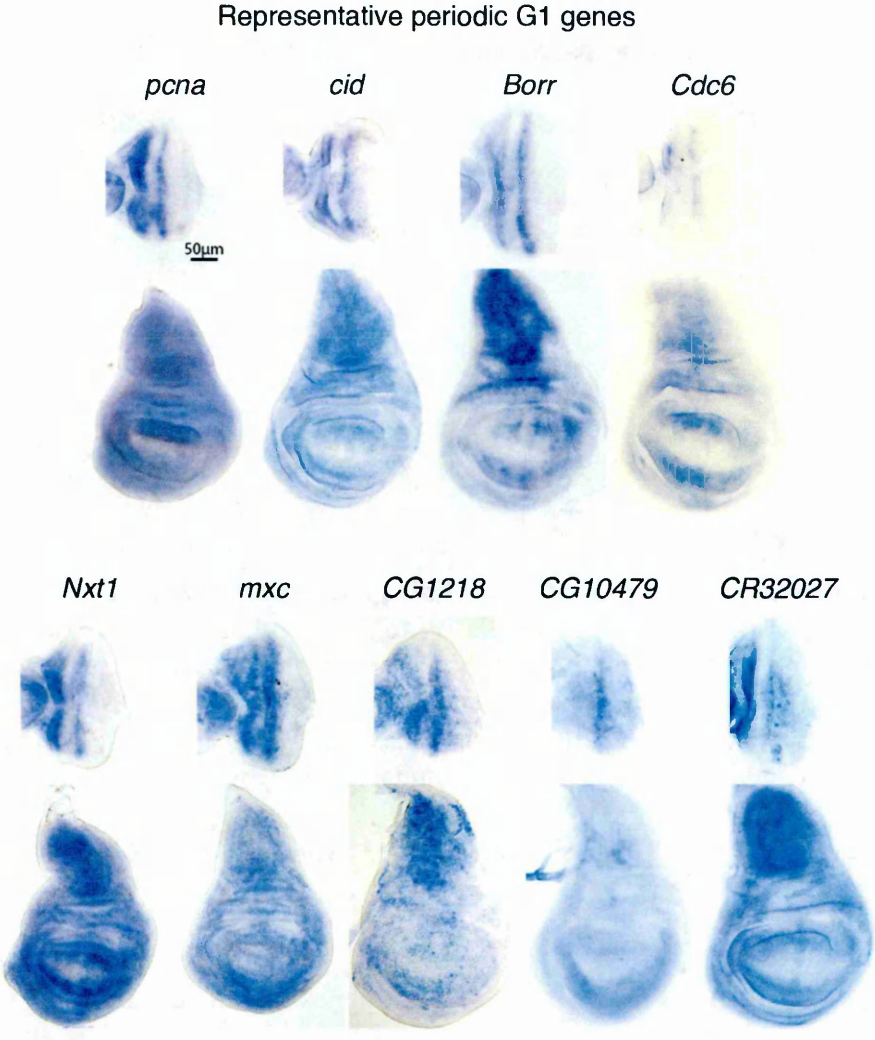


**Figure 3-7 Examples of validated G1 periodic gene expression *in vivo*.**
Cell cycle phase-associated expression relative to the morphogenetic furrow was confirmed for 22 genes by *in situ* hybridization in developing eye discs (the top image for each gene). These genes also exhibited heterogeneous expression in wing discs (the bottom image for each gene). Other genes confirmed but not shown: *CDC45L*, *Pole2*, *asf1*, *Caf1-180*, *Caf1-105*, *scrib*, *Flo-2*, *CG5491*, *CG4951*. Scale bar: 50μm.

Most of the periodic genes we analyzed were expressed broadly in the wing disc (Figure 3-7 and Figure 3-8). However, *CG10200* showed specific expression pattern in the wing disc. It expressed predominantly in the peripodial membrane, and in two stripes of cells in the wing pouch at anterior-posterior compartment boundary adjacent to the dorsal-ventral boundary, related with Hh signaling (Figure 3-8).

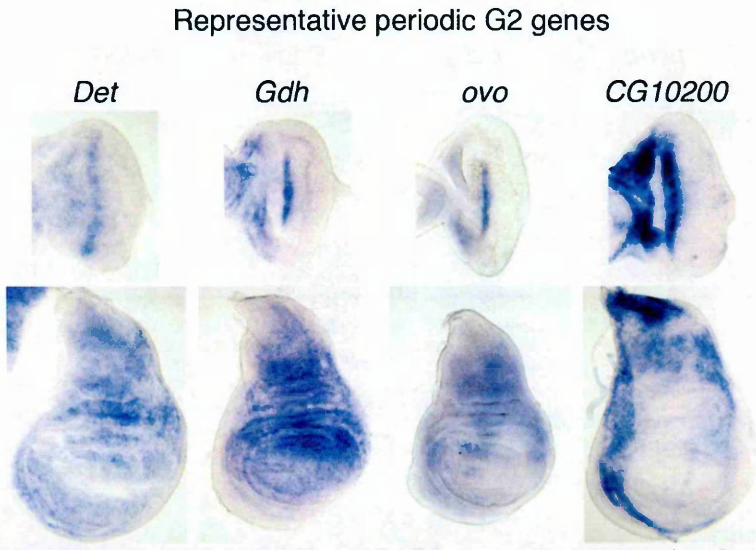


**Figure 3-8 Examples of validated G2 periodic gene expression *in vivo*.**
Cell cycle phase-associated expression relative to the morphogenetic furrow was confirmed for 22 genes by *in situ* hybridization in developing eye discs (the top image for each gene). These genes also exhibited heterogeneous expression in wing discs (the bottom image for each gene), except *CG10200* showing enriched expression in the peripodial membrane and two stripes at anterior-posterior boundary of the disc proper.

Additionally, one G1 gene showed elevated expression in myoblasts (*Sox100B*) and one G2 gene (*CG3168*) showed enriched expression in neural lineages (Figure 3-9). Together, these results identify a core set of periodic genes shared between wing disc and S2 cells, demonstrate the robustness of periodic transcription in the wing disc, and reveal substantial differences in periodic gene expression between different cellular contexts.

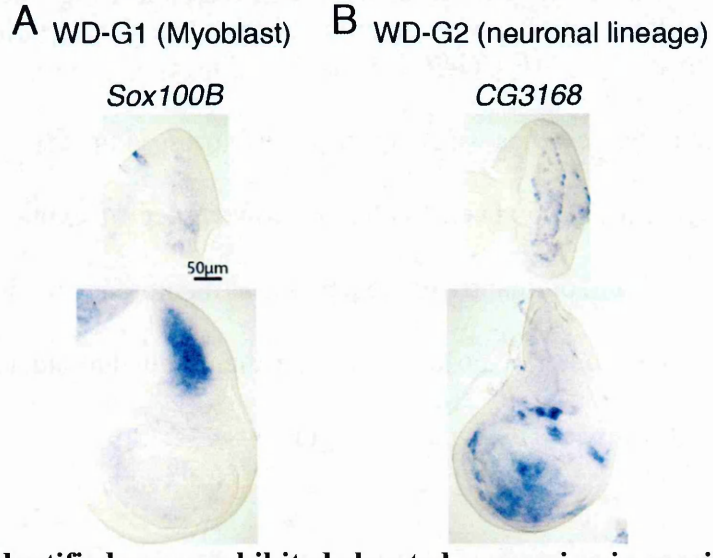


**Figure 3-9 Two identified genes exhibited elevated expression in specific cell types of the developing wing disc.**
(A) *Sox100B* exhibited enriched expression in myoblasts of the wing disc (the bottom image).
(B) *CG3168* exhibited enriched expression in neural lineages of the wing disc (the bottom image). Both exhibited little expression in the eye discs (the top images). Scale bar: 50μm.

## 3.2 The context-dependence of cell cycle-associated gene expression

### 3.2.1 The global pattern of cyclic transcription: pathway analysis

To gain a global perspective on functional implications of cell cycle-entrained transcription, I first used a Kyoto Encyclopedia of Genes and Genomes (KEGG) pathway analysis to identify molecular processes enriched in either G1 or G2. As expected, G1 transcripts were enriched for factors likely to be specifically required in S phase, including proteins involved in DNA replication, pyrimidine and purine metabolism, DNA repair, and homologous recombination. Interestingly, we also found RNA transport factors to be enriched in G1, including many genes encoding components of the nuclear pore complex (NPC), a few genes encoding components of nuclear export complex, and genes functioning in RNA processing. The increased expression of NPC components in G1 may correlate with the increasing area of the nuclear envelop and NPC in G1 phase (Winey *et al.*, 1997), while the elevated expression of RNA transport components in G1 may also prepare the cells for an efficient nuclear import and export during cell division or interphase (Gavet and Pines, 2010a).

While progression through the G1 phase involves a strict regime of transcriptional control in preparation for S phase (Duronio and O'Farrell, 1995; Dyson, 1998; Johnson *et al.*, 1993), there is little precedent for a generalized transcriptional program coordinating events in G2. Consistent with this, a scan for enriched regulatory sequences 2000 kb upstream of G1 genes identified E2F binding sites *de novo* (computational analysis done by Alexander Garruss), while no clear consensus elements were enriched in G2 genes (Figure 3-10). Based on the KEGG pathway analysis, genes with elevated expression in G2 were enriched for the pathways of endocytosis, ubiquitin-mediated proteolysis, protein processing in the ER, lipid metabolism (glycerophospholipid, sphingolipid and glycerolipid) and Wnt signaling. We note that aside from Wnt signaling, these pathways fall into the

general category of protein and lipid recycling, which suggests a lipid turnover during mitotic processes (e.g., cytokinesis) in wing discs. Less predictably, periodically-expresssing G2 genes were also enriched for the three branches of the Wnt signaling pathway: canonical, planar cell polarity (PCP), and Wnt/$Ca^{2+}$. These periodic genes include many of the known receptors, ligands and downstream genes of the Wnt signaling pathway, indicating that Wnt signaling might predominant function during G2/M phase. Indeed, it has previously been shown that canonical Wnt signaling peaks at G2/M, mediated by G2/M Cyclin-dependent phosphorylation of Wnt receptor LRP5/6 (Davidson *et al.*, 2009).

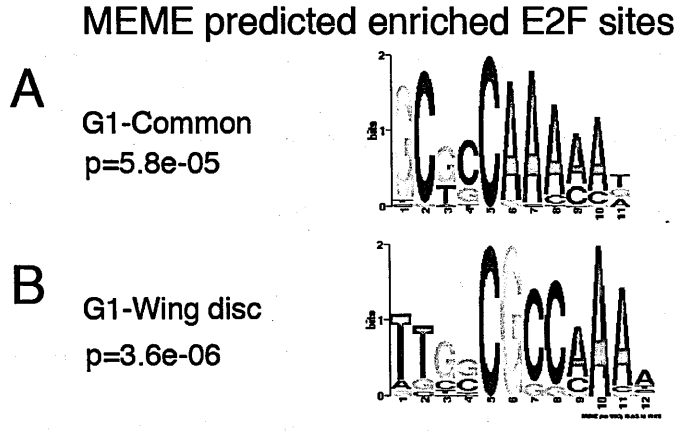


**Figure 3-10 Consensus E2F binding motifs that were enriched in the upstream regions of G1-Com and G1-WD specific genes.**

### 3.2.2 The global pattern of cyclic transcription: gene ontogeny categorization

Additional to KEGG analysis, Chris and I applied gene ontology (GO) analysis to the periodic genes from six main categories (Figure 3-5, and Table S1). GO analysis showed each of these categories to be enriched for distinct biological processes (Figure 3-11). As expected, G1 genes with similar expression profiles in wing discs and S2 cells (G1-Com) were enriched for DNA replication. Likewise, G2 genes exhibiting similar regulation in both cell types (G2-Com) were enriched for functions in mitosis.

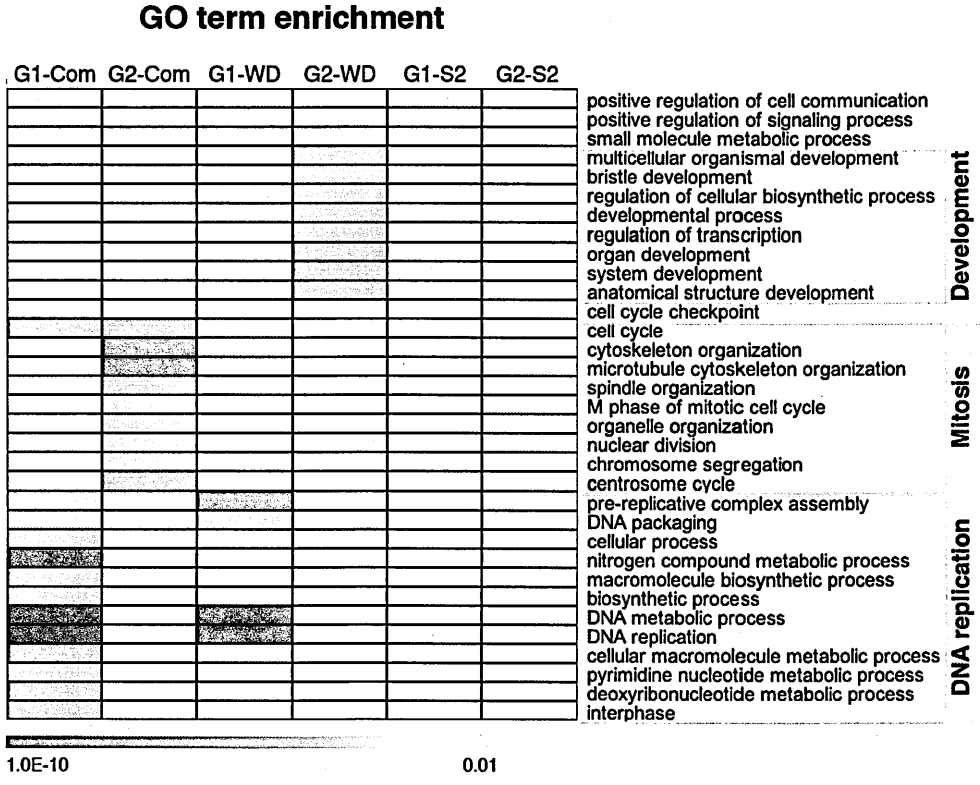


**Figure 3-11 Gene ontology category enrichment for the periodic gene classes.** The grey boxes on the right indicate the Development, Mitosis and DNA replication-related GO categories.

### 3.2.3 The plasticity of periodic gene expression: DNA replication

Unexpectedly, several core elements of the DNA replication machinery exhibited elevated G1 expression only in wing disc cells (G1-WD). These included *Orc1-Orc3*, *Mcm2-Mcm5*, and *dup (Cdt1)* of the pre-replication complex (pre-RC), and *Sld5* of the GINS complex (Figure 3-12 and Figure 3-13).

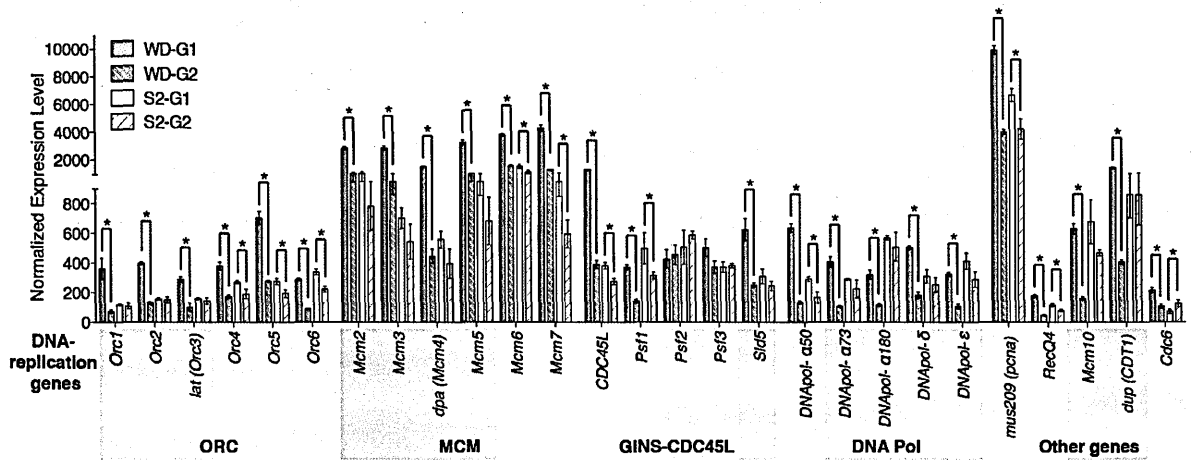


**Figure 3-12 Normalized expression levels of individual DNA replication genes by microarray.**

Values are the mean (±SD) of 3 biological replicates. The asterisks indicate statistical significance of periodic expression by t-statistics with a Benjamini-Hochberg adjusted p value $< 0.05$. The colors under the gene names at the bottom correlate with the colors in Figure 3-13. Note that the Normalized Expression Level scale is not linear.

Furthermore, CDC6, another component of the pre-RC (Cocker *et al.*, 1996), was one of the 16 genes exhibiting opposing patterns of periodic transcription between wing disc and S2 cells (Figure 3-12, Figure 3-13 and Table S1). This result is particularly interesting since CDC6 plays an essential role in the initiation of DNA synthesis by loading MCM proteins onto chromatin (Coleman *et al.*, 1996; Donovan *et al.*, 1997). In budding yeast, this process requires *de novo* synthesis of CDC6, consistent with its peak expression near the G1/S transition (Donovan *et al.*, 1997; Zhou and Jong, 1990). Consistent with the importance of its temporal regulation, ectopic *CDC6* causes an M phase delay in fission and budding yeast (Boronat and Campbell, 2007; Bueno and Russell, 1992), and induces EMT-like changes in mouse and human epithelial cell lines (Sideridou *et al.*, 2011).

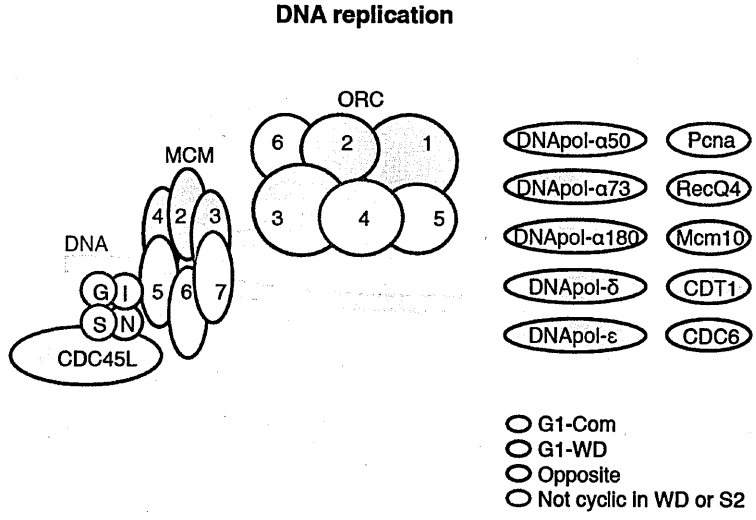


**Figure 3-13 Context-specific periodic transcription of genes involved in DNA replication.**
Note that Orc1-Orc3 and Mcm2-Mcm5 were significantly periodic only in wing disc cells (dark blue).

On a more general level, it is unclear why key elements of the DNA replication machinery would exhibit different periodic expression profiles in wing disc versus S2 cells, since most of these genes are known E2F targets (Dimova *et al.*, 2003). Further, computational analysis of regulatory regions from both common and wing disc-specific G1 genes revealed significant enrichment for the consensus motifs recognized by E2F (Figure 3-10). These results suggest that there may be context-dependent transcriptional regulation of cell cycle factors targeted by E2F (e.g., DNA replication factors). Whether this context-dependent activity is controlled through distinctive E2F binding sites (e.g., Figure 3-10) remains unclear.

### 3.2.4 The plasticity of periodic gene expression: mitosis

The differences between the periodic transcriptomes of wing disc and S2 cells were not limited to G1 genes. Many known mitotic genes exhibited elevated G2 expression only in S2 cells (Figure 3-14 and Figure 3-15). These include *pim* (encoding *Drosophila* Securin), *wee* (encoding *Drosophila* Wee1 kinase), *CycB3*, as well as the checkpoint protein encoding genes *lok* (homolog with human CHEK2) and *mad2*.

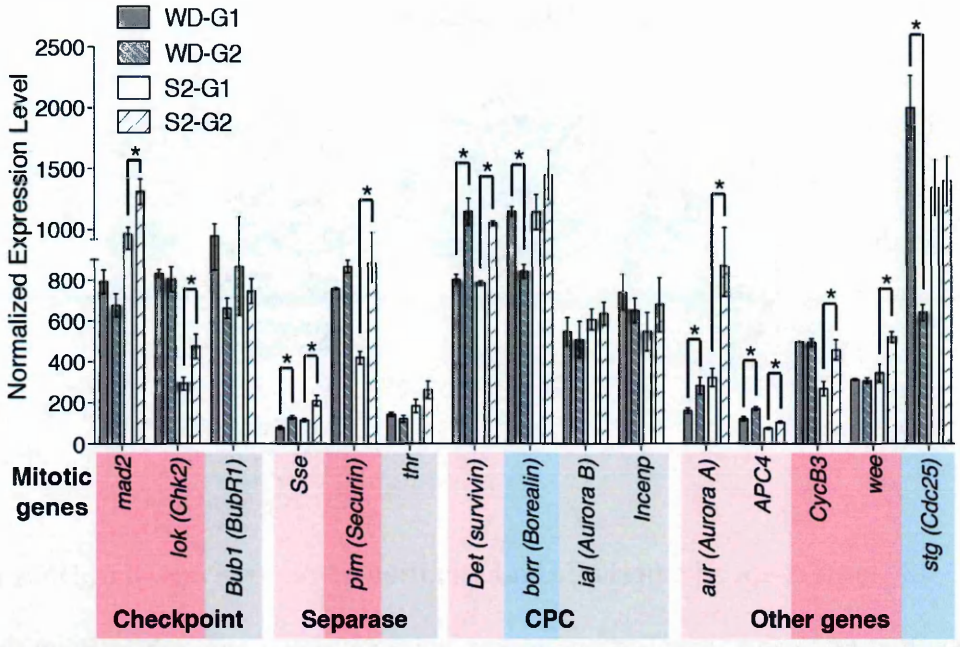


**Figure 3-14 Normalized gene expression level of individual genes involved in mitosis.** Values are the mean (±SD) of 3 biological replicates from the microarray. The asterisks indicate statistical significance of periodic expression by t-statistics with a Benjamini-Hochberg adjusted p value < 0.05. The colors under the gene names at the bottom correlate with the colors in Figure 3-15. Note that the Normalized Expression Level scale is not linear.

In addition, a few genes with known functions in mitosis exhibited higher G1 expression only in the wing-disc, such as *string* (*Drosophila* CDC25), *cid* and *Borr* (*boreal-in-related*) (Figure 3-14, Figure 3-15, and Figure 3-7). This suggests that some genes are transcribed before their protein function is required, or they may have unexplored functions outside of G2/M in wing disc cells.

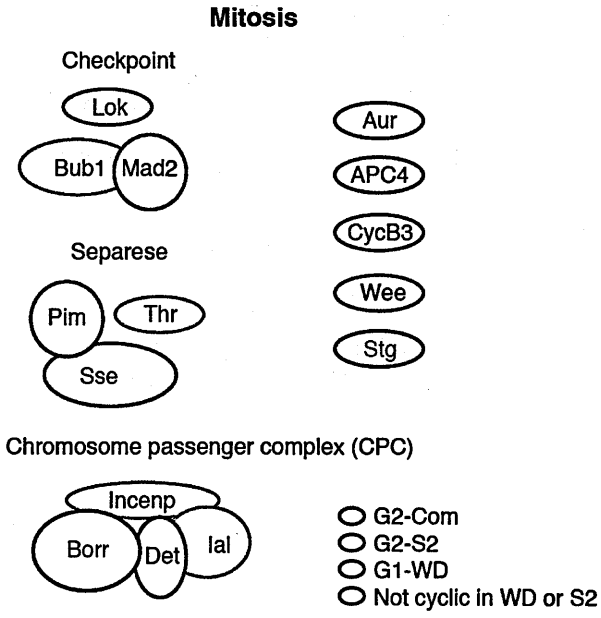


**Figure 3-15 Model of the context-specific periodic transcription of genes involved in mitosis.**
The color of each component correlates with the colors in Figure 3-14.

Taken in sum, my transcriptional profiling experiments revealed an unexpected degree of context-dependence in cell cycle-associated transcription, even for genes encoding core components of the DNA replication machinery and the mitotic apparatus. Additionally, these experiments allowed us to define the core periodic transcriptome of proliferating epithelial cells *in vivo*. Many of the periodic genes we identified were uncharacterized or not thought to play a role in cell proliferation. I therefore systematically disrupted these genes to determine their functions *in vivo*. Detailed results of the transcriptional profiling and phenotypic experiments can be accessed through the searchable online database at http://odr.stowers.org/FlyCycle.

## 3.3 Functional identification of periodic genes required for wing development

### 3.3.1 Examining the function of periodic genes in wing development through tissue-specific RNAi knockdown

To circumvent the limitations of whole-animal mutant analysis, I used tissue-specific RNAi to interrogate requirements for genes from the Common, WD-specific, and

Opposite classes during wing development. I obtained transgenic RNAi lines from the Vienna *Drosophila* RNAi Center (VDRC) P-Element RNAi Library and screened 461 RNAi lines targeting 311 genes (multiple lines from the GD library were tested whenever possible; Table S3). To identify the subset of periodic genes that functionally contribute to growth of the wing, male flies carrying each *UAS-RNAi* construct were crossed to females of the genotype: *Bx-GAL4; UAS-dicer2* (Figure 3-16). Bx-GAL4 was selected for the RNAi screen because of its wing-specific expression as well as its relative stronger knockdown effects compared with other wing disc drivers (such as nubbin-GAL4, compared in a pilot experiment using selected RNAi lines; data not shown).

### 3.3.2 Enrichment of developmental function among wing disc periodic genes

For each cross, we scored for adult viability and wing phenotypes using specific terms (described in Table S3). When there were multiple RNAi constructs available for a single gene, the relevant phenotypes were quantified and averaged (Table S4 and Figure 3-17). In sum, almost 80% of all genes tested were required for normal wing development (244/311; Figure 3-16 and Table S4), suggesting a significant enrichment of developmental function among wing disc periodic genes (compared with 32/66 S2-specific periodic genes, Table S5, and 35/67 random genes required for wing development, Table S6; p value < 0.005 by Fisher's exact test).

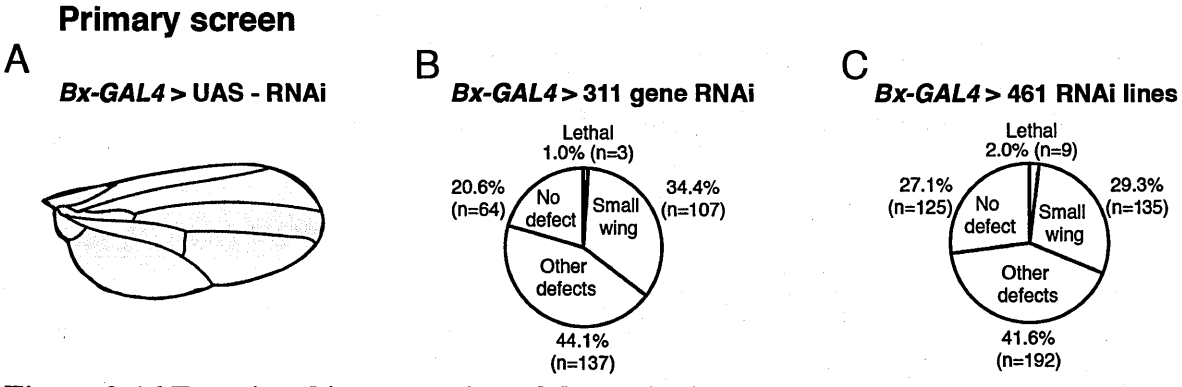


**Figure 3-16 Functional interrogation of the periodic transcriptome in the developing *Drosophila* wing.**
(A) *Bx-GAL4* drives gene knockdown predominantly in the wing pouch area that gives rise to the adult *Drosophila* wing.
(B) Phenotypic distribution of 311 periodic genes identified through transcriptional profiling.

(C) Summary of adult wing phenotypes for 461 VDRC RNAi lines corresponding to periodically expressed genes.

### 3.3.3 RNAi screen defined putative loss-of-function phenotypes for 244 periodically expressed genes, many of which were growth defects

Among these, 107 gene knockdowns led to a small wing phenotype, representing a strong growth defect. In addition, 137 produced other morphological defects such as curly, canoe-shaped, blistered or notched wings (Table S4 and Figure 3-17).

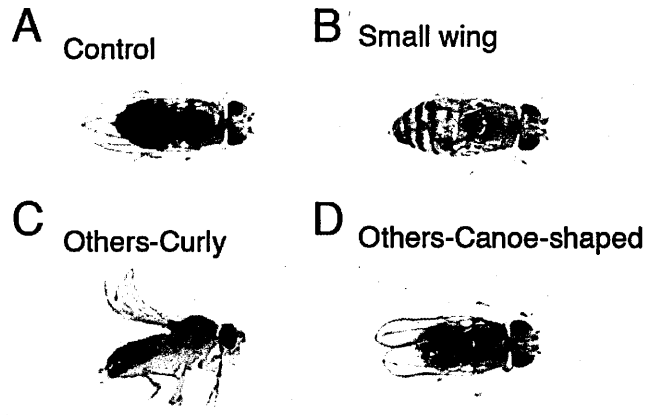


**Figure 3-17 Representative adult wing phenotypes from the RNAi screen.**
(A) A control adult fly with normal wings.
(B) Small wing phenotype represents a strong growth defect. (C-D) Other phenotypes include curly and canoe-shaped wing, which may reflect imbalanced growth of the dorsal and ventral sides of the wing blade.

The curly and canoe-shaped wing phenotypes may reflect imbalanced growth of dorsal and ventral sides of the wing blade due to the stronger dorsal expression of *Bx-GAL4* (Figure 3-17 and Figure 3-18).

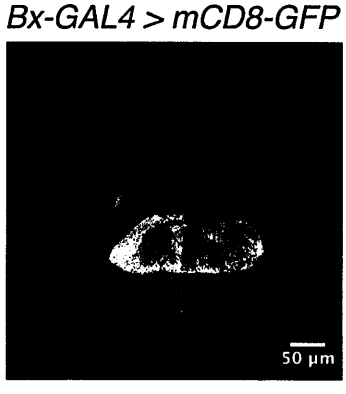


**Figure 3-18 RNAi knockdown region in the primary screen.**
*Bx-GAL4; UAS-dicer2 > mCD8-GFP* expression domain (*green*) in the third instar wing disc. Note the elevated dorsal expression in the wing pouch (compared with the uniform wing pouch expression of *nub-GAL4*; Figure 3-28). Scale bar: 50µm.

This initial screen defined putative loss-of-function phenotypes for 244 periodically expressed genes, many of which were growth defects. Hypothetically, these genes could directly control cell cycle progression, but might also indirectly affect growth by regulating related processes. Thus, I next tested the cellular basis for the observed wing defects using both cytometric analysis of DNA content as well as direct confocal imaging.

## 3.4 Identification of periodic genes required for cell cycle progression *in vivo*

### 3.4.1 Examining the function of periodic genes in cell cycle progression by flow cytometry

To determine which periodic genes were required for wing development through effects on cell cycle progression, I analyzed the phenotypes of RNAi knockdown cells by flow cytometry. For these experiments, I knocked down each gene in GFP-labeled cells of the posterior compartment of the wing disc using flies of the genotype: *UAS-dicer2; engrailed-GAL4, UAS-EGFP*. For each analysis, the corresponding GFP-negative anterior compartment cells were used as an internal control (Figure 3-19). Jeff and Ruihong at the SIMR cytometry core help me with running the samples.

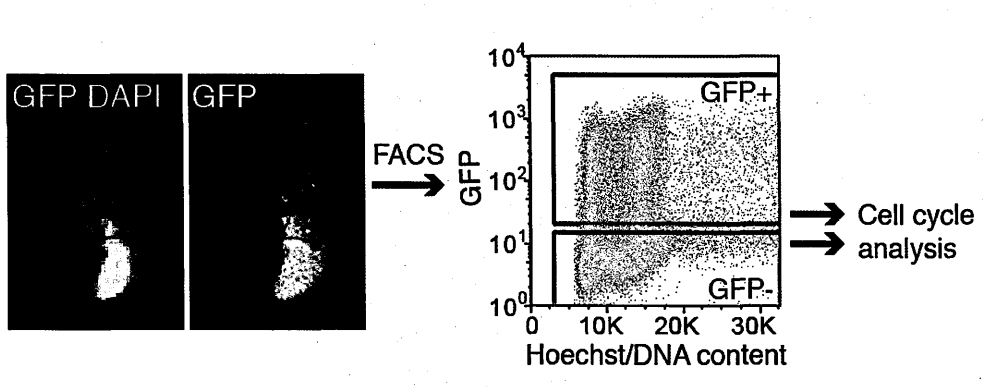


**Figure 3-19 Strategy of the cell cycle analysis in GFP-labeled posterior compartment cells by flow cytometry.**
Wing disc cells were dissociated and stained by Hoechst and 7AAD. GFP+ and GFP- populations were separately analyzed for cell cycle phasing using FlowJo and Modfit softwares.

In total, 156 RNAi lines were tested, representing 133 genes that produced wing defects in the primary RNAi screen (Figure 3-20). Among these, RNAi knockdown for 13 genes could not be analyzed owing to early lethality or severely reduced wing disc sizes (Figure 3-20). Flow cytometry data for the other 120 genes (138 lines) was analyzed for defects in cell proliferation and cell cycle phasing (Figure 3-20, Table S7, Table S8, and http://odr.stowers.org/FlyCycle).

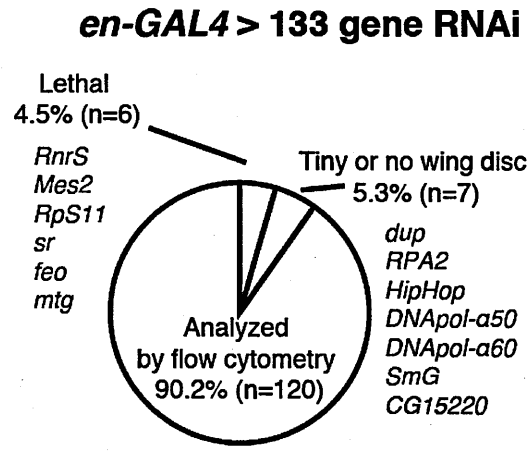


**Figure 3-20 Phenotypic distribution following en-GAL4 > UAS-RNAi knockdown of 133 periodic genes.**
We were only able to analyze 120 of these by flow cytometry. G1 genes are in blue text, G2 genes are in red.

### 3.4.2 Identification of periodic genes regulating cell proliferation and cell cycle phasing

Using the quantitative analysis of DNA content and cell numbers in the individual dsRNA knockdowns, I next clustered the lines according to phenotypic categories (Figure 3-22A). Knockdown of 36 genes produced a highly significant reduction in GFP+ cell numbers relative to GFP- controls (Proliferation defects (> 3 SD); Figure 3-21, Figure 3-22A, and Table S7).

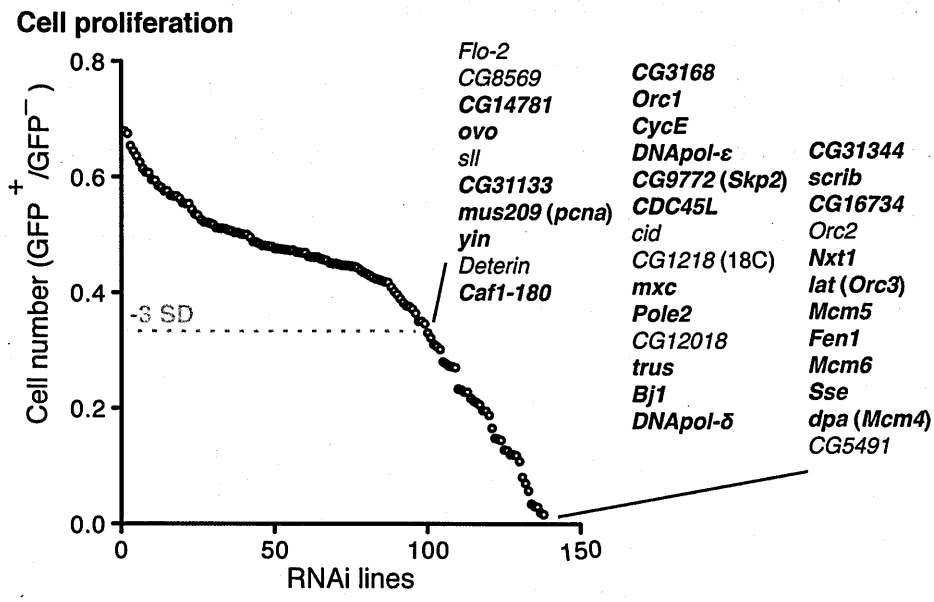


**Figure 3-21 Scatter plots of screened RNAi lines for cell proliferation defects as measured by cytometry.**
Genes with significant defects in cell numbers after RNAi knockdown are listed. Colored gene names indicate the expression phase of the targeted genes: *blue*- G1, *red*- G2/M. Genes in bold font also produced cell cycle phasing defects after knockdown. The dashed grey lines indicate a cutoff of Mean -3 SD calculated from the control.

Compared with cell cycle phasing in the cognate $GFP^-$ internal controls, 27 of these knockdowns also caused highly significant changes in the distribution of cells in G1, S and G2/M phases (Increased G1, Increased S, Increased G2/M (> 3 SD); Figure 3-22 and Table 3-1).

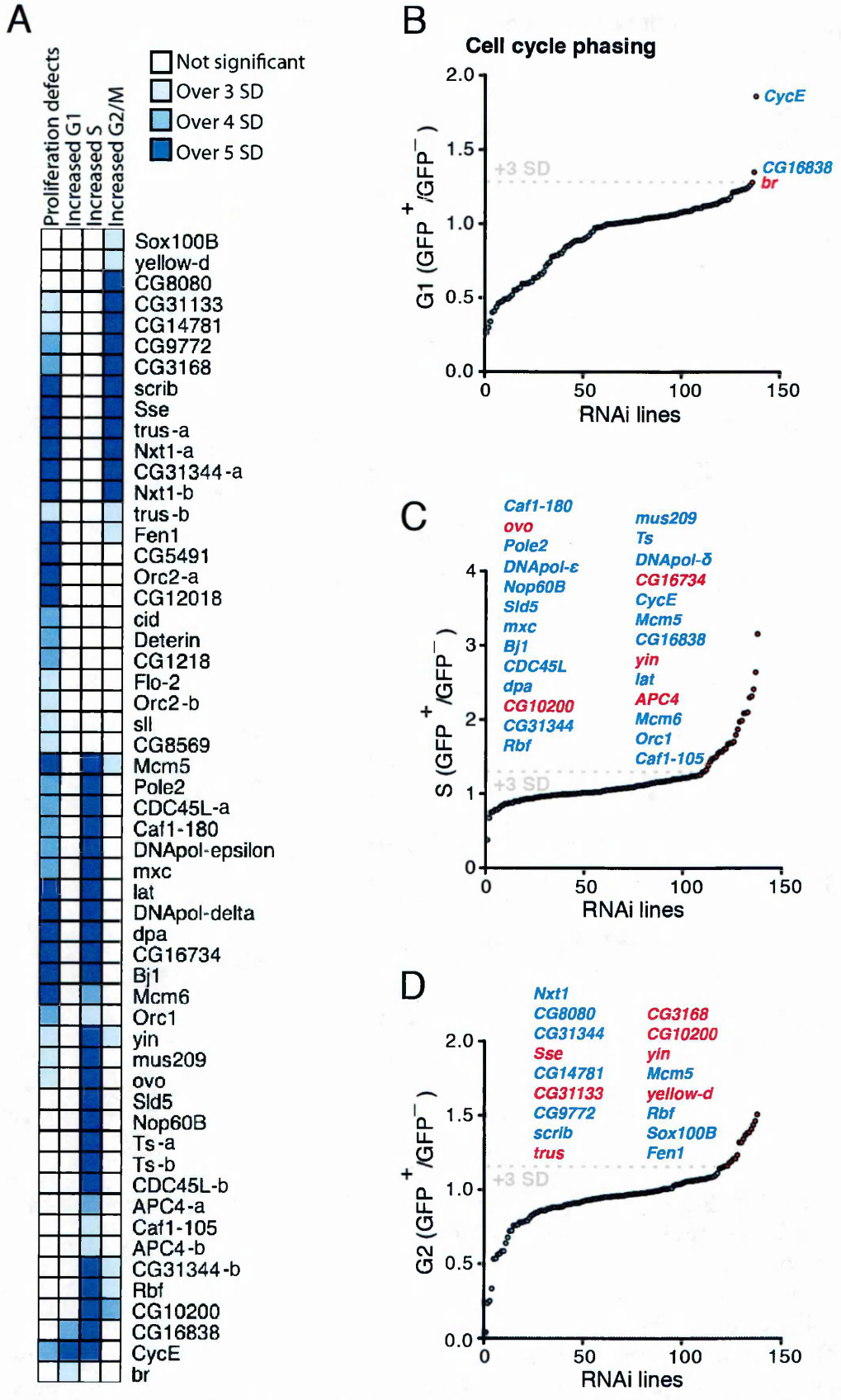


**Figure 3-22 Gene clustering based on proliferation and cell cycle phasing phenotypes.** (A) Only genes with significant cell cycle phasing defects (> 3 SD) in the flow cytometry screen are shown. Note that two distinct RNAi lines for a gene were designated by *a* or *b*. (B-D) Scatter plots of screened RNAi lines for cell cycle phasing defects. Text colors of the gene names represent the expression phase of the targeted genes: blue- G1, red- G2/M. The dashed grey lines indicate cutoff of Mean +3 SD calculated from controls. Listed genes in the plots had significant increases in G1 (B), S (C) or G2/M (D) following RNAi.

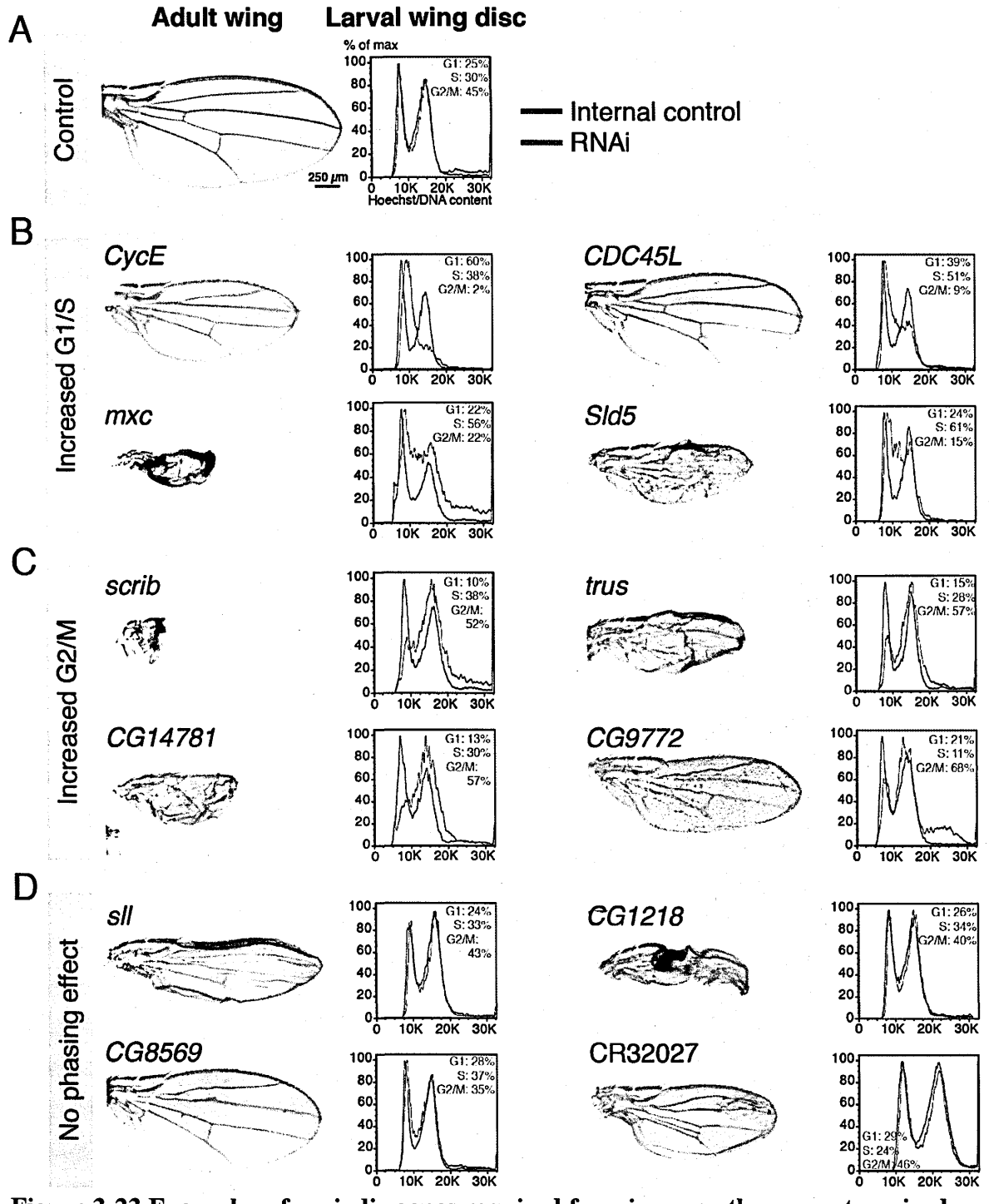


**Figure 3-23 Examples of periodic genes required for wing growth were categorized according to their cytometry profiles.**
(A) Control.
(B) Increased G1/S.
(C) Increased G2/M.
(D) No phasing effect. Note that knockdown of CG9772 (Skp2) in the wing disc resulted in an increased cell population with DNA content at or above 4N. For each gene knockdown, representative adult wings and cell cycle phasing phenotypes are shown.

In addition, nine gene knockdowns led to a decrease in cell number and no significant effect on cell cycle phasing (Figure 3-22A and Figure 3-23). These genes may therefore function in the control of other developmental processes, such as apoptosis (e.g.,

*CG5491*; data not shown). Conversely, knockdown of 12 genes did not significantly affect cell numbers, but produced defects in cell cycle phasing (Figure 3-22A and Table 3-1).

### 3.4.3 Majority of the identified cell cycle genes were not found in pervious S2 RNAi screens

As described above, we identified a total of 39 periodically expressed genes that were required for normal cell cycle phasing (Figure 3-22, Figure 3-23, and Table 3-1). These included many known genes, including cell cycle regulators (e.g., *Cyclin E* (*CycE*)) and DNA replication factors (e.g., *mus209* (*pcna*), *CDC45L*, *Sld5*, *dpa* (*Mcm4*) and *lat* (*Orc3*)) for G1/S phase, and the anaphase cysteine protease-encoding gene, *Separase* (*Sse*) for G2/M (Figure 3-22, Figure 3-23, and Table 3-1). Besides known cell cycle regulators, we also identified several periodic genes with unknown cell cycle functions, including *NTF2-related export protein 1* (*Nxt1*), *trus*, *Nop60B*, *ovo*, *CG14781*, *CG10200*, CG31344 and *CG16734* (Figure 3-22, Figure 3-23, and Table 3-1). Strikingly, of the 39 genes required for cell cycle phasing in the wing, only four were previously identified in genome-wide *Drosophila* RNAi screens in S2 cells (Table 3-1; Bjorklund *et al.*, 2006). Only two of these (*CycE* and *CDC45L*) showed similar phenotypes after knockdown in wing discs and S2 cells. In contrast, *trus* knockdown increased the G2/M population in discs but decreased the G2/M population in S2 cells (Table 3-1; Bjorklund *et al.*, 2006). Knockdown of *CG9772* (Skp2; Shibutani *et al.*, 2008) increased the G2/M population in both discs and S2 cells, but also caused an accumulation of aneuploid or polyploid cells not reported in cell culture (with > 4N DNA content; Figure 3-23). *CG9772* is a member of ubiquitin-protein ligase SCF. Consistent with our data, a recent study shows that knockdown of *CG9772* in *Drosophila* plasmatocytes leads to accumulation of *dup* (*double parked*, *Drosophila Cdt1*) in the nucleus and a consequence of DNA re-replication (Kroeger *et al.*, 2013). In general, the divergence in genes identified by the two screens may reflect technical differences, but may also suggest a critical difference in cell cycle regulation and pe-

riodic gene activity between different cell types or between the *in vivo* and *in vitro* contexts.

**Table 3-1 Periodic genes required for normal cell cycle phasing.**

| Cell cycle phenotype | Cyclic Expression Class | Gene | RNAi Wing phenotype | Indentified in previous S2 RNAi screen for cell cycle phenotypes* |
|---|---|---|---|---|
| **Increased G1** | G1-Com | *CycE* | Small wing | Increased G1 |
| | | *CG16838* | Others-disrupted vein pattern | - |
| | G2-WD | *br* | Small wing | - |
| **Increased S** | G1-Com | *CDC45L* | Small wing | Increased G1 |
| | | *Rbf, Mcm6, mus209 (pcna), Pole2, Ts, Bj1, CG31344* | Small wing | - |
| | G2-Com | *APC4* | Small wing | - |
| | | *CG16734* | Others-curly | NA |
| | G1-WD | *Orc1, Mcm5, dpa, DNApol-δ, DNApol-ε, Caf1-180, Caf1-105, mxc, Nop60B* | Small wing | - |
| | | *lat* | Others-curly and blistered | - |
| | | *Sld5* | Small wing | NA |
| | G2-WD | *yin, CG10200* | Small wing | - |
| | | *ovo* | Lethal | - |
| **Increased G2/M** | G1-Com | *Fen1, Nxt1* | Small wing | - |
| | | *CG9772* | Small wing | Increased G2/M |
| | G2-Com | *Sse* | Small wing | - |
| | | *CG31133* | Others-curly | - |
| | | *trus* | Small wing | Increased G1 |
| | G1-WD | *CG8080* | Others- canoe shaped and blistered | - |
| | | *scrib, CG14781* | Small wing | - |
| | | *Sox100B* | Small wing | NA |
| | G2-WD | *yellow-d, CG3168* | Small wing | - |

* Four genes (*CycE*, *CDC45L*, *CG9772* and *trus*) were previously identified in a genome-wide S2 RNAi screen using flow cytometry analysis (Björklund *et al.*, 2006). The GenomeRNAi database (Gilsdorf *et al.*, 2010) was also used for checking previous cell- based RNAi phenotypes, and no additional genes were identified in previous cell cycle screens using S2 cells. The cell cycle phenotypes listed here are the primary defects (refer Figure 3-22A for the phenotype overview). Notably, knockdown of *CG9772* (*Skp2*) in wing disc results in not only an increased G2/M population as in S2 cells (Björklund *et al.*, 2006), but also an accumulation of cells with an over 4N DNA content (Figure 3-23).

Finally, for all the transcriptional and functional analysis of the periodic genes, we have summed up the relevant data in a single master table (Table S8). In addition, to make the data easier to navigate and access, we have constructed a searchable website which includes: 1) Genome-wide periodic gene expression data from wing discs and S2 cells; 2) The phenotypic results of RNAi screening for hundreds of cyclic genes represented by

1,435 adult fly images that were taken during the original screening process; 3) Flow cytometry data for cell proliferation and cell cycle phasing defects for over a hundred candidate genes studied by RNAi *in vivo*; and 4) Homology information for each gene we identified. As mentioned above, the website is at: http://odr.stowers.org/FlyCycle.

### 3.4.4 Protein-protein interaction map between periodic genes required for normal cell cycle phasing

To assess potential functional relationships between periodic genes required for normal cell cycle phasing, we next constructed a protein-protein interaction (PPI) map using known physical interactions in *Drosophila* and predicted interactions based on orthology (Warde-Farley *et al.*, 2010). The resulting network (Figure 3-24) exhibited tight interactions between genes whose RNAi led to an increase in the G1/S population, but no direct interactions between genes whose RNAi increased the G2/M population. This indicates that G2/M accumulation may be triggered by the disruption of diverse and unrelated pathways, while G1/S accumulation may be primarily attributable to defects in DNA replication.

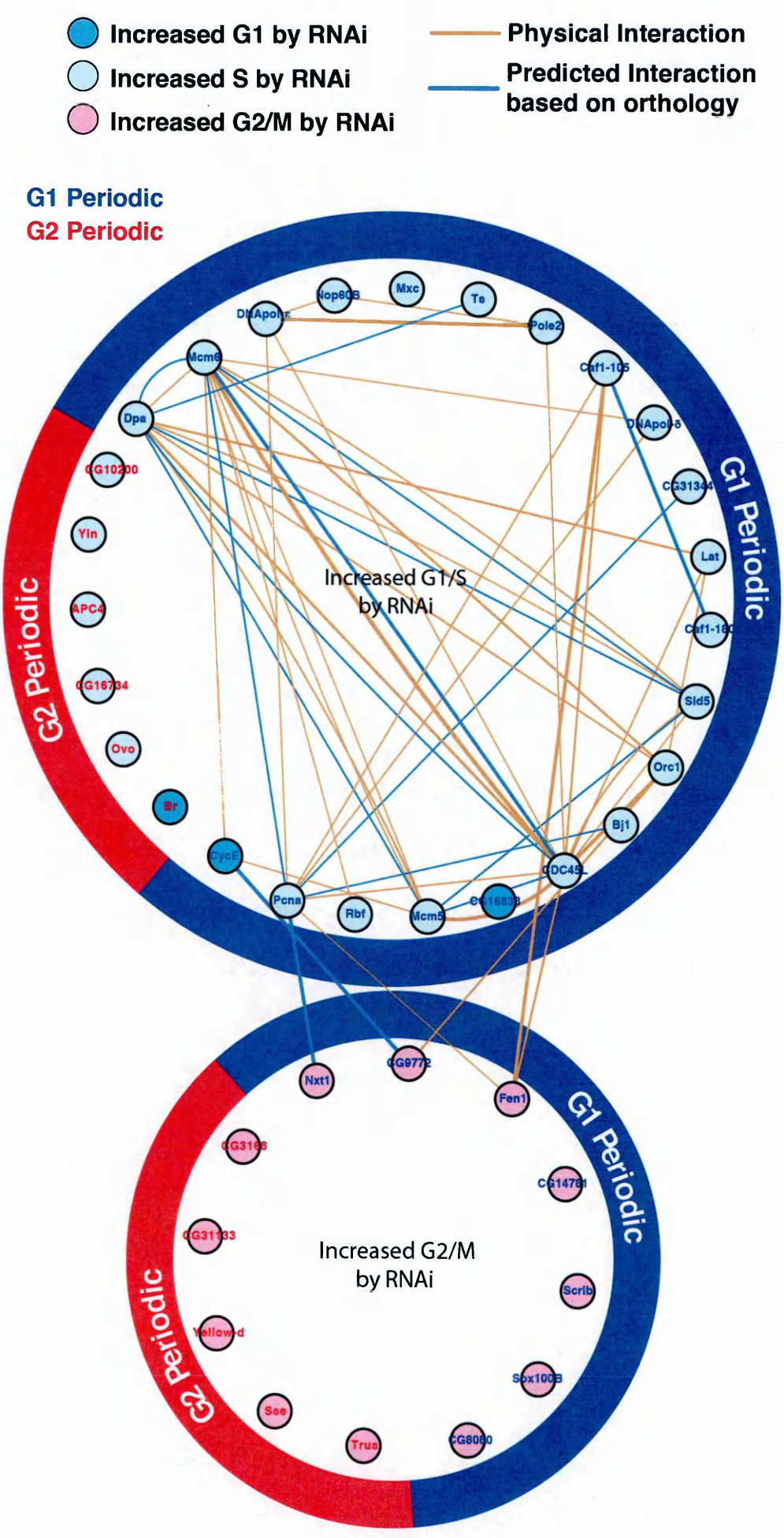
Increased G1 by RNAi
Increased S by RNAi
Increased G2/M by RNAi
Physical Interaction
Predicted Interaction based on orthology
G1 Periodic
G2 Periodic
Increased G1/S by RNAi
Increased G2/M by RNAi
Mxc
Te
Pole2
Mcm6
Caf1-105
Dpa
CG10200
CG31344
Yin
Lat
APC4
Caf1-180
CG16734
Sld5
Ovo
Orc1
Br
Bj1
CycE
CDC45
Pcna
Rbf
Mcm5
Nxt1
Fen1
Scrib
Sse
True

**Figure 3-24 A protein interaction network of identified cell cycle genes.**
Genes whose knockdown produced increased G1 or S phases exhibited a larger number of interactions than genes with increased G2/M after RNAi. Proteins are shown as nodes, and physical and predicted interactions are shown as edges. The colors of the edges represent types of interaction: *brown-* physical interaction in *Drosophila*, *blue-* predicted interaction based on orthology. Text colors of the protein names represent expression phases of targeted genes: *blue-* G1, *red-* G2/M. Periodic expression phases are indicated in the circles around the nodes. For CG31344, two different RNAi lines showed cell cycle phase accumulations in S and G2, respectively. We inferred the primary defect during S phase, supported by a predicted interaction with Pcna.

Among the genes with G1/S defects, 21/27 were expressed at elevated levels in G1 (Figure 3-24 and Figure 3-25), and 19 of these formed a tight PPI network (Figure 3-24 and Figure 3-25). Within the network, protein complexes involved in DNA replication emerged, including ORC, MCM, GINS and DNA polymerases (Figure 3-25). Additionally, a few novel genes were connected to the DNA replication protein network, including *Nop60B* (encoding a pseudouridine synthase) and *CG31344* (a putative target of E2f2 in *Drosophila* (Roy *et al.*, 2010); Figure 3-25). Their periodic expression, requirements for cell cycle progression, and interactions with known DNA replication factors indicate a likely function in DNA replication-related processes. There were also six genes highly expressed in G2 whose RNAi led to G1/S accumulation (Figure 3-25). Interestingly, none of these were connected to the DNA replication PPI network (Figure 3-25), suggesting that they may control cell cycle phasing through other processes.

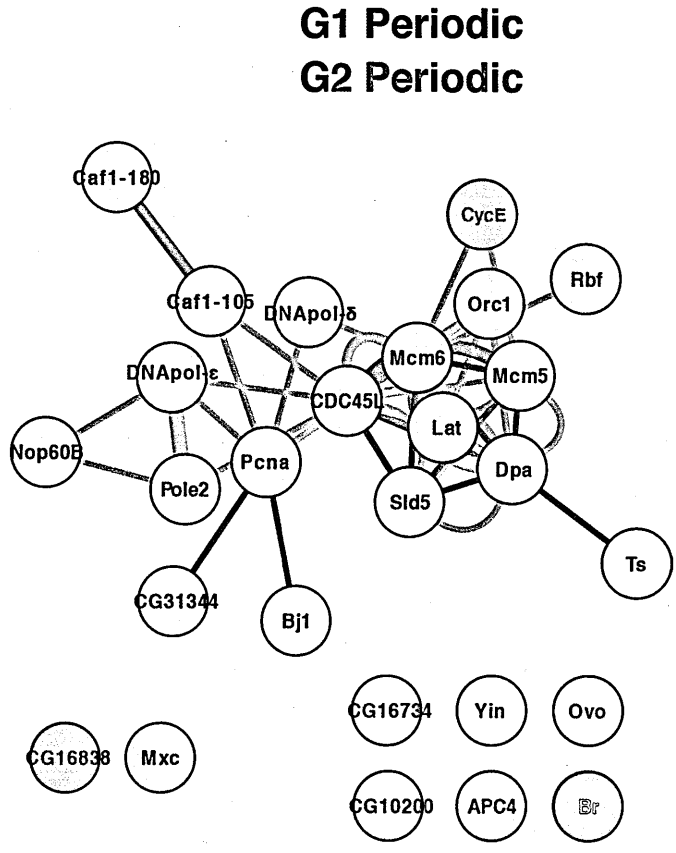


**Figure 3-25 The PPI network for factors whose knockdown produced increased G1 or S phases.**
Proteins are shown as nodes, and physical and predicted interactions are shown as edges. The colors of the edges represent types of interaction: *brown-* physical interaction in *Drosophila*, *blue-* predicted interaction based on orthology. Text colors of the protein names represent expression phases of targeted genes: *blue-* G1, *red-* G2/M.

## 3.5 Periodic genes required for cell division in the developing eye

To test whether these wing periodic genes have a more general function in cell proliferation in other epithelial tissues, we next examined their function in the developing eye (Figure 3-26A). We accomplished this by region-specific knockdowns. RNAi strains were crossed to flies carrying either GMR-GAL4, which is expressed in cells behind the MF (Freeman, 1996) or ey-GAL4, which is expressed in both dividing and differentiated cells (Lyko *et al.*, 1999). Using this approach, we identified 18 genes that were required for proliferation of the eye primordium (with ey-GAL4) but not differentiation (with GMR-GAL4) (Figure 3-26 and Figure 3-27, except *ovo*). Knockdown of *ovo* in the differentiation domain of the eye disc leaded to extensive generation of bristle cells (Figure 3-27). *Ovo* is

a transcription factor required for both germline (Garfinkel *et al.*, 1992; Mevel-Ninio *et al.*, 1991; Oliver *et al.*, 1990; Oliver *et al.*, 1987) and somatic cells (Delon *et al.*, 2003). Our data suggest *ovo* may play a role in eye cell differentiation, which is along the same line with its somatic role of regulating denticle formation during epidermal differentiation (Delon *et al.*, 2003).

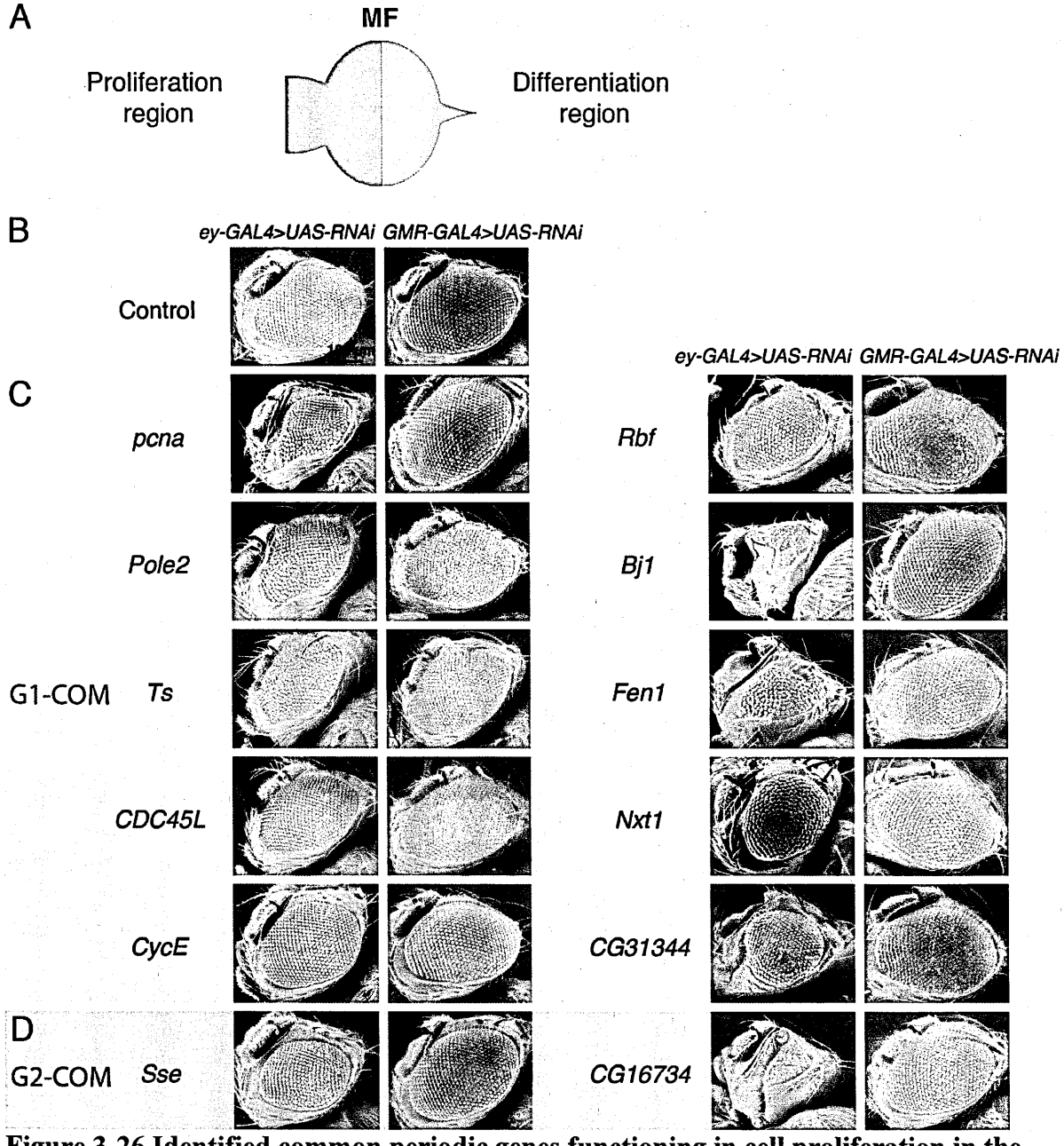


**Figure 3-26 Identified common periodic genes functioning in cell proliferation in the developing eye.**
(A) Scheme of developing eye imaginal disc with active-proliferation region (*ey-GAL4*, *blue*) before the morphogenetic furrow (MF) and limited cell division in the differentiation region (*GMR-GAL4*, *red*) after the MF.
(B) SEM images of control adult fly eyes.

(C-D) Examples of common periodic genes controlling cell proliferation in both wing and eye systems. Note that the effects of adult-eye-size reduction by *ey-GAL4* driven gene knockdown varied between individual flies and different RNAi lines. At least 5 male and 5 female flies were observed and imaged by SEM and the representative images are presented here. Scale bar: 100μm.

Under the same assay conditions, there are more common periodic genes required for cell division in both wing and eye (75.0%; N=16; Figure 3-25), compared with wing disc specific genes (43.7%; N=16; Figure 3-26). As a result, we showed that some periodic genes in the wing disc are also involved in the cell cycle control of the developing eye (Figure 3-25 and Figure 3-26).

My results highlight the importance for further studies in context specific cell cycle regulation. The common and wing disc specific periodic genes potentially provide an initial collection of gene sets for that purpose.

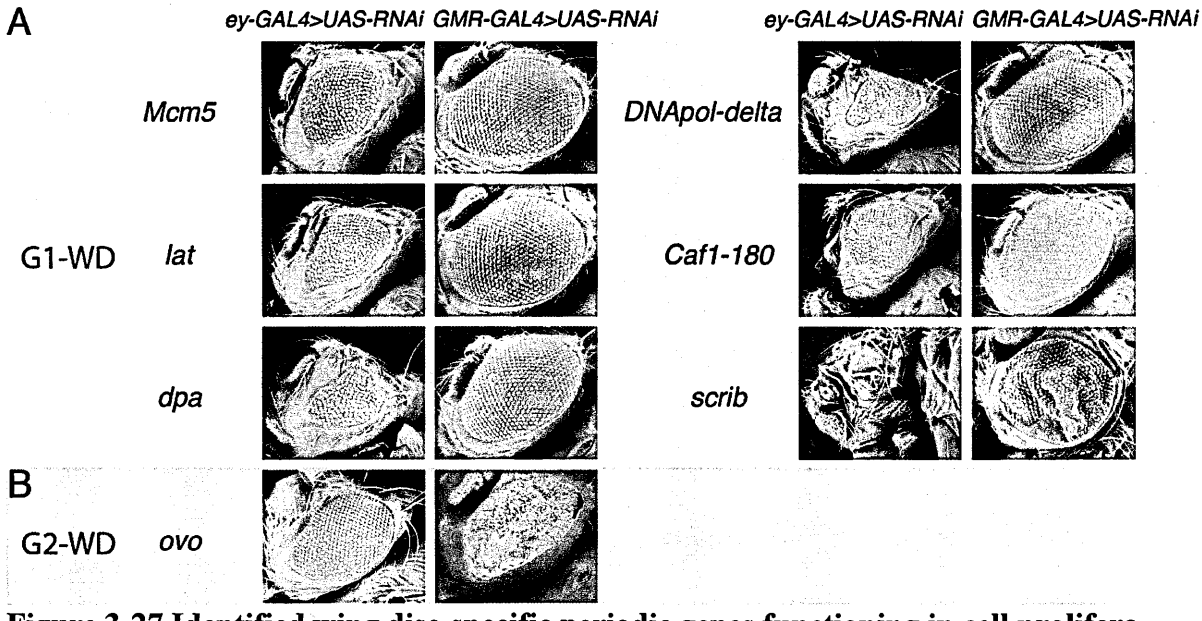


**Figure 3-27 Identified wing disc-specific periodic genes functioning in cell proliferation in the developing eye.**
(A-B) Examples of wing disc-specific periodic genes controlling cell proliferation in both wing and eye systems.

## 3.6 Periodic genes required for mitotic chromosome segregation

### 3.6.1 Examining the mitotic function of periodic genes by confocal and live imaging analysis

The cytometry screen described above provided us with a rough profile of cell proliferation and cell cycle phasing defects for a large number of periodic gene knockdowns. To better understand the wing growth defects and identify periodic genes directly involved in mitosis or other cellular processes, I also analyzed a subset of phenotypes at the cellular level. To achieve a relatively late wing pouch-specific knockdown, 71 RNAi lines that produced strong growth defects in the primary screen were crossed with *nubbin-GAL4* (Figure 3-28).

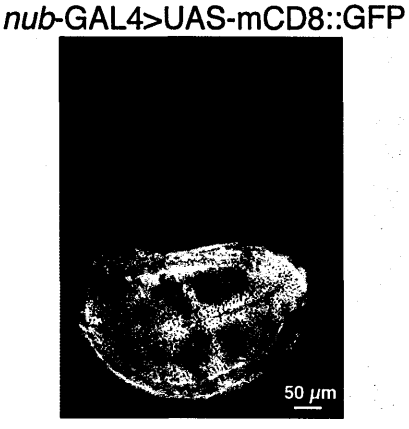


**Figure 3-28 RNAi knockdown region in the confocal analysis.**
*UAS-dicer2; nub-GAL4 > mCD8-GFP* expression domain (*green*) in the pouch region of the third instar wing disc. Scale bar: 50μm.

63/71 of these RNAi lines caused a similar wing growth reduction compared with results from the primary screen. For imaging analysis, we dissected wing discs from 3$^{rd}$ instar larvae and labeled microtubules, F-Actin and DNA. Of the 63 genes examined, we identified a number of mitotic abnormalities, including defective metaphase chromosome alignment (Figure 3-29), multipolar spindles (Figure 3-30J), and lagging or bridging chromosomes in anaphase (Figure 3-30B-J). Furthermore, for a few selected candidates, we also dissected the dynamics of mitotic defects in *ex vivo* cultured wing discs (Figure 3-32, Figure 3-33, and Movies S1-S5).

### 3.6.2 Six periodic genes involving in DNA replication resulted in chromosome alignment and segregation defects after knockdown

The knockdown of eight genes resulted in significant chromosome alignment and segregation defects during mitosis (Figure 3-29 and Figure 3-30).

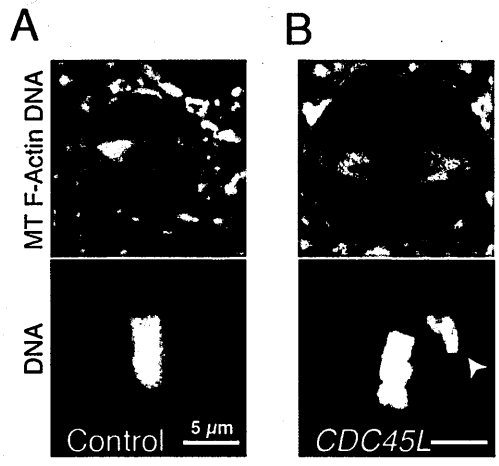


**Figure 3-29 Metaphase chromosome alignment defects after *CDC45L* knockdown.** A metaphase figure from a control (A) wing disc and a misaligned chromosome (*arrow-head*) in a metaphase cell after *CDC45L* knockdown (B). Cells were stained for α-tubulin (MT, *green*), DNA (*blue*), and F-Actin (*red*). Scale bar: 5μm.

Among these, only *cid* (Figure 3-30G) is known to directly function in kinetochore assembly and chromosome segregation (Blower and Karpen, 2001). Six other genes had direct or indirect functions in the process of DNA replication, including *dpa* (*Mcm4*; Figure 3-30B), *CDC45L* (Figure 3-29 and Figure 3-30C), *pcna* (Figure 3-30D), *RPA2* (Figure 3-30E), *RnrS* (Figure 3-30F) and *DNA-ligI* (Figure 3-30I).

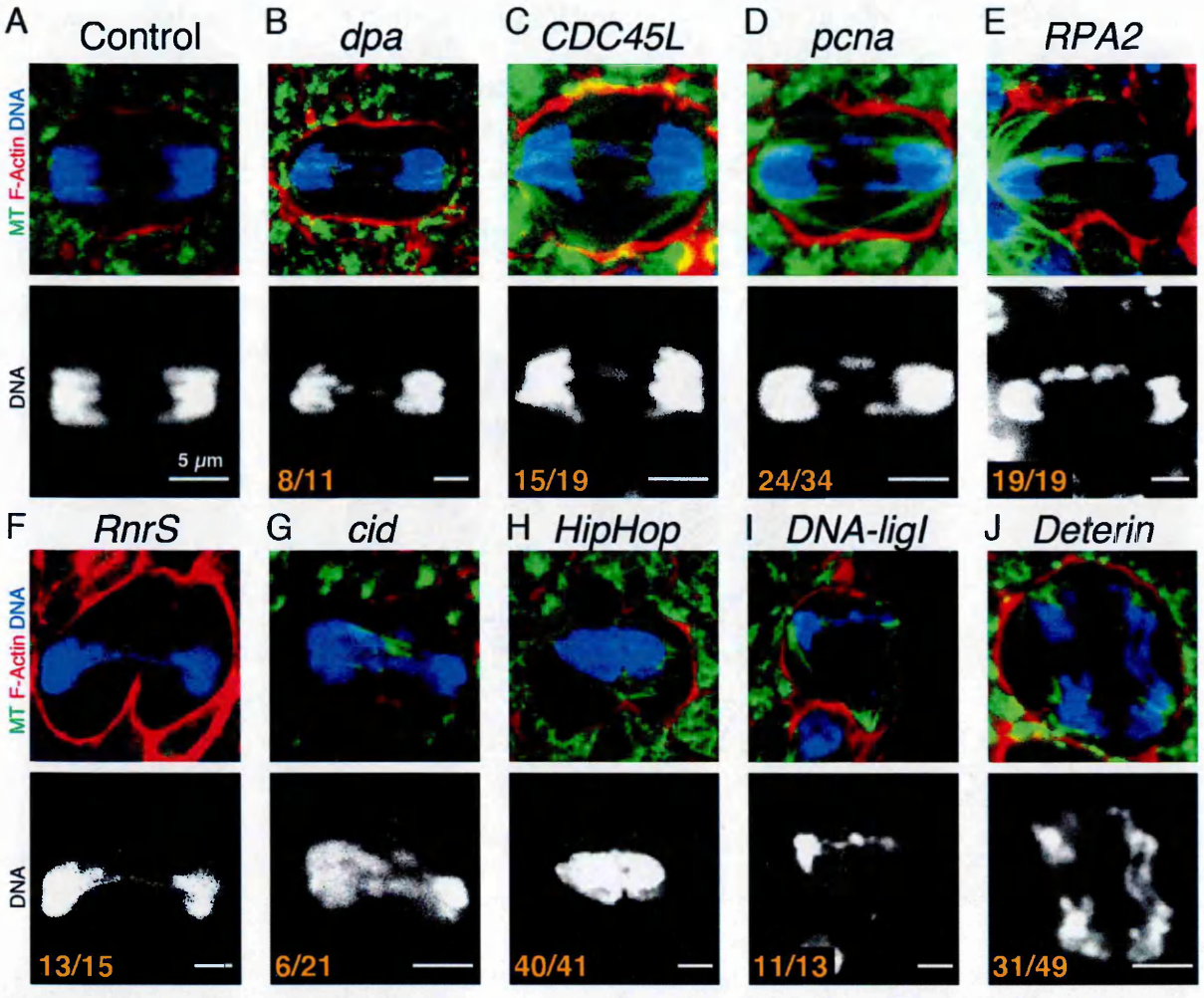


**Figure 3-30 Mitotic abnormalities associated with periodic gene knockdown,** *in vivo*. (A) Normal anaphase chromosome segregation in a control wing disc. Cells are labeled for α-tubulin (MT, *green*), DNA (*blue*), and F-Actin (*red*). Scale bar: 5μm. (B-E) Abnormal anaphase segregation with lagging chromosomes after *dpa*, *CDC45L*, *pcna* and *RPA2* knockdown. (F-I) Abnormal anaphase segregation with chromosome bridges observed after *RnrS, cid, HipHop* and *DNA-ligI* knockdown. (J) Abnormal multipolar spindles observed after *Deterin* knockdown.

Insufficient levels of DNA replication factors and incomplete DNA replication could lead to a cell cycle accumulation in late S phase. Under these conditions, abnormal cells that are able to pass through the DNA replication checkpoint may have incompletely replicated DNA and broken chromosomes, resulting in mitotic arrest or chromosome segregation defects (Balasov *et al.*, 2009; Loupart *et al.*, 2000; Pflumm and Botchan, 2001). Indeed, after DNA replication factor knockdown we frequently observed apoptotic cells, perhaps triggered by an active DNA damage checkpoint (data not shown).

### 3.6.3 HipHop, a telomere protein, also associated with defects in chromosome segregation

One final gene associated with defects in chromosome segregation was *HipHop,* which encodes a protein localized to telomeric regions (Gao *et al.*, 2010). Following knockdown, we observed tightly bound anaphase chromosomes in *HipHop* RNAi wing discs (97.6%, $n$=41 anaphase figures; Figure 3-30H and Figure 3-31). This could reflect telomere fusion, which has been reported in *HipHop* RNAi S2 cells (Gao *et al.*, 2010). In *HipHop* RNAi wing discs, aberrant chromosome bridges were largely resolved by telophase, although a thread of DNA often persisted between daughter nuclei. In these cases, we observed high levels of phosphorylated histone H3 in the bridging chromosomes (Figure 3-31). We suspect that the bridging chromosomes might be the telomeric regions, which will be interesting to test by telomeric FISH or a double-staining with another telomere marker, such as HOAP (Shareef *et al.*, 2001) in the future study.

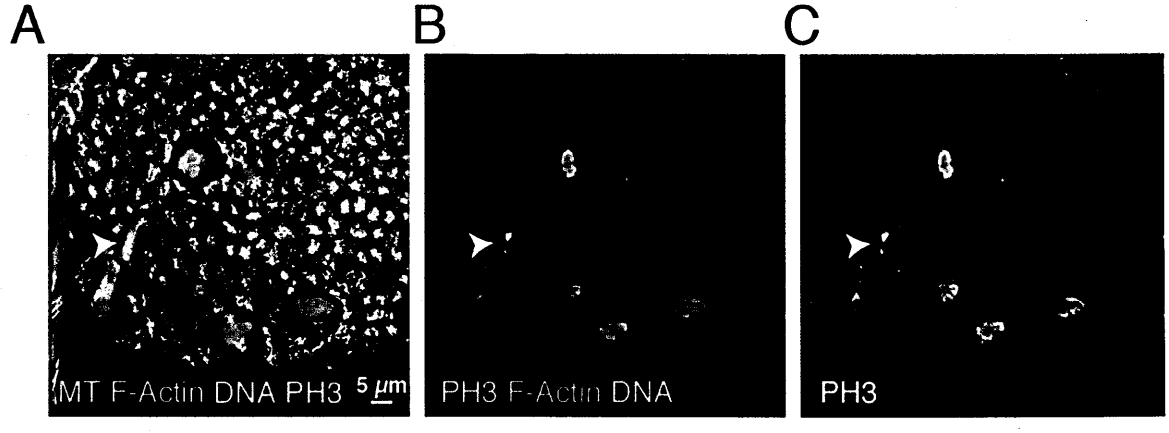


**Figure 3-31 Cells with mitotic chromosome segregation defects in *HipHop* RNAi wing disc.**
Aberrant chromosome bridges were largely resolved by telophase, however, a thread of DNA persisted between the daughter nuclei with high levels of phosphorylated histone H3 in the bridging chromosomes (*arrowheads*). Scale bar: 5μm.

By live imaging of cultured wing discs, we confirmed a metaphase delay associated with lagging and bridging chromosomes in *HipHop* RNAi wings discs which was similar to that observed for knockdown of the DNA replication factor *DNA-ligI* (Figure 3-32, Movie S1-S3).

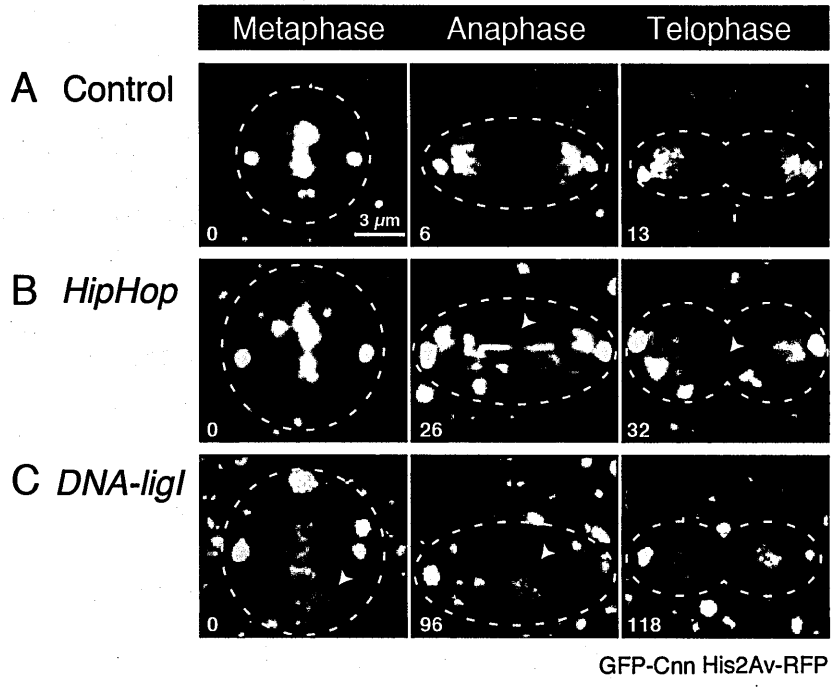


**Figure 3-32 Live imaging of a representative mitotic division in an ex vivo cultured control wing disc, as well as bridging chromosomes, lagging chromosomes, and mitotic delays following HipHop and DNA-ligI knockdown.**
Number in each panel shows the elapsed time (minutes). Bridging or lagging chromosomes are indicated by arrowheads. Scale bar: 3μm.

### 3.6.4 Deterin RNAi wing disc cells exhibited multipolar spindles without mitotic delay

Defects in chromosome segregation were occasionally associated with additional cellular phenotypes. In addition to lagging chromosomes, *Deterin* RNAi wing disc cells exhibited a high frequency of multipolar spindles (31/49 mitotic figures; Figure 3-30J). Mitotic figures with multipolar spindles typically either segregated the chromosomes into two units (Figure 3-33A and Movie S4) or failed at segregation entirely (Figure 3-33B and Movie S5). It is possible that multipolar spindles in *Deterin* RNAi wing cells formed as a consequence of a previous incomplete cytokinesis. In the future, it will be interesting to test if the ploidy of the cell matches with the centrosome number in *Deterin* RNAi. In addition, some MTOCs may consist of multiple centrosomes that were separated during telophase (Figure 3-33B) in the live imaging. However, I didn't see centrosome clustering (multipolar spindles become bipolar) in *Deterin* RNAi cells, an event that was observed in the reported *Drosophila* lines with extra centrosomes. In these reported mutants with extra

centrosomes, the process of centrosome clustering requires a mitotic delay, which is mediated by the spindle assembly checkpoint (SAC) (Basto *et al.*, 2008). With *Deterin* RNAi, we did not observe an obvious delay or arrest in mitotic progression (Figure 3-32, Figure 3-33 and Movie S4-S5), which may explain the failure of centrosome clustering. Interestingly, mitotic delay and multipolar spindle are both observed in the mutant of *Borealin*, a *Deterin* interacting partner (Gassmann *et al.*, 2004). If Deterin involves in the regulation of SAC *in vivo* remains to be explored, though a very recent study in S2 cells suggests a knockdown of *Deterin* might lead to a compromised SAC function or additional aspects of spindle assembly (Moutinho-Pereira *et al.*, 2013).

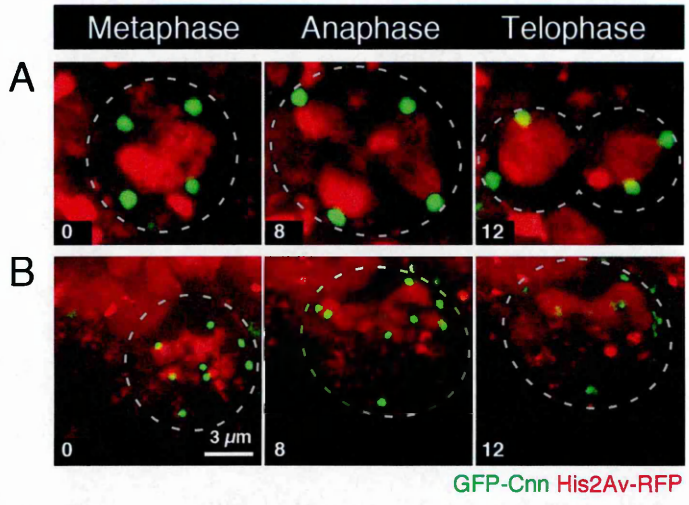


**Figure 3-33 Live imaging of the multipolar spindles following *Deterin* knockdown in ex vivo cultured wing discs.**
(A) Chromosomes finally clustered and segregated into two units in a representative cell with four mitotic spindle poles following *Deterin* knockdown.
(B) A representative cell with 8 spindle poles that failed to divide following *Deterin* knockdown. Number in each panel shows the elapsed time (minutes). Bridging or lagging chromosomes are indicated by arrowheads. Scale bar: 3μm.

Deterin's human homolog has been shown to function in the chromosomal passenger complex and is required for normal mitotic division (Lens *et al.*, 2006; Li *et al.*, 1999; Szafer-Glusman *et al.*, 2011). Here, my microarray expression data (Figure 3-14 and Figure 3-15) are consistent with the known cell-cycle-dependent expression of *Deterin* during G2/M phase in human cells (Li *et al.*, 1998). Further, my results indicate a function for

Deterin in chromosome segregation and perhaps mitotic checkpoint activation in *Drosophila* wing disc epithelium.

## 3.7 Periodic genes required for mitotic cell size and spindle size control additional to the function in mitosis

### 3.7.1 Mitotic cell size and spindle size increase in scale after *RnrS* and *RPA2* knockdown

In the proliferating tissue, mitotic division is directly linked with cell size and mitotic apparatus size. From my imaging screen, I identified several genes required for chromosome segregation that also disrupted mitotic cell size (Figure 3-34K-P). Cell size increased significantly in *RnrS*, *RPA2*, *DNA-ligI* and *HipHop* RNAi. Based on the live imaging analysis of mitotic division, the cell size increases observed in *DNA-ligI* and *HipHop* (possibly also *RnrS* and *RPA2*) RNAi may due to a significant cell cycle delay (Figure 3-32), since a similar cell size change was not observed for genes without a mitotic delay (e.g., *Deterin*). Metaphase spindle length increased proportionally with the cell diameter for *RnrS* and *RPA2* RNAi (Figure 3-34L-M and Figure 3-34P), which is consistent with the scaling of spindle length with cell size (Brown *et al.*, 2007; Goshima and Scholey, 2010; Hara and Kimura, 2009; Wuhr *et al.*, 2008).

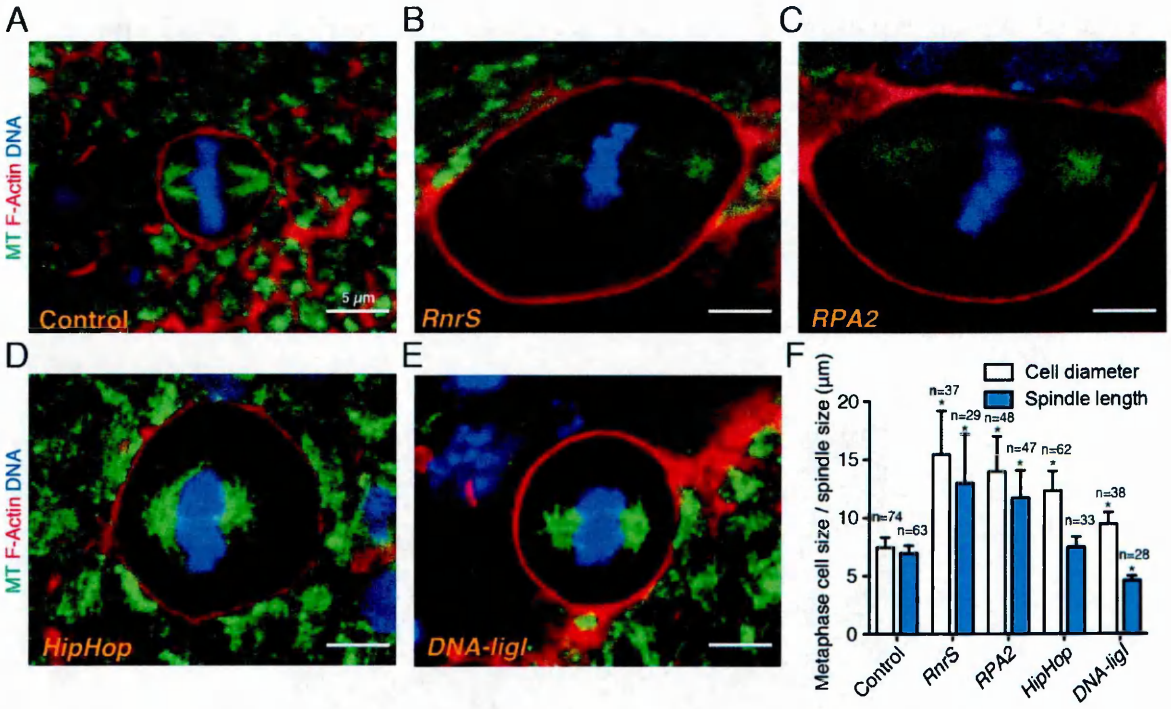


**Figure 3-34 Cell size increased significantly after *RnrS*, *RPA2*, *DNA-ligI* and *HipHop* knockdown.**
(A) A normal metaphase cell in a control wing disc. Cells are labeled for α-tubulin (MT, *green*), DNA (*blue*), and F-Actin (*red*). Scale bar: 5μm.
(B-C) Abnormally enlarged metaphase cells with increased spindle size after *RnrS* and *RPA2* knockdown.
(D-E) Abnormally enlarged metaphase cells without increased spindle size after *HipHop* and *DNA-ligI* knockdown.
(F) Bar plot showing quantification of metaphase cell size and spindle size in *RnrS*, *RPA2*, *HipHop*, and *DNA-ligI* knockdowns. Values are mean (±SD). The asterisks indicate statistical significance compared to controls by t-test with a p value < 0.005.

### 3.7.2 DNA-ligI and HipHop regulate mitotic cell size but not spindle size

In contrast, the spindle did not scale to the increased cell size after *HipHop* knockdown, and was actually slightly smaller than controls in enlarged *DNA-ligI* RNAi cells (Figure 3-34N-P). Both HipHop and DNA-ligI are involved in the regulation of chromosome integrity and structure. My data are consistent with the conjecture that spindle size scales with cell size and that abnormalities in chromosome structure may disrupt the scaling mechanism.

### 3.7.3 Apical extrusion of enlarged mitotic cells after RnrS and RPA2 knock-down

Interestingly, the enlarged mitotic cells after *RnrS* and *RPA2* knockdown (Figure 3-35) could get extruded from the epithelium. In some rare cases, individual floating cells were observed in the wing disc lumen (Figure 3-35).

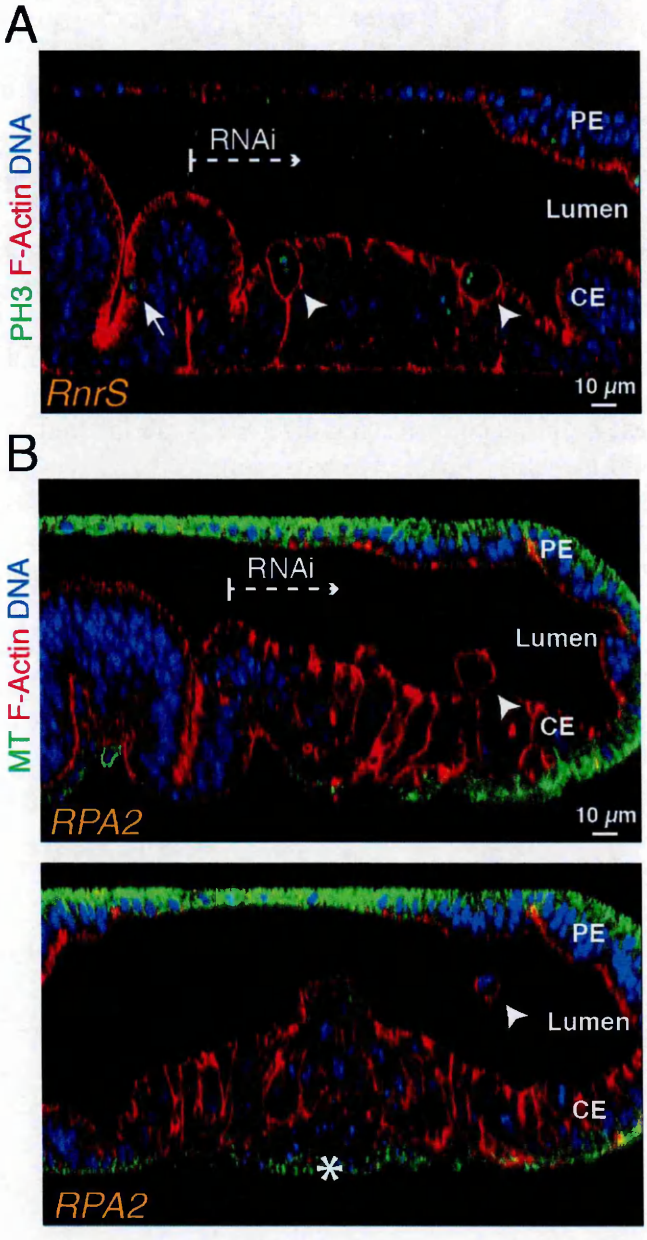


**Figure 3-35 Abnormally enlarged mitotic cells in wing discs after *RnrS* and *RPA2* knockdown.**
(A) Abnormally enlarged metaphase cells (*arrowheads*) after *RnrS* knockdown (RNAi knockdown region is indicated), compared with normal mitotic cell (*arrow*) in the control region. Scale bar: 5μm.
(B) Abnormally enlarged cells (*arrowheads*) after *RPA2* knockdown (RNAi knockdown region is indicated) extruded from the wing disc epithelium into the lumen. Note that there were dying cells with fragmented DNA (*asterisk*) extruded from the basal side of the disc. PE: peripodial epithelium; CE: columnar epithelium. Scale bar: 5μm.

Furthermore, with the enlarged mitotic cells extruding from the apical side and dying cells extruding from the basal side (Figure 3-35), the apical epithelium organized into a rosette geometric shape (Figure 3-36B), instead of the polygon topology in the control wing disc (Figure 3-36A). These results suggest that normal mitotic cell size is critical in maintaining an organized epithelial structure. A disruption of mitotic process *in vivo* may not only lead to individual cell catastrophe, but also dramatic changes in epithelial organization.

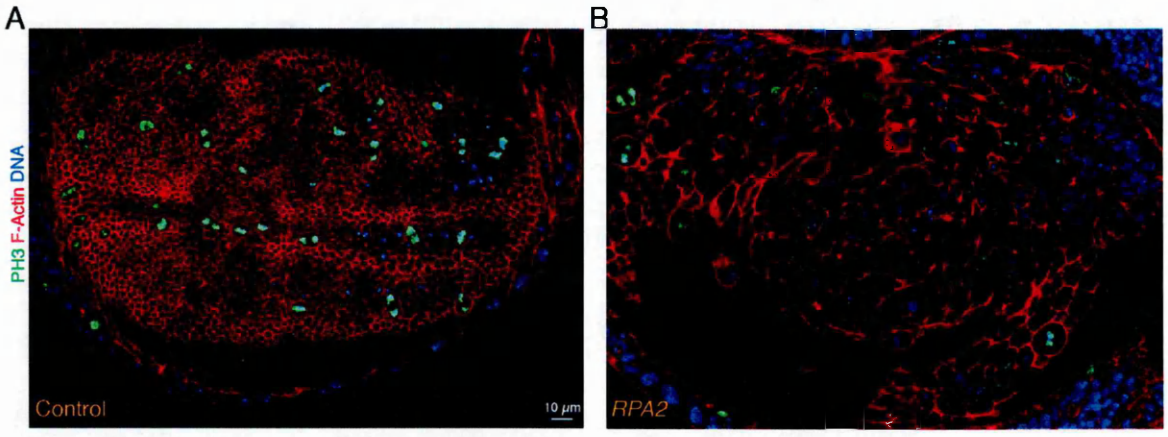


**Figure 3-36 Disrupted epithelial organization after *RPA2* knockdown.**
Apical views of the wing disc show that the epithelial cells organized into a rosette geometric shape after *RPA2* knockdown (B), instead of the polygon topology in the control wing disc (A). Scale bar: 10μm.

Neither *RnrS* nor *RPA2* have been previously identified in RNAi screens of S2 cells for cell cycle or cell size defects. However, they both were shown to affect neuroblast cell size in an *in vivo* RNAi screen of the nervous system (Neumuller *et al.*, 2011), indicating RnrS and RPA2 could play a similar role in mitotic cell size control in both epithelial and nervous systems.

## 3.8 Periodic genes required for cell size but not cell cycle phasing

### 3.8.1 Cell size increases after tumor suppressor gene *dlg1* knockdown

Despite cyclic genes involved in cell cycle progression, my flow cytometry screen also identified a number of periodic genes that function in wing growth without affecting cell cycle phasing, such as *CG8569*, *CG1218*, *dlg1* and *sll* (Figure 3-23). Among them,

*CG8569*, *CG1218* and *dlg1* knockdown caused significant increases in G1 and G2 cell sizes. None of the genes have been suggested to have a function in cell size control.

Interestingly, as tumor suppressor genes functioning in the DLG1/SCRIB polarity complex, both *dlg1* and *scrib* have cell cycle-associated expression patterns in the wing disc with higher mRNA levels in G1 (also true in S2 cells for *dlg1*, Table S1), and knockdown of either gene produced an increased cell size. The *dlg1* knockdown didn't affect cell cycle phasing, whereas the knockdown of *scrib* resulted in a striking increase in the number of G2/M cells (Figure 3-22 and Figure 3-23), both of which were validated using independent RNAi lines. In the previous mosaic analysis of *dlg1*, mutant clones failed to outcompete with wild-type cells (Woods and Bryant, 1991). Combined with my flow cytometry result, *dlg1* knockdown may lead to a slowdown of the cell cycle without affecting the G1, G2 distribution or the cell growth rate. It will be interesting to link their cell cycle/growth function with epithelial polarity.

### 3.8.2 Cell size increases after *CG8569* and *CG1218* knockdown

Unlike *dlg1*, which is the well-known tumor suppressor gene, *CG8569* and *CG1218* genes have not been previously characterized. *CG8569* encodes a protein containing a Zinc finger and Bromodomain, suggesting its potential function in transcriptional regulation. CG1218 is a highly conserved (putative homolog in *H. sapiens*: C4orf27) unknown protein containing an uncharacterized DUF2228 domain. Although there are no obvious similarities between their protein function, RNAi knockdown of either of these genes produced proliferation defects with normal cell cycle phasing (Figure 3-12 and Figure 3-23). This result indicates these genes could specifically affect the cell cycle length or cell growth rate but not cell cycle phasing. Further clonal analysis can eliminate the compartment compensation effect and help understand the function of these genes in cell size control.

## 3.9 Two wing disc-specific periodic genes implicated in IKNM

### 3.9.1 Identification of two novel periodic genes involving in IKNM

Interkinetic nuclear migration is a fundamental cellular process by which mitotic nuclei translocate to the apical epithelial surface during prophase (Baye and Link, 2008; Del Bene *et al.*, 2008; Meyer et al., 2011, b; Norden *et al.*, 2009). These events permit the subsequent alignment of the mitotic spindle to the plane of the epithelium as defined by apically polarized cell junctions (Nakajima *et al.*, 2013). Despite its likely conservation in pseudostratified epithelia throughout animals, the molecular mechanisms which link apically directed nuclear movements with cell cycle progression remain poorly understood. My imaging analysis revealed genes whose knockdown led to significant mitotic defects (Figure 3-29 and Figure 3-30), some of which were also coupled with significant increases in mitotic cell size (Figure 3-34) or dramatic increase of mitotic figures (e.g., *APC4*; Figure 3-37). Nevertheless, even in the most severe cases, mitotic nuclei remained restricted to the apical epithelial surface.

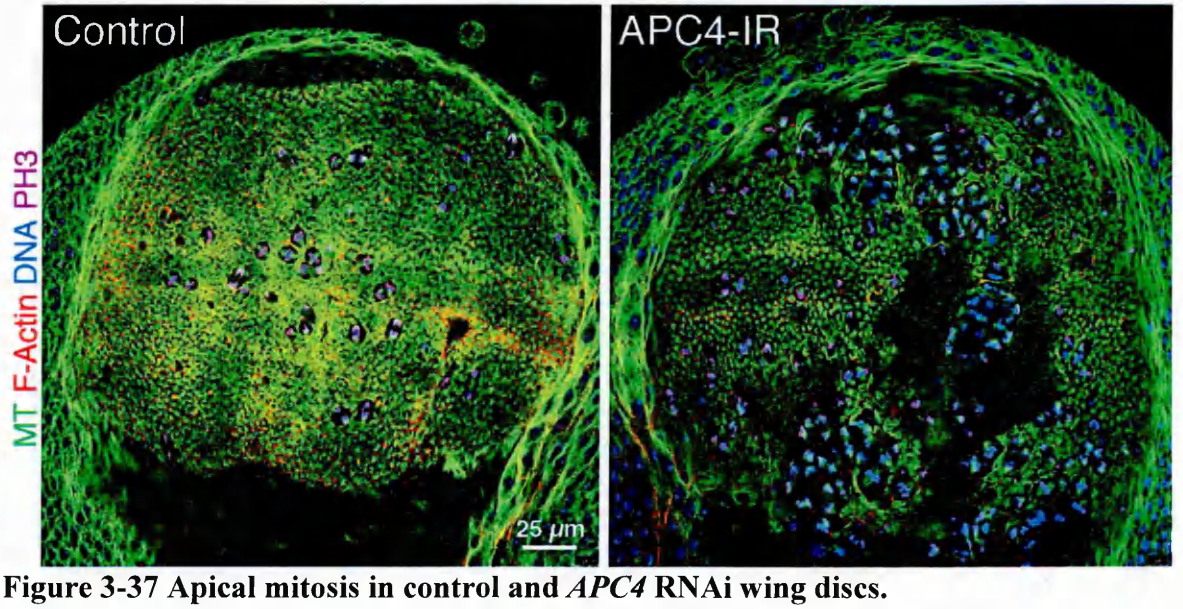


**Figure 3-37 Apical mitosis in control and *APC4* RNAi wing discs.**
(A) An apical view of a representative control wing disc, showing the mitotic nuclei (anti-PH3+, *purple*). Samples were also stained for F-Actin (*red*), MT (*green*) and DNA (*blue*). (B) Mitotic figures are largely increased but still retained at the apical surface in a representative wing disc following *APC4* (driven by *UAS-dicer2, w*$^{1118}$; *nubbin-GAL4*). Scale bar: 25$\mu$m.

To search for genes specifically involved in IKNM, I analyzed mitotic nuclear position following knockdown of the 71 periodic genes strongly required for wing development. Among these, IKNM was specifically disrupted by RNAi lines targeting *CR32027* (predicted to be a long non-coding RNA) and *CG10479* (predicted to encode a novel SH2-domain containing protein). In both cases, the total number of mitotic nuclei localized below the septate junction-delimited mitotic zone (MZ) was significantly increased (the out-of-MZ nuclei were referred to as basal or basally mislocalized nuclei in the following sections; Figure 3-38). Also in both cases, the normal polarized architecture of the epithelium was largely intact, confirmed by localization of the septate junction-associated protein Dlg (Figure 3-38A).

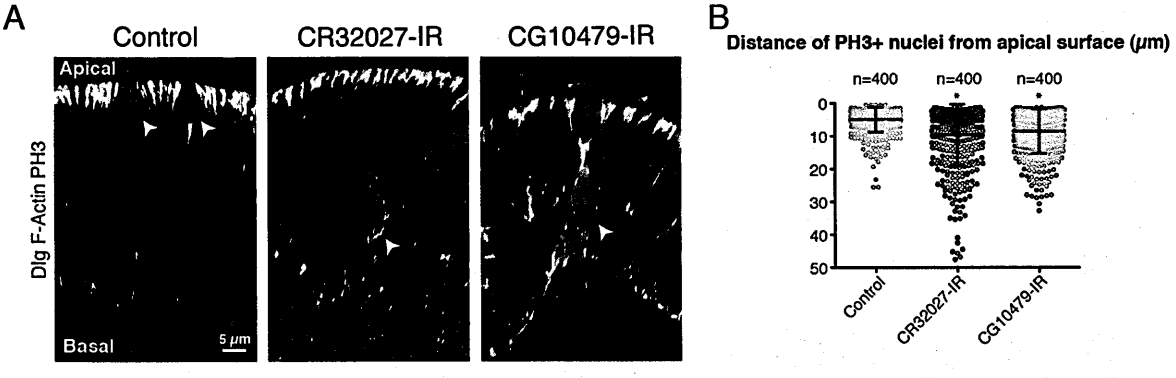


**Figure 3-38 Identification of *CR32027* and *CG10479* as novel periodic genes functioning in IKNM.**
(A) Basally mislocalized mitotic nuclei (anti-PH3+, *blue*; *white arrowheads*) in *CR32027* and *CG10479* RNAi wing discs (driven by *UAS-dicer2, w*$^{1118}$; *nubbin-GAL4*). Samples were also stained for F-Actin (*red*) and septate junctions, labeled by Discs large (DLG, *green*). Scale bar: 5$\mu$m.
(B) Scatter plot shows the distance of 400 anti-PH3+ nuclei from the apical surface of wing discs in control and following *CR32027* and *CG10479* RNAi. Error bars show mean ±SD. The asterisks indicate statistical significance compared to control by Mann-Whitney U test with a p value < 0.0001.

It is proposed that Rho-kinase controls IKNM, at least in part, through phospho-regulation of Myosin activity (Meyer et al., 2011). The myosin II activity was then measured using a rabbit polyclonal phosphor-myosin regulatory light chain II antibody (anti-p-MRLC). In control discs, we observed strong cortical anti-p-MRLC staining in mitotic cells (Figure 3-39). Following *CG10479* RNAi, however, anti-p-MRLC staining was severely reduced in basally mislocalized mitotic cells (Figure 3-39). This indicates that

*CG10479* is not only periodically expressed, but may also function in the regulation of IKNM at or above the level of Rho kinase activity. In contrast with this result, normal anti-p-MRLC signal levels were observed following disruption of *CR32027*, even in basally mislocalized mitotic cells (Figure 3-39). Consistently, these mitotic cells exhibited mislocalized anti-PH3+ nuclei, but had normal cortical F-Actin accumulation and underwent normal mitotic rounding (Figure 3-38 and Figure 3-39). These experiments indicate that *CR32027* likely functions in the regulation of IKNM independently from both Rho-kinase activity and actomyosin contractility.

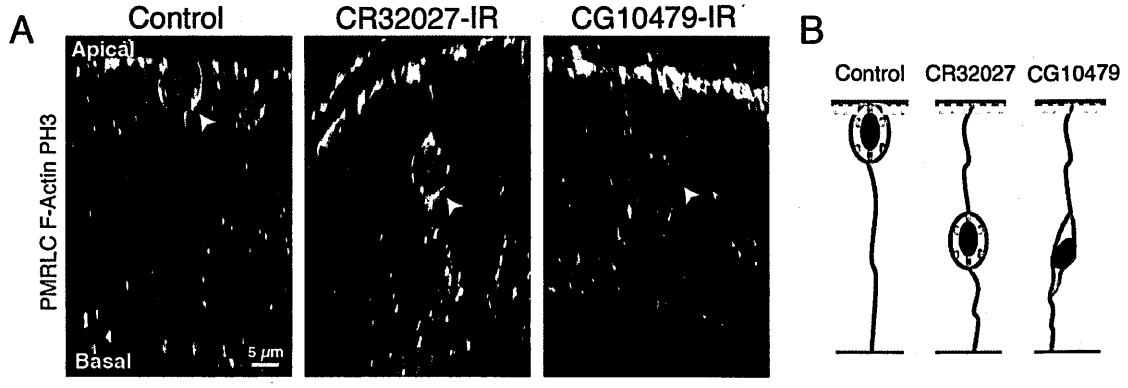


**Figure 3-39 *CR32027* and *CG10479* function in IKNM though actomyosin independent and dependent mechanisms.**
(A) Anti-p-MRLC (*green*) accumulates at the cortex of rounded mitotic cells (*arrowheads*; nuclei are anti-PH3+, *blue*; F-actin, *red*) in controls and following *CR32027* RNAi, but not in mitotic cells following *CG10479* RNAi (driven by *UAS-dicer2, $w^{1118}$; nubbin-GAL4*). Scale bar: 5μm.
(B) Schematic summary of phenotypes for *CR32027* and *CG10479* RNAi. Knockdown of either gene produced basally mislocalized mitotic nuclei (*blue*) without disrupting the septate junctions (*yellow*). Notably, in *CR32027* RNAi, mitotic rounding appears to be normal and anti-p-MRLC (*green*) accumulates at the cortex.

Indeed, we observed a strong additive effect on nuclear position when we inhibited Actin dynamics with Cytochalasin D in *CR32027 RNAi* wing discs (Figure 3-40). Under these conditions, anti-PH3+ mitotic nuclei showed a roughly uniform distribution throughout the epithelium (Figure 3-40C), consistent with a maximal defect in IKNM.

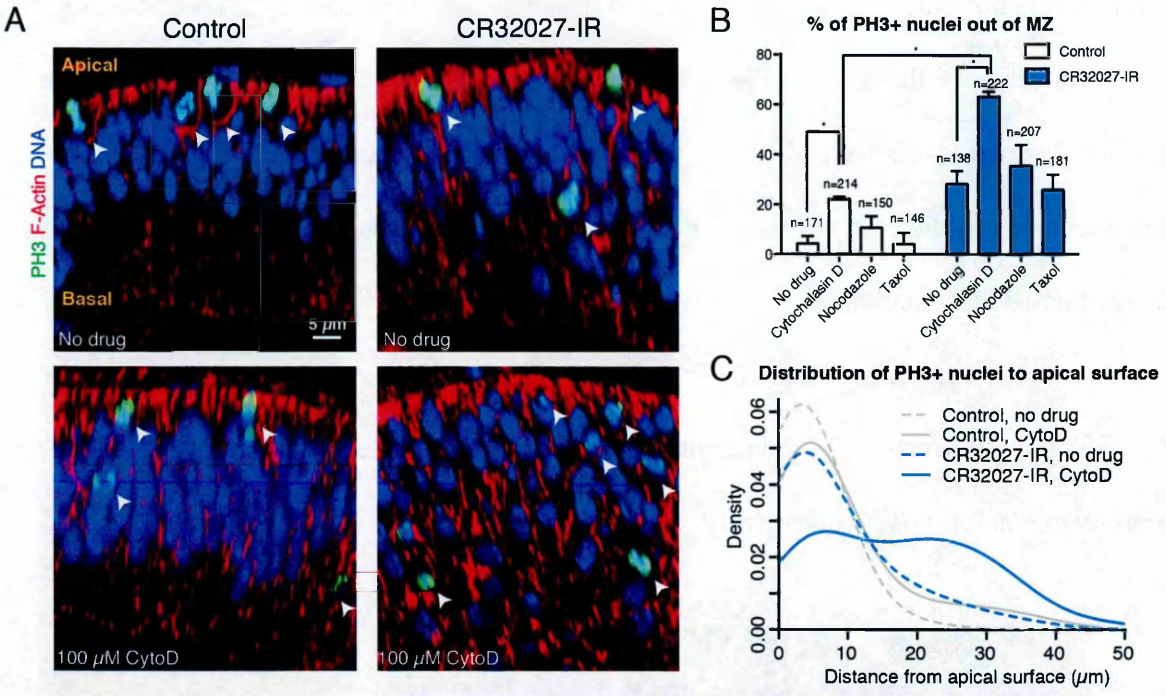


**Figure 3-40 *CR32027* functions in IKNM though actomyosin independent mechanism.**
(A) Increased numbers of basally mislocalized mitotic nuclei (anti-PH3+, *green*; *white arrowheads*) were observed in *A9-Gal4 > UAS-CR32027* RNAi wing discs treated with 100μM Cytochalasin D (CytoD) for 30 minutes. Samples were also stained for F-Actin (*red*) and DNA (*blue*). Scale bar: 5μm.
(B) Bar plot showing the percentage of basal anti-PH3+ nuclei in controls and in *CR32027* RNAi wing discs with and without cytoskeletal inhibitor treatments. Values are mean (±SD). The asterisks indicate statistical significance compared to control by t-test with a p value < 0.005.
(C) Histogram showing the distribution of anti-PH3+ nuclei relative to the apical epithelial surface in controls and *CR32027* RNAi wing discs, with and without cytoskeletal inhibitor treatments. The density plot is generated using kernel density estimation with a bandwidth equal to 0.6. Mann-Whitney U test between all 4 groups is significant (p value < 0.005).

### 3.9.2 CR32027 controls IKNM potentially through regulating centrosome function

To extend these results, we validated the function of *CR32027* using a second RNAi construct (*CR32027-IR2*; Figure 3-42A-B) and also confirmed the reduction of *CR32027* transcript levels in the experimental wing discs (Figure 3-41).

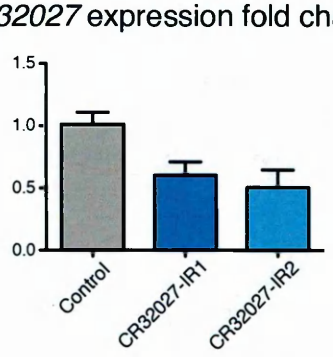


**Figure 3-41 Reduced *CR32027* transcript level following RNAi knockdown.**
qRT-PCR analysis of *CR32027* transcript levels in wing discs with *CR32027* knockdown (with $w^{1118}$, *Bx-GAL4; UAS-dicer2*), relative to control.

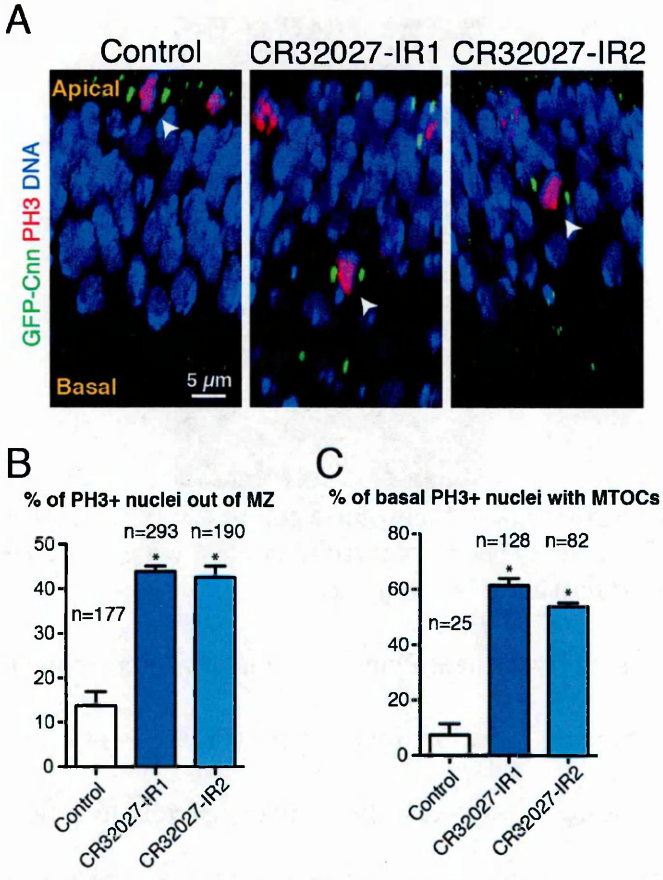


**Figure 3-42 Basally-mislocalized mitotic nuclei and MTOCs in two independent RNAi lines of *CR32027*.**
(A) Basally-mislocalized mitotic nuclei (anti-PH3+, *red*; DNA, *blue*; *arrowheads*) and MTOCs (GFP-Cnn, *green*) in both *CR32027-IR1* and *CR32027-IR2* wing discs (driven by *A9-GAL4*). Scale bar: 5μm.
(B) Bar plot showing the percentage of anti-PH3+ nuclei outside the MZ in control, *CR32027-IR1* and *CR32027-IR2* wing discs. Values are mean (±SD). The asterisks indicate statistical significance compared to control by t-test with a p value < 0.005.
(C) Bar plot showing the percentage of basal anti-PH3+ nuclei associated with basal MTOCs in control, *CR32027-IR1* and *CR32027-IR2* wing discs. Values are mean (±SD). The asterisks indicate statistical significance compared to control by t-test with a p value < 0.005.

Phenotypically, in addition to mislocalized mitotic nuclei, expression of both *CR32027-IR1* and *CR32027-IR2* resulted in a significant increase in basally localized microtubule-organizing centers (MTOCs, marked by the pericentriolar matrix marker Centrosomin; Figure 3-42C).

In *CR32027-IR1*, we observed basal cells in every mitotic phase, including telophase (7.7±2.3%, $n$=128; Figure 3-43), indicating that the abnormal cells can still complete mitotic division.


**Figure 3-43 A basally-mislocalized telophase cell in *CR32027-IR1* wing disc.**
Basal dividing cells have never been observed in control wing discs. Here, wing disc was stained for anti-PH3 (*green*) and F-Actin (*red*).

Furthermore, using live Single Plane Illumination Microscopy (SPIM), we observed aberrant basal mitoses in cultured wing discs (Figure 3-44). In some cases, aberrant mitotic figures first appeared basally and then moved apically to complete mitosis (Figure 3-44C and Movie S8). This may explain how a small but relatively normal adult wing phenotype was observed in these lines (Figure 3-23D). Importantly, mitotic timing in *CR32027* RNAi cells was normal compared with controls (Figure 3-44 and Movie S6-8). Since *CR32027* RNAi did not disrupt cell cycle timing or phasing (Figure 3-23D), my results suggest that IKNM is not required for mitosis, and that *CR32027* may link mitotic division with nuclear migration without affecting other mitotic processes (i.e., cell rounding, cell cycle phasing, and mitotic progression).

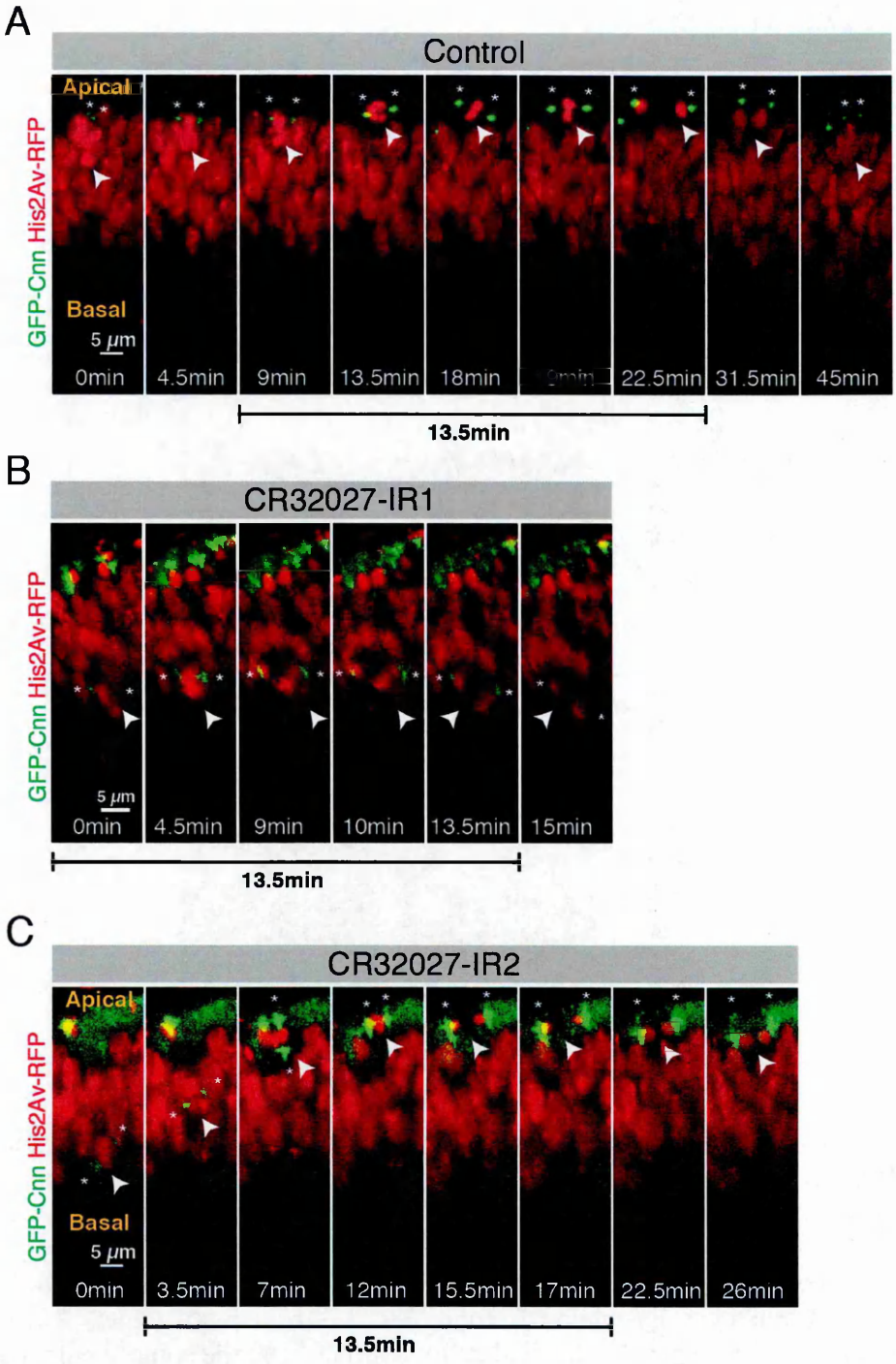


**Figure 3-44 *CR32027* specifically regulates IKNM without affecting normal mitotic progression.**

SPIM live XZ imaging of mitosis in *ex vivo* cultured control and *CR32027* RNAi wing discs (driven by *A9-GAL4*).

(A) In controls, nuclei (His2Av-mRFP, *red*; *arrowheads*) rise to the apical surface to divide and move basally after division. During division, MTOCs (GFP-Cnn, *green*, *asterisks*) generally remain apical.

(B) In *CR32027-IR1* wing discs, we observed basally mislocalized mitotic cells associated with abnormally basal MTOCs. Note that mitotic timing in the *CR32027* RNAi cell was similar to controls.

(C) Following *CR32027* RNAi in a representative *CR32027-IR2* wing disc, the nucleus (His2Av-mRFP, *red*; *arrowheads*) entered mitosis basally with mislocalized MTOCs (GFP-Cnn, *green*; *asterisks*), and then translocated to the apical surface to complete mitosis. Note that mitotic timing in the *CR32027* RNAi cell was similar to controls. Scale bar: 5μm.

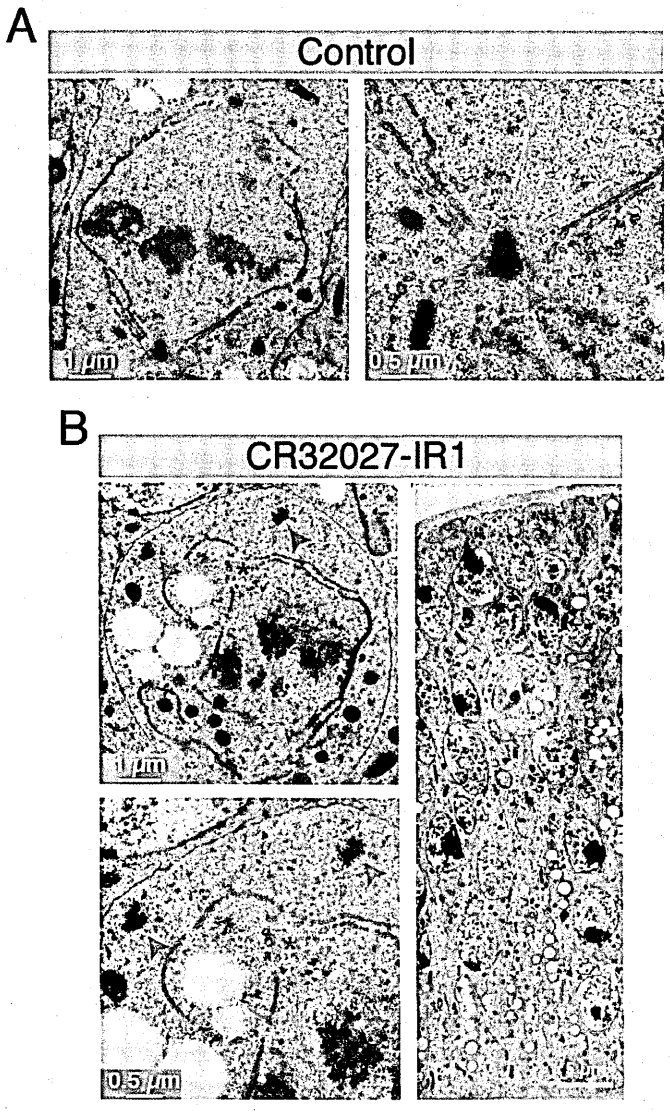


**Figure 3-45 *CR32027* is required for IKNM, potentially through modulation of centrosome function.**
(A) Mitotic centrosomes containing two centrioles (*arrowheads*) were associated with radial arrays of MTs in a control wing disc cell.
(B) Putatively non-functional centrioles (*arrowheads*) were not associated with MTs at the MTOC (*asterisks*) in a basally-mislocalized mitotic cell from an *A9-Gal4 > UAS-CR32027 RNAi* wing disc. Left two panels: detailed cellular structure at the spindle pole. Right: basal localization of the representative mitotic cell (highlighted in pink; colors in the image were adjusted for better viewing) after *CR32027* knockdown.

One possible interpretation is that *CR32027* directly or indirectly regulates centrosome positioning and function, and misregulation of this process may allow aberrant cell division to happen at basal positions in the epithelium. Consistent with this, centrioles in mitotic *CR32027* RNAi wing disc cells were not consistently associated with the spindle poles or MTs (Figure 3-45). Further suggesting a link between *CR32027* expression and

centrosome function, *CR32027* transcript abundance was recently reported to be sensitive to centrosomal manipulations in *Drosophila* (Baumbach *et al.*, 2012).

Interestingly, I sometime observed centrosome hopping events in the fly wing disc (Figure S6D; also in control for rare cases) as recently reported in the chicken neural tube, mouse cortical slices, and rat brain (Hu *et al.*, 2013; Spear and Erickson, 2012), in which when mitotic nuclei fail to reach apical epithelium before mitosis, MTOCs go basally right before mitotic entry, approach closely with the mitotic nuclei and then move apically together. This suggests the cell-cycle phase specific regulation of MT motor protein and centrosome function could be a conserved feature in maintaining normal IKNM process.

### 3.9.3 *CR32027* control IKNM potentially through Klp54D

While it remains unclear how a putative non-coding RNA might directly regulate centrosome localization, a number of long non-coding RNAs have been proposed to function by directly controlling transcription of specific targets or by regulating the basal transcriptional machinery (Rinn and Chang, 2012). We therefore used transcriptional profiling to identify gene expression changes in the wing pouch following *CR32027* RNAi. For both *CR32027-IR1* and *CR32027-IR2* knockdown, the putative target genes *Cyp6A17* and the kinesin-like protein *Klp54D* were highly downregulated (> 500 fold). We used RNAi to test the function of both genes in IKNM, and observed a high frequency of basally mislocalized mitotic nuclei in *Klp54D* RNAi wing discs. Similar results were obtained with two independent lines targeting *Klp54D*, whereas no defects were observed after *Cyp6A17* knockdown (Figure 3-46). Notably, *Klp54D* knockdown did not produce a small wing phenotype, presumably because aberrant basal mitotic figures ultimately moved apically to complete mitosis (data not shown).

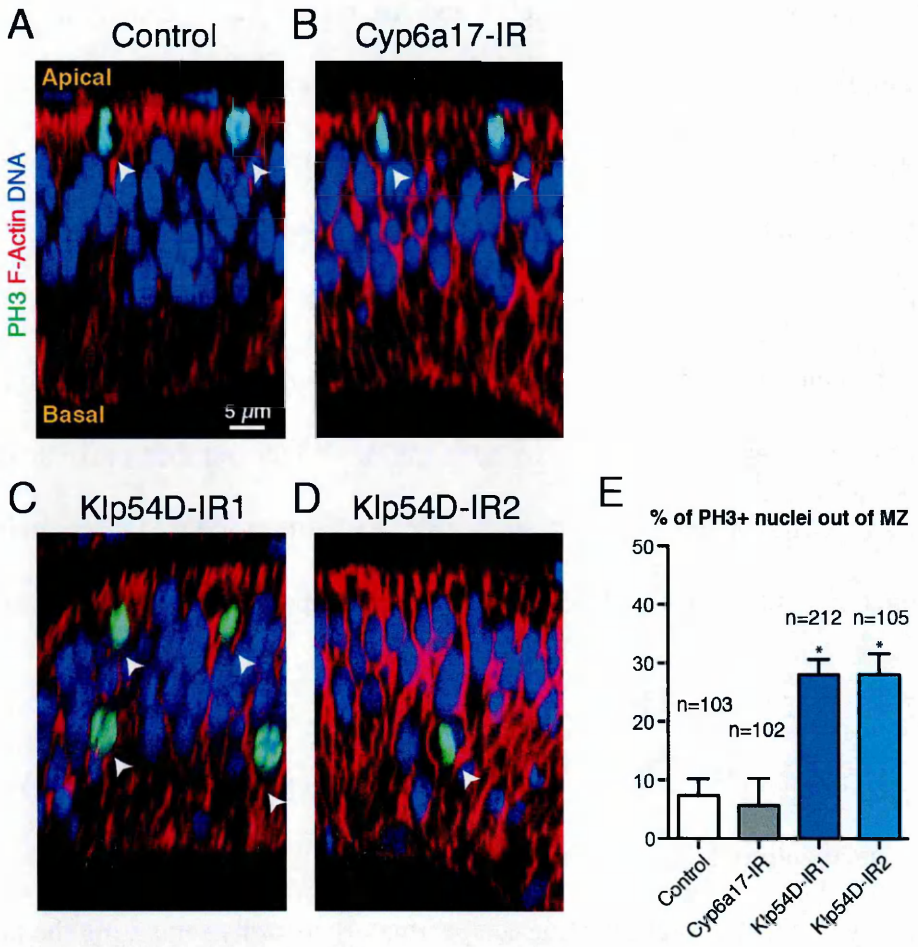


**Figure 3-46 *CR32027* controls IKNM, potentially through the transcriptional regulation of *Klp54D*.**
(A-D) Basally-mislocalized mitotic nuclei (anti-PH3+, *green*; *white arrowheads*) were observed in wing discs of *Klp54D-IR1* and *Klp54D-IR2*, but not *Cyp6a17-IR* (driven by *A9-GAL4*, at 29°C). Samples were also stained for F-Actin (*red*) and DNA (*blue*). Scale bar: 5μm.
(E) Bar plot shows the percentage of anti-PH3+ nuclei outside the MZ in wing discs of control, *Cyp6a17-IR*, *Klp54D-IR1*, and *Klp54D-IR2*. Values are mean (±SD). The asterisks indicate statistical significance compared to control by t-test with a p value < 0.005.

Together these results suggest that *CR32027* may function directly or indirectly through transcriptional control of *Klp54D,* which could in turn regulate centrosome positioning or other mitotic processes. Looking forward, the regulation of centrosome positioning and dynamics may represent an important avenue for future studies of epithelial cell proliferation *in vivo*.

# Discussion

Rapid and continuous cell division is a fundamental aspect of early animal development, and must therefore be integrated with other processes, such as cell growth, tissue patterning, and epithelial morphogenesis. In this thesis I provided a global functional perspective on cell cycle-dependent periodic genes in the *Drosophila* wing disc, an established *in vivo* model for development and morphogenesis. On a genomic level, my experiments define the *in vivo* periodic transcriptome of an epithelial tissue for the first time, and also reveal an unexpected degree of plasticity in global periodic transcription between different cell types from the same organism. Experimentally, using a phenotypic screen validated by both flow cytometry and direct confocal analysis, I also report a large number of periodically expressed genes required for the regulation of cell proliferation. This approach led us to several new genes required for tissue growth and cell cycle progression, as well as two novel genes, *CG10479* and *CR32027*, which appear to function in IKNM, a conserved aspect of epithelial cell division not observed in tissue culture cells. In sum, I hypothesize that similar approaches in vertebrate systems could uncover additional novel regulators of mitotic processes that may be difficult or impossible to study *in vitro*.

## 4.1 The global periodic transcriptome, *in vivo*

### 4.1.1 New dissociation-FACS-microarray method reliably identified global cell-cycle-associated transcription

#### 4.1.1.1 New dissociation-FACS method separated cells according to DNA content without cell synchronization

In any analysis of cell cycle-dependent gene expression in an intact tissue, the chief technical hurdle is efficient dissociation and sorting of cells according to their DNA content. My dissociation-FACS-microarray method (see Methods) allowed me to sort wing disc cells into G1 and G2/M populations without the need to impose artificial synchroniza-

tion (Figure 1A). This is the principle difference in the methodology between my thesis study and the previous periodic gene analysis in single-cell systems. Synchronization by arrest-release (e.g., double-thymidine block) has been widely used and was thought to be the only approach for sorting cells from different cell cycle phases. However, arguments have been raised about the method: whether the cells are actually synchronized and whether the apparent periodic expression is a result of chance fluctuations or stress from the treatments, especially when large variations were observed with replicate experiments (Shedden and Cooper, 2002). These concerns were addressed in this study by directly sorting the cell from a near natural state after a quick dissociation, without artificial synchronization. Based on repeated post-sort analysis between experiments (Figure 3-1) and microscopic examination, I believe that we can apply FACS in live wing disc cells to reliably separate them based on their cell cycle phase. Moreover, using my optimized FACS-microarray technique instead of synchronization methods, the genes we identified are clearly cell-cycle related, but not due to the induction of synchrony. Potentially, a similar approach could be applied to other tissue types for cell-cycle associated gene analysis, or other gene expression studies.

#### 4.1.1.2 Triplicates and two genetic backgrounds validate the general strategy to robustly identify periodic genes

Previous studies in single-cell systems have revealed that periodic transcription of individual genes varies greatly among experiments (Jensen *et al.*, 2006). Hence, it was argued that some differences in the gene expression measurements could arise from chance fluctuations (Shedden and Cooper, 2002) and in some systems, the numerous cell-cycle-dependent expressed genes identified may come from experimental noise. In my experiments, three biological replicates were examined for each sample, and a stringent statistical test was applied to define the significant cyclic genes in wing disc cells or S2 cells (adjusted p value $< 0.05$). In this way, we have defined over 700 cyclic genes in wing disc cells,

over 600 cyclic genes in S2 cells, as well as over 100 common cyclic genes between the two systems, in which a large number of well-known cell cycle genes were identified, validating the general strategy. Moreover, by comparing G1 and G2/M wing disc cells from distinct genetic backgrounds, we eliminated the possibility that the identified cell cycle-associated transcripts were simply a product of random noise (Figure 3-6). These findings validate a general methodology for future studies while demonstrating the robustness of global periodic transcription in the developing wing disc.

### 4.1.2 Periodic transcription is a highly robust process and not a stochastic event

#### 4.1.2.1 Periodic transcription is robust and context-dependent

The periodic expression patterns of many conserved genes vary greatly among systems derived from distantly related organisms (Jensen *et al.*, 2006; Rustici *et al.*, 2004). Despite the evolutionary distance, these single-cell systems are also derived from distinct cell or tissue contexts. Thus, it is unclear if the expression differences can be purely explained by evolution, or different contexts, or moreover, a stochastic process. To answer these questions, we compared the periodic transcriptome between different cell contexts of the same organism, as well as the same cellular context in two distinct genetic backgrounds. To accomplish this, *Drosophila* S2 cells were analyzed in parallel with wild-type wing disc cells from distinct *OreR* and $w^{1118}$ backgrounds. From these comparisons, my results suggest that periodic transcription is robust within the same cell context, but also has great context-specificity.

#### 4.1.2.2 Periodic gene expression in G1/S is primarily controlled by E2F

How is robust but context-specific periodic transcription achieved? By searching the upstream regulatory regions of the identified periodic genes using computational analysis, we identified (*de novo*) a strong enrichment for E2F binding sites among G1 genes, but no consensus motifs related to G2 expression (Figure 3-10). Further, we observed a tight

correlation between G1 expression, G1 function, and physical interaction between proteins involved in DNA replication (Figure 3-24), and again, no such correlation in G2. This suggests that the waves of periodic gene expression primarily reflect the action of E2F during G1/S. Interestingly, we observed differences in the nucleotide sequences of the predicted E2F binding sites from common and wing disc-specific G1 genes (Figure 3-10). This may partially explain the context specific periodic gene expression in G1 phase. More discussion of the regulation and function of periodic expression is included in the following section.

### 4.1.3 Functional implication of context-dependent periodic gene expression

#### 4.1.3.1 The periodic expression of core cell cycle genes may contribute to the control of cell cycle duration in *Drosophila*

One key functional implication of periodic gene expression is to ensure 'just-in-time' assembly, a conserved process in eukaryotes (de Lichtenberg *et al.*, 2005; Jensen *et al.*, 2006). It is therefore surprising that we identified many well-known DNA replication genes that exhibited different patterns of periodic transcription between wing disc and S2 cells (Figure 3-12 and Figure 3-13). These results demonstrate that within the same organism, cell cycle-associated transcription may vary significantly, even for genes known to be functioning in core processes. How these differences in periodic expression are achieved remains unclear, though subtle changes in binding sites for upstream regulatory factors (e.g., E2F) may play a role (Figure 3-10). The differences in the upstream binding sites identified may indicate an involvement of different transcriptional cofactors that assists the function of E2F in diverse contexts. To test the effectiveness of the different binding sites to the periodic transcription, it will be interesting to replace one form (e.g., the sequence identified upstream of the common genes) with the other (the sequence identified upstream of the wing disc-specific genes) to examine the outcomes to the transcriptional pattern.

Notably, for the two model systems we used, wing disc cells at third instar have a cell doubling time around 12 hours (Neufeld *et al.*, 1998) and S2 cells have a cell cycle of roughly 24 hours with a relatively shorter duration of G1 and a longer G2/M phase (Figure 3-1). This relative timing difference may be one of the factors underlying the differential periodic transcription in the two contexts. Conversely, the differential periodic expression of certain genes could contribute to the temporal regulation of cell division. For example, peak expression of *CDC6* during G2/M in S2 cells correlates with a longer G2/M duration. Since CDC6 stabilizes APC and delays mitosis (Boronat and Campbell, 2007; Bueno and Russell, 1992), we reason that the periodic expression of *CDC6* could contribute to the control of cell cycle length in *Drosophila.*

#### 4.1.3.2 Context-dependent cell cycle regulation at the post-translational level and its disease implications

Differential regulation of periodic transcription (as we report in wing disc and S2 cells) is not likely to be the only way of controlling context-dependent cell cycle regulation. Interestingly, periodically expressed subunits of protein complexes involved in core cell-cycle processes (e.g., DNA replication, mitosis) are proposed to be three times as likely to be phosphorylated as constitutively expressed components (Jensen *et al.*, 2006). Through the lens of my results, this raises the intriguing possibility that there may also be significant context-dependent regulation at the post-translational level.

These findings have some potential implications for human health. For example, Meier-Gorlin syndrome is a disease caused by mutations in pre-RC complex components but is associated with tissue-specific effects, such as reduced ear size (Bicknell *et al.*, 2011a; Bicknell *et al.*, 2011b; Guernsey *et al.*, 2011). A deeper understanding of context-specific cell cycle regulation could shed light on the tissue-specific effects in such conditions. It may also provide further insight into context-dependent features of cell cycle progression during proliferative disease.

#### 4.1.3.3 The periodic gene expression and function correlated on a genome-wide scale

This thesis project suggests a correlation between periodic gene expression and function on a genome-wide scale. In the developing wing, we found that a significantly higher percentage of wing disc periodic gene knockdowns (78.5%) produced a wing phenotype compared with either randomly selected (52.2%) or S2-specific periodic genes (48.5%). The detailed analyses are included in Table S5 and S6. Consistently, based on published S2 RNAi screen data, we found that the S2 periodic genes were more likely to be required for S2 cell proliferation or cell cycle phasing. Specifically, among common and S2 specific periodic genes, 3.5% (9/257) showed either G1 or G2 phasing defects, whereas in wing disc specific periodic genes, only 2.5% (5/200) showed cell cycle phasing defects. We have included this comparison in Table S8. However, since there were a very limited number of genes identified in the published S2 screen, there is not sufficient data to make a blanket statement on the correlation between periodic gene expression and function in S2 cells.

Following the finding of context-specific periodic gene expression, in the future, it will be of great interest to dissect the functional significance of periodic transcription on a global scale *in vivo*. However, this is a hard question and may not have a common answer for all periodic genes. Hypothetically, in some cases, periodic transcription may not be functionally necessary, but may simply serve to limit needless transcription and thus optimize cellular energy homeostasis (only expressing DNA replication proteins when they are required, for example). Thus, the functional importance of periodic transcription can not be determined from a few individual gene examples. Technically, simply replacing a periodic promoter with a constitutive (non-periodic) or opposite-phase promoter would not guarantee a similar expression level, which could complicate the interpretation of any observed phenotypes. This kind of experiment must be carefully designed to conduct, control and interpret.

In conclusion, this thesis project opens up many interesting questions about the regulation and function of periodic expression, especially in terms of context-specificity. For the current study, my primary objective was to use periodic patterns of gene expression as a potential indicator for genes involved in cell proliferation *in vivo*. Indeed, this approach led me to identify a number of novel periodic genes required for wing development, cell cycle phasing, mitotic regulation, and novel genes specifically involved in IKNM.

## *4.2* Periodically expressed genes represent good candidates for cell cycle related screens *in vivo*

### 4.2.1 Periodically expressed genes represent good candidates for a cell cycle screen

#### 4.2.1.1 Novel periodic genes were identified functioning in cell proliferation

As I discussed in the previous section, periodically expressed genes were enriched for factors required for normal cell cycle phasing in the developing wing disc. A previous genome-wide screen in S2 cells using a similar flow cytometry approach found that roughly 4% of all genes screened were required for cell cycle progression, cell size or apoptosis (Bjorklund *et al.*, 2006). Here, by functionally screening 311 periodically expressed genes *in vivo*, we identified over a hundred factors involved in wing growth and 39 (among 120 genes screened by flow cytometry) required for normal cell cycle phasing. Among the 39 periodic genes required for normal cell cycle phasing in the wing disc, only four were previously identified by S2 cell-based screening approaches (Bjorklund *et al.*, 2006; Gilsdorf *et al.*, 2010). The subset identified only in my screen included some very well-studied cell cycle genes, including *pcna*, *Separase* and *Rbf* (Table 3-1), which validated my *in vivo* approach. I have also identified numerous uncharacterized periodically expressed genes required for normal cell cycle phasing *in vivo*, such as *CG10200, CG31344, CG16734, CG8080, CG31133* and *CG14781*, in addition to several factors not previously known to

have a role in cell cycle progression (Figure 3-22 and Table 3-1). Currently, none of these factors are known to be periodically expressed and none have been implicated in the regulation of cell cycle progression (even in S2 RNAi screens).

#### 4.2.1.2 The potential of the *in vivo* screen approach

The differential identification of these and other factors from my screen and previous S2 screens may simply be due to differences in RNAi efficiency or other technical discrepancies between the two systems. It is also possible that the cell cycle machinery is more sensitive to gene expression levels in the developmental context. Nevertheless, my ability to identify both known and novel cell cycle genes confirms the potential of the *in vivo* approach. Since I only tested approximately 20% of the total wing disc periodic genes by flow cytometry and confocal imaging, additional periodic genes regulating cell proliferation may yet be identified.

### 4.2.2 Wing disc-specific periodic genes include candidates that link the cell cycle with epithelial development

In addition to the identification of cell cycle genes in the developing wing, by screening periodically expressed genes *in vivo*, we also identified interesting candidates that link the cell cycle with other aspects of epithelial development. Here, I discuss examples of periodic genes and their functions in developmental signaling, epithelial architecture and polarity.

#### 4.2.2.1 The wing disc-specific G2 periodic gene, *CG10200*, potentially links cell cycle progression with the Hh signaling pathway

Among the periodic genes that were periodically expressed in the wing disc but not in S2 cells (wing disc-specific periodic genes), one G2 gene, *CG10200*, potentially links the cell cycle with the Hh signaling pathway. From flow cytometry analysis, we observed the *CG10200* knockdown produced an increased S and G2/M phase phenotype (Figure 3-

22). Interestingly, *CG10200* RNA expression exhibited a Hh signaling-related pattern in the wing imaginal disc (Figure 3-8). We have hypothesized that *CG10200* could be a downstream factor of Hh signaling, by which its periodic expression may link wing disc signaling events with cell cycle and growth *in vivo*. Indeed, a very recent report confirmed that *CG10200* responds to ectopic Hh signaling in the wing disc (Ibrahim *et al.*, 2013). As a future direction, it would be interesting to understand how *CG10200* links Hh developmental signaling with G2 phase of the cell cycle.

#### 4.2.2.2 *RnrS* and *RPA2* are essential for maintaining normal mitotic cell size and epithelial architecture

In addition to wing disc-specific periodic genes that link the cell cycle with wing development, common periodic genes in the epithelial context could also control tissue-specific developmental aspects. From confocal imaging analysis, I identified two G1 common genes, *RnrS* (Ribonucleoside diphosphate reductase small subunit) and *RPA2* (Replication protein A2), that not only control mitosis, but are also important for maintaining a normal mitotic cell size (Figure 3-34 and Figure 3-35) and the epithelial architecture (Figure 3-36). Both genes directly function in the process of DNA replication. Incomplete DNA replication (low DNA staining signal) may trigger a cell cycle arrest in both knockdowns, which led to a cell size increase. Indeed, I observed enlarged epithelial cells in wing discs with knockdowns of some other DNA replication factors, such as *CDC45L*, *dpa*, *pcna* (Figure 3-29 and Figure 3-30), and *cyclin E* (data not shown). Intriguingly, including cases with a very strong cell cycle arrest (e.g., *cyclin E* RNAi; Figure 3-23), *RnrS* and *RPA2* represent the two examples with the largest cell size increases (cell volume became eight times larger than that of normal cells; Figure 3-34). It is equally interesting that only in *RnrS* and *RPA2* RNAi wing discs, we observed that the enlarged epithelial cells were often extruded from the epithelium during mitosis. In the future, phenotypically, we can look into the dynamics of the apical extrusion (and floating; Figure 3-35) by live imag-

ing. Mechanistically, we can examine if this extrusion is a cell-autonomous process by generating mosaic clones among control cells. We can also examine whether cell adhesion complex levels and localization dynamics may play a role in this apical mitotic extrusion process in both control and discs with enlarged cells. Neither *RnrS* nor *RPA2* have been identified in previous RNAi screens in S2 cells, but both of them came out as targets from a recent *in vivo* screen using the nervous system. Knockdown of either gene produces a larger cell size in neuroblast cells (Neumuller *et al.*, 2011), a similar effect to what we have seen in the developing wing discs. This again validates the merits of *in vivo* screen approaches.

#### 4.2.2.3 The tumor suppressor genes, *dlg1* and *scrib* are periodically expressed during G1 phase

There are other examples of periodic genes identified in my screens that link with epithelial development. For example, *dlg1* and *scrib* have been well documented as tumor suppressor genes in the DLG1/SCRIB complex, controlling both tissue growth and cell polarity (Bilder *et al.*, 2000). However, specifically, how they directly interact with the cell cycle machinery remains unclear. Here, we showed that *dlg1* and *scrib* are regulated in a cell cycle-dependent manner at the gene expression level (*dlg1*: G1-Common, and *scrib*: G1-WD specific), and knockdown of both induced interruption of cell cycle progression or cell growth. Moreover, we identified potential E2F binding sites *de novo* from the upstream regulatory region of *dlg1*. This suggests that the activity of the DLG1/SCRIB complex may not only be directly regulated by the cell cycle, but important for normal cell cycle phasing and cell size control. Along similar lines, it has been observed that the localization and stability of DLG1 protein is regulated in a cell cycle-dependent manner. This regulation may be directly controlled at the phosphorylation sites of DLG1 by CDK proteins (Narayan *et al.*, 2009). In the future, it would be interesting to extend the functional study from using ectopic expressing constructs and cultured cell lines, and test the cell cy-

cle-dependent regulation of DLG1/SCRIB complex in a tissue context, potentially linking with epithelial polarity.

### 4.2.3 Wing disc-specific periodic genes also include factors involved in myoblast or neuronal precursor development

Does every gene identified in my microarray cyclically express in the developing wing disc? We believe most of them do, as most of the epithelial cells are still actively proliferating at the stage we did the microarray, and by RNA *in situ* hybridization, we know many of the genes express ubiquitously in the wing disc. Besides, many of them show periodic expression pattern in the developing eye imaginal disc. However, from my microarray experiment, I also identified an additional type of gene expressed in specific small groups of cells. In the developing wing disc, there is a group of cells in the neuronal lineage which arrest early in G2 phase (Johnston and Edgar, 1998). Among wing disc cyclic G2 genes, we have indeed identified the known proneural genes *achaete* and *scute* (Cubas *et al.*, 1991; Skeath and Carroll, 1991), as well as novel gene *CG3168*, encoding a protein with major facilitator superfamily domain, which is predominantly expressed in cells with neuronal identify (Figure 3-9). Interestingly, among wing disc cyclic G1 genes, we also identified genes with known expression patterns and functions in the myoblast cell lineage of the adepithelial layer, such as *Twist*, *mef2*, the fly FGF receptor Heartless/DFR1 (Emori and Saigo, 1993; Shishido *et al.*, 1993), *Him* (Butler *et al.*, 2003; Rebeiz *et al.*, 2002). We have also discovered a novel myoblast gene, *Sox100B*, by *in situ* hybridization (Figure 3-9), which has transcription factor activity and was previously linked with male gonad development (DeFalco *et al.*, 2003). This suggests that the wing disc associated myoblast cells may arrest in G1/G0 phase at the third instar larval stage as in other myoblast systems. These suggest my microarray data not only identified cyclic genes in the developing wing disc, but also defined a group of genes involved in myoblast or neuronal precursor cell development, which express in specific cell types due to early cell cycle arrests. In the

future, it will be interesting to confirm the lineage-specific expression of target genes using myoblast and neuronal precursor specific markers (FISH or double-staining).

A few genes in this category also show defects in cell cycle phasing. Those genes could either control cell division of cells in disc proper non-autonomously or they have a ubiquitous low-level expression in the disc proper. However, we also can not rule out the possibility that the cell cycle phasing phenotypes we observed are owing to potential off-target effect of certain RNAi lines.

## 4.3 Periodic genes provide novel insights into IKNM

### 4.3.1 The putative lncRNA *CR32027* potentially links cell cycle progression with centrosome dynamics and nuclear movement

Although the underlying molecular mechanisms are still largely unclear, IKNM is a critical process that ensures the apical mitotic rounding of polarized epithelial cells. In this respect, IKNM represents a facet of cell proliferation control that can only be fully understood *in vivo*. From my list of periodically expressed genes, two candidates were implicated in the regulation of IKNM in the developing wing disc. Both *CR32027* (which encodes a long ncRNA) and *CG10479* (which encodes a novel SH2-domain containing protein) showed ubiquitous expression in the wing disc (Figure S2A) and exhibited elevated G1 phase expression only in the wing disc and not in the S2 cells. The knockdown of both genes by RNAi caused wing growth defects (Figure 3E and Table S3) and led to a significant increase in basal mitotic nuclei without a corresponding disruption of epithelial integrity (Figure 6A and Figure 6B).

I have obtained additional RNAi lines targeting *CG10479* from the NIG stock center, knockdown of which showed a different adult wing phenotype from the VDRC stock (wing notching rather than growth defects). The NIG lines target the conserved SH2 domain, and may therefore have significant off target effects. The conserved SH2 domain is avoided in the sequence of the VDRC line that we used for the study. Although I could not

validate requirements for *CG10479* with multiple RNAi constructs, my data suggest that it controls mitotic rounding upstream of the known actomyosin contractility cassette (Meyer et al., 2011). In contrast, it appears that *CR32027* functions through an independent mechanism, perhaps related to the regulation of MTOC localization and centrosome function (Figure 7A, Figure 7C-7G, and Figure S6D-S6F).

Notably, the periodic genes *CG10479* and *CR32027* are required for IKNM, while they produced no cell cycle or cell size defects after knockdown in S2 cells (Bjorklund *et al.*, 2006). In the future, it would be reasonable to extend my confocal screen for IKNM defects to the 401 additional periodic genes identified in wing disc (which were also not screened for defects in wing growth).

### 4.3.2 Periodic expression of *CR32027* potentially controls IKNM through a temporal control in Klp54D abundance

Mechanistically, *CR32027* may regulate the process of IKNM through transcriptional regulation of the kinesin family motor protein, Klp54D (Figure 3-46). Interestingly, 216 putative lncRNA were identified in human cells that exhibit periodic expression during the cell cycle (Hung *et al.*, 2011). One recently identified periodically expressed lncRNA, MALAT1 controls expression of multiple targets, including the centromere-associated kinesin-like protein, CENPE (Tripathi *et al.*, 2013). A number of kinesin-like proteins (e.g., Xklp2, kinesin-12/KIF15) localize to the spindle poles and regulate centrosome separation in *Xenopus*, mouse embryos, and human cells (Boleti *et al.*, 1996; Courtois *et al.*, 2012; Sturgill and Ohi, 2013). In addition, a stronger *CR32027* knockdown effect was observed using *nubbin*-GAL4, wherein mitotic spindle poles were splayed out and the splayed MTs were anchored to the cell cortex (Figure 4-1 and Figure 4-2). This is similar to the cellular phenotype of kinesin RNAi in S2 cells (Goshima and Vale, 2003). Based on my results, elevated G1 expression of the putative long non-coding RNA *CR32027* could play a temporal role in controlling the microtubule motor protein Klp54D abundance, thus linking

cell cycle progression with centrosome dynamics and nuclear movement. Future study is needed to characterize the motor protein function of Klp54D in detail, such as its localization and motion direction on the MT. We hypothesize that it could function as a MT plus end motor that locates at the apical centrosomes and pull the MT with the mitotic nuclei, or it may serve as a minus end motor protein that transport the nuclei along the MT to the apical centrosomes. Along similar lines of motor protein function in IKNM, it was recently reported that dynein is recruited to nuclei during G2 to drive IKNM in the vertebrate neocortex (Hu *et al.*, 2013). Combined, these independent results suggest that the cell cycle phase-specific regulation of motor proteins could be a conserved feature of cell proliferation in epithelial tissues.

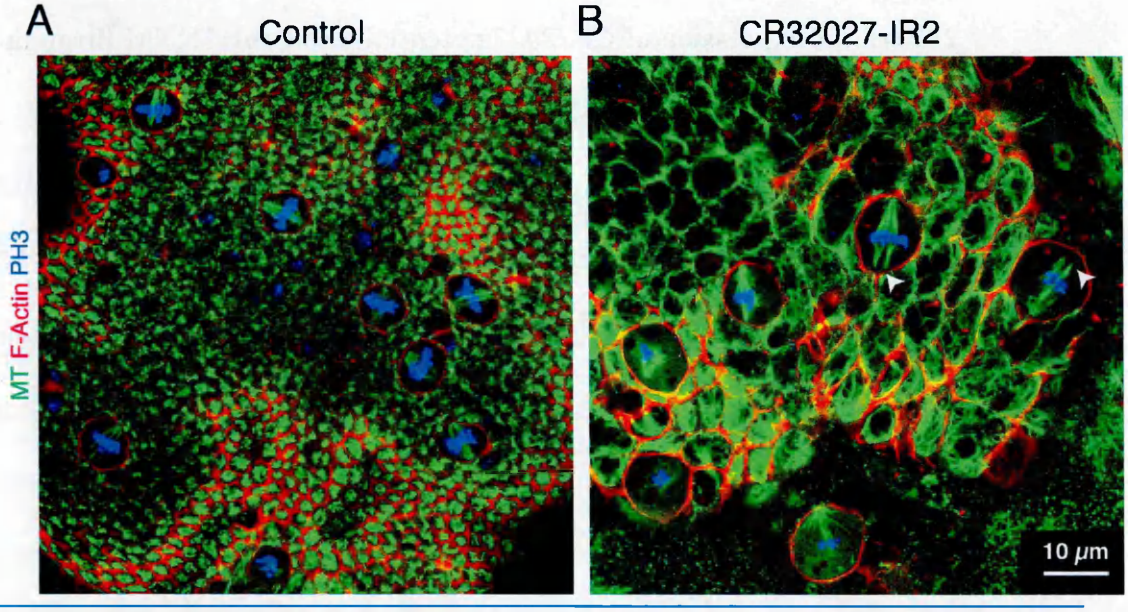


**Figure 4-1 The splayed spindles in metaphase cells with *CR32027* strong knockdown.**
(A) Multiple metaphase cells in a control wing disc with normal spindles.
(B) The splayed spindles (*arrowheads*) in metaphase cells of wing disc with *CR32027* strong knockdown (*UAS-dicer2*; *nubbin-GAL4>CR32027-IR2*). Note that the mitotic cells of *CR32027 RNAi* are bigger than control cells, probably due to a cell cycle delay. Samples are labeled for α-tubulin (MT, *green*), anti-PH3 (*blue*), and F-Actin (*red*). Scale bar: 10μm.

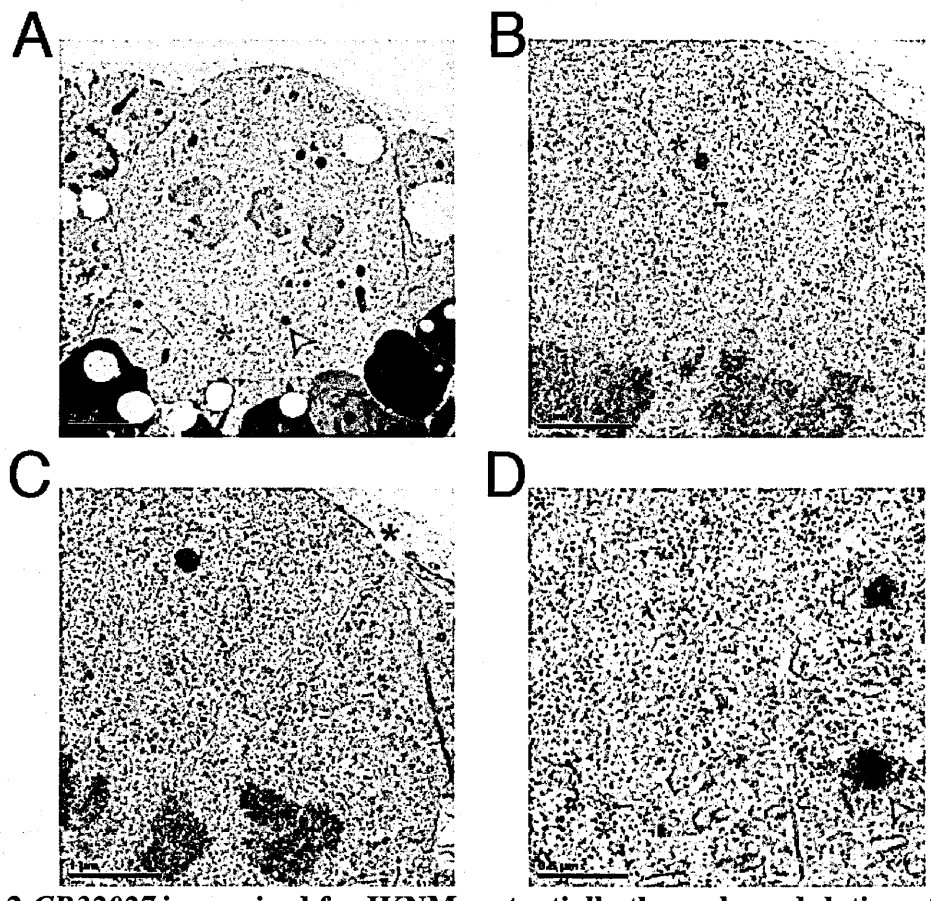


**Figure 4-2 *CR32027* is required for IKNM, potentially through modulation of centrosome function.**
TEM images of an apical localized mitotic cell in a wing disc with *CR32027* strong knockdown (driven by *UAS-dicer2, $w^{1118}$; nubbin-GAL4 > CR32027-IR2*). Images were taken at different sections to show putatively non-functional centrioles (*arrowheads*) that were not associated with MTs. Instead, bundled MTs appear to radiate into the cytoplasm from either membrane structures (*asterisks*, B and D) or the cell cortex (*asterisk*, C).

Based on our results, *CR32027* and *klp54D* is highly likely to regulate the process of IKNM independent of the actomyosin pathway (Figure 3-39 and Figure 3-40). It is interesting to notice that the p-MRLC staining is symmetric (both apical and basal to the nucleus) in the *CR32027* RNAi cells (Figure 3-39). This raised a possibility that *CR32027* might function by controlling the asymmetry distribution of myosin activity. However, due to the heterogeneity of the mitotic nuclei positioning and movement (either complete division basal or finish division at apical, Figure 3-44), detailed analysis on the distribution of active myosin is needed. Based on the current data, *CR32027* and *klp54D* probably function through controlling centrosome function. We would expect that inhibit actin dynamic by Cytochalasin D in *klp54D* RNAi wing disc may also lead to a significant increase in the

number of basally mislocalized mitotic nuclei. In the future, it will be interesting to examine if centrosome hopping and the control of MT dynamic may serve as a backup mechanism for normal IKNM regulation in the wing disc epithelium. If so, combining the MT drugs with Cytochalasin D would enhanced the IKNM defects observed with only Cytochalasin D treatment.

### 4.3.3 Another potential downstream target of *CR32027* in controlling IKNM: *piwi*

In addition to Klp54D, I also identified *piwi* as another potential target gene of *CR32027*. The expression level of *piwi* was down-regulated (four fold) after *CR32027* knockdown. Importantly, two independent RNAi lines of *piwi* phenocopied the IKNM defects observed in *CR32027* knockdowns. This is particularly interesting, since *piwi* has been mostly investigated for its function in interacting with piRNA. In germline stem cells, it promotes cell division autonomously, while it also modulates germline stem cell division through somatic expression (Cox *et al.*, 2000). Does *piwi* function in wing disc by regulating the cell cycle-specific process of IKNM? Does the potential long non-coding RNA, *CR32027* control IKNM partially through interacting with the pathways of piRNA? To answer these questions, in the future, we need to thoroughly investigate the function of piwi in the context of wing disc development, especially using *piwi* null mutants.

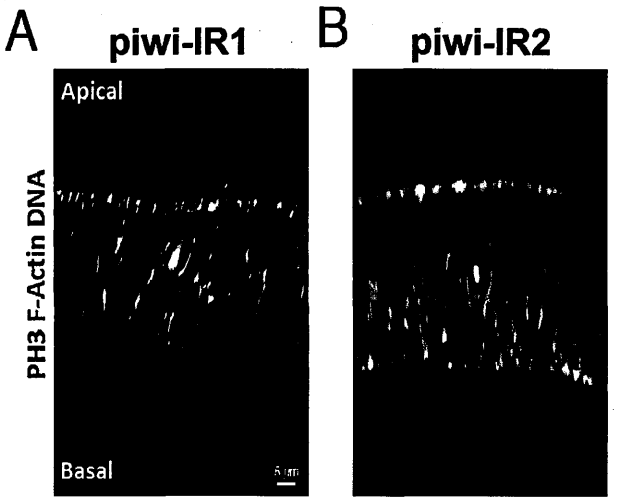


**Figure 4-3 *piwi* may be another downstream target of *CR32027* in controlling IKNM.** Basally-mislocalized mitotic nuclei (anti-PH3+, *white*) were observed in wing discs of *piwi-IR1* and *piwi-IR2* (driven by *A9-GAL4*, at 29°C). Samples were also stained for F-Actin (*red*) and DNA (*blue*). Scale bar: 5μm.

### 4.3.4 Independent mechanisms may regulate the normally associated processes of mitotic division, apical mitotic cell rounding, and mitotic nuclear migration

One of the most surprising observations was that mitotic progression can not only initiate but also reach completion at the basal side of the epithelium in *CR32027* RNAi discs (Figure 7E). To the best of our knowledge, *CR32027* RNAi represents the first separation of function between the control of mitotic nuclear position and the control of cell division itself. This indicates that apical rounding, mitosis and mitotic nuclear migration, though normally tightly associated, are regulated by partially independent mechanisms. Given the importance of these issues and their likely implications for epithelial cell division in a multitude of systems, further study of *CR32027* will be important to expand our understanding of the molecular mechanisms of IKNM. On a broader level, my genomic analyses provide a global perspective on cell cycle regulation in the *in vivo* epithelial context, at both the transcriptional and functional level. Further detailed analyses of interesting candidates and their human counterparts should improve our understanding of epithelial cell proliferation in both development and disease.

# Appendix A: Supplemental Information

## 5.1 Supplemental Tables

(All Supplemental materials can be accessed at Liang's published paper in the journal of *Developmental Cell* at http://dx.doi.org/10.1016/j.devcel.2014.02.018. Additional information and original data can be viewed at the Stowers Original Data Repository site at: http://odr.stowers.org.)

### 5.1.1 Table S1. Microarray analysis identified 8 classes of periodic genes.

Eight classes of periodic genes are listed separately, including the 6 main categories (G1-Com, G2-Com, G1-WD, G2-WD, G1-S2, and G2-S2). For each gene, the probe ID from the Affymetrix array, G1/G2 expression ratios, related p values and the adjusted p values for wing discs, S2 cells, and their differences (Diff) are listed. Genes are also annotated by their Gene Symbol, Gene Title, FlyBase ID, Representative Public ID, and associated GO terms.

### 5.1.2 Table S2. 19 transcripts showing different periodic behavior between *OreR* and $w^{1118}$ wing discs.

For each gene, probe ID from the Affymetrix array, G1/G2 expression ratios and related p values in *OreR* wing disc cells, $w^{1118}$ wing disc cells, and their differences (Diff) are listed. Genes are also annotated by their Gene Symbol, Gene Title, FlyBase ID, Representative Public ID, and associated GO terms.

### 5.1.3 Table S3. RNAi phenotypes in adult wings.

For each gene, the periodic class, gene name and RNAi lines screened (VDRC RNAi line transformant ID) are listed. For each line, the knockdown phenotypes were observed for at least 10 male and/or female progeny, and a score from 1 to 3 was given based on the phenotypic severity.

### 5.1.4 Table S4. RNAi wing phenotypes, summarized for individual genes.

For each gene, the scores of knockdown phenotypes were averaged based on two separate RNAi lines wherever possible.

### 5.1.5 Table S5. RNAi phenotypes for 66 S2-specific genes.

The periodic class, gene name and RNAi line screened (VDRC RNAi line transformant ID) are listed. For each line, knockdown phenotypes were observed for at least 10 male and/or female progeny, and a score from 1 to 3 was given based on the phenotypic severity.

### 5.1.6 Table S6. RNAi phenotypes for 67 randomly-selected genes (Random).

The periodic class, gene name and RNAi line screened (VDRC RNAi line transformant ID) are listed. For each line, knockdown phenotypes were observed for at least 10 male and/or female progeny, and a score from 1 to 3 was given based on the phenotypic severity.

### 5.1.7 Table S7. Flow cytometry results for 138 RNAi lines (120 periodic genes).

For each gene, the gene name, periodic class, and VDRC RNAi line transformant ID are listed. Flow cytometry data include $GFP^-$ and $GFP^+$ cell events, as well as cell number distributions (by percentage) in G1, S and G2/M phases based on Modfit analysis. Cell number (pos/neg, cell proliferation), G1 (pos/neg, cell cycle phasing), S (pos/neg, cell cycle phasing), and G2/M (pos/neg, cell cycle phasing) were calculated for each line by dividing the $GFP^+$ cell number by corresponding $GFP^-$ cell number.

### 5.1.8 Table S8. Summary of periodic genes identified in this study.

This table organizes data obtained during the course of my periodic expression studies, functional experiments and bioinformatic analyses. Multiple human orthologs for *Drosophila* genes or multiple GO terms under 'cell cycle' were not included here. Identified genes were manually compared with their published S2 RNAi phenotypes (Bjorklund

*et al.*, 2006). Note that the cell cycle phasing analysis in the S2 RNAi data (Bjorklund *et al.*, 2006) includes percentages of cells in G1, G2, subG1, overG2, but not S phase. *ND*, not done.

## 5.2 Supplemental Movies

### 5.2.1 Movie S1. Normal mitosis in an *ex vivo* cultured control wing disc.

Cell division was monitored with GFP-labeled centrosomes (*green, UASp-GFP-Cnn*) and RFP-labeled chromatin (*red, His2Av-mRFP*). One second represents 8 minutes in real time.

### 5.2.2 Movie S2. Aberrant mitosis following *DNA-ligI* RNAi knockdown.

Cell division was monitored with GFP-labeled centrosomes (*green, UASp-GFP-Cnn*) and RFP-labeled chromatin (*red, His2Av-mRFP*). One second represents 8 minutes in real time.

### 5.2.3 Movie S3. Aberrant mitosis following *HipHop* RNAi knockdown.

Cell division was monitored with GFP-labeled centrosomes (*green, UASp-GFP-Cnn*) and RFP-labeled chromatin (*red, His2Av-mRFP*). One second represents 8 minutes in real time.

### 5.2.4 Movie S4. Aberrant mitosis following *Deterin* RNAi knockdown.

Cell division was monitored with GFP-labeled centrosomes (*green, UASp-GFP-Cnn*) and RFP-labeled chromatin (*red, His2Av-mRFP*). Note the presence of four spindle poles. One second represents 8 minutes in real time.

### 5.2.5 Movie S5. Aberrant mitosis following *Deterin* RNAi knockdown.

Cell division was monitored with GFP-labeled centrosomes (*green, UASp-GFP-Cnn*) and RFP-labeled chromatin (*red, His2Av-mRFP*). Note the presence of eight spindle poles and that the cell failed to divide. One second represents 8 minutes in real time.

### 5.2.6 Movie S6. SPIM time-lapse movie of a representative apical cell division in an *ex vivo* cultured control wing disc.

Cell division was monitored with GFP-labeled centrosomes (*green, UASp-GFP-Cnn*) and RFP-labeled chromatin (*red, His2Av-mRFP*). One second represents 3.5 minutes in real time.

### 5.2.7 Movie S7. SPIM time-lapse movie of an aberrant basal mitotic event following *CR32027* RNAi knockdown.

Cell division was monitored with GFP-labeled centrosomes (*green, UASp-GFP-Cnn*) and RFP-labeled chromatin (*red, His2Av-mRFP*). One second represents 3.5 minutes in real time.

### 5.2.8 Movie S8. SPIM time-lapse movie of an aberrant mitosis following *CR32027* RNAi knockdown.

In this case, cell division initiated at the basal side of the epithelium, but the mitotic figure subsequently translocated to the apical surface to complete division. Cell division was monitored with GFP-labeled centrosomes (*green, UASp-GFP-Cnn*) and RFP-labeled chromatin (*red, His2Av-mRFP*). One second represents 3.5 minutes in real time.

# References


Aggarwal, B.D., and Calvi, B.R. (2004). Chromatin regulates origin activity in *Drosophila* follicle cells. Nature *430*, 372-376.

Alberts, B. (2002). Molecular biology of the cell, 4th edn (New York: Garland Science).

Aparicio, O.M., Weinstein, D.M., and Bell, S.P. (1997). Components and dynamics of DNA replication complexes in S. cerevisiae: redistribution of MCM proteins and Cdc45p during S phase. Cell *91*, 59-69.

Bailey, T.L., and Elkan, C. (1994). Fitting a mixture model by expectation maximization to discover motifs in biopolymers. Proc Int Conf Intell Syst Mol Biol *2*, 28-36.

Baker, N.E. (2001). Cell proliferation, survival, and death in the *Drosophila* eye. Seminars in cell & developmental biology *12*, 499-507.

Balasov, M., Huijbregts, R.P., and Chesnokov, I. (2009). Functional analysis of an Orc6 mutant in *Drosophila*. Proceedings of the National Academy of Sciences of the United States of America *106*, 10672-10677.

Bandura, J.L., Beall, E.L., Bell, M., Silver, H.R., Botchan, M.R., and Calvi, B.R. (2005). humpty dumpty is required for developmental DNA amplification and cell proliferation in *Drosophila*. Current biology : CB *15*, 755-759.

Barr, F.A., Sillje, H.H., and Nigg, E.A. (2004). Polo-like kinases and the orchestration of cell division. Nat Rev Mol Cell Biol *5*, 429-440.

Bartek, J., Bartkova, J., and Lukas, J. (1997). The retinoblastoma protein pathway in cell cycle control and cancer. Experimental cell research *237*, 1-6.

Basto, R., Brunk, K., Vinadogrova, T., Peel, N., Franz, A., Khodjakov, A., and Raff, J.W. (2008). Centrosome amplification can initiate tumorigenesis in flies. Cell *133*, 1032-1042.

Baumbach, J., Levesque, M.P., and Raff, J.W. (2012). Centrosome loss or amplification does not dramatically perturb global gene expression in *Drosophila*. Biol Open *1*, 983-993.

Baye, L.M., and Link, B.A. (2008). Nuclear migration during retinal development. Brain Res *1192*, 29-36.

Bell, S.P., and Dutta, A. (2002). DNA replication in eukaryotic cells. Annu Rev Biochem *71*, 333-374.

Bell, S.P., and Stillman, B. (1992). ATP-dependent recognition of eukaryotic origins of DNA replication by a multiprotein complex. Nature *357*, 128-134.

Bettencourt-Dias, M., and Goshima, G. (2009). RNAi in *Drosophila* S2 cells as a tool for studying cell cycle progression. Methods Mol Biol *545*, 39-62.

Bicknell, L.S., Bongers, E.M., Leitch, A., Brown, S., Schoots, J., Harley, M.E., Aftimos, S., Al-Aama, J.Y., Bober, M., Brown, P.A., *et al.* (2011a). Mutations in the pre-replication complex cause Meier-Gorlin syndrome. Nature genetics *43*, 356-359.

Bicknell, L.S., Walker, S., Klingseisen, A., Stiff, T., Leitch, A., Kerzendorfer, C., Martin, C.A., Yeyati, P., Al Sanna, N., Bober, M., *et al.* (2011b). Mutations in ORC1, encoding the largest subunit of the origin recognition complex, cause microcephalic primordial dwarfism resembling Meier-Gorlin syndrome. Nature genetics *43*, 350-355.

Bilder, D., Li, M., and Perrimon, N. (2000). Cooperative regulation of cell polarity and growth by *Drosophila* tumor suppressors. Science *289*, 113-116.

Bjorklund, M., Taipale, M., Varjosalo, M., Saharinen, J., Lahdenpera, J., and Taipale, J. (2006). Identification of pathways regulating cell size and cell-cycle progression by RNAi. Nature *439*, 1009-1013.

Blower, M.D., and Karpen, G.H. (2001). The role of *Drosophila* CID in kinetochore formation, cell-cycle progression and heterochromatin interactions. Nature cell biology *3*, 730-739.

Boleti, H., Karsenti, E., and Vernos, I. (1996). Xklp2, a novel Xenopus centrosomal kinesin-like protein required for centrosome separation during mitosis. Cell *84*, 49-59.

Boronat, S., and Campbell, J.L. (2007). Mitotic Cdc6 stabilizes anaphase-promoting complex substrates by a partially Cdc28-independent mechanism, and this stabilization is suppressed by deletion of Cdc55. Mol Cell Biol *27*, 1158-1171.

Boutros, M., Kiger, A.A., Armknecht, S., Kerr, K., Hild, M., Koch, B., Haas, S.A., Paro, R., Perrimon, N., and Heidelberg Fly Array, C. (2004). Genome-wide RNAi analysis of growth and viability in *Drosophila* cells. Science *303*, 832-835.

Brown, K.S., Blower, M.D., Maresca, T.J., Grammer, T.C., Harland, R.M., and Heald, R. (2007). Xenopus tropicalis egg extracts provide insight into scaling of the mitotic spindle. The Journal of cell biology *176*, 765-770.

Brust-Mascher, I., Sommi, P., Cheerambathur, D.K., and Scholey, J.M. (2009). Kinesin-5-dependent poleward flux and spindle length control in *Drosophila* embryo mitosis. Mol Biol Cell *20*, 1749-1762.

Bryant, P.J. (1974). Determination and pattern formation in the imaginal discs of *Drosophila*. Current topics in developmental biology *8*, 41-80.

Bryant, P.J. (1975). Regeneration and duplication in imaginal discs. Ciba Foundation symposium *0*, 71-93.

Budirahardja, Y., and Gonczy, P. (2009). Coupling the cell cycle to development. Development *136*, 2861-2872.

Bueno, A., and Russell, P. (1992). Dual functions of CDC6: a yeast protein required for DNA replication also inhibits nuclear division. EMBO J *11*, 2167-2176.

Butler, M.J., Jacobsen, T.L., Cain, D.M., Jarman, M.G., Hubank, M., Whittle, J.R.S., Phillips, R., and Simcox, A. (2003). Discovery of genes with highly restricted expression patterns in the *Drosophila* wing disc using DNA oligonucleotide microarrays. Development *130*, 659-670.

Campbell, G., and Tomlinson, A. (1999). Transducing the Dpp morphogen gradient in the wing of *Drosophila*: regulation of Dpp targets by brinker. Cell *96*, 553-562.

Capdevila, J., and Guerrero, I. (1994). Targeted expression of the signaling molecule decapentaplegic induces pattern duplications and growth alterations in *Drosophila* wings. EMBO J *13*, 4459-4468.

Cappello, S., Attardo, A., Wu, X., Iwasato, T., Itohara, S., Wilsch-Brauninger, M., Eilken, H.M., Rieger, M.A., Schroeder, T.T., Huttner, W.B., *et al.* (2006). The Rho-GTPase cdc42 regulates neural progenitor fate at the apical surface. Nat Neurosci *9*, 1099-1107.

Chan, G.K., Liu, S.T., and Yen, T.J. (2005). Kinetochore structure and function. Trends in cell biology *15*, 589-598.

Chenn, A., Zhang, Y.A., Chang, B.T., and McConnell, S.K. (1998). Intrinsic polarity of mammalian neuroepithelial cells. Mol Cell Neurosci *11*, 183-193.

Cho, R.J., Campbell, M.J., Winzeler, E.A., Steinmetz, L., Conway, A., Wodicka, L., Wolfsberg, T.G., Gabrielian, A.E., Landsman, D., Lockhart, D.J., *et al.* (1998). A genome-wide transcriptional analysis of the mitotic cell cycle. Molecular cell *2*, 65-73.

Cho, R.J., Huang, M., Campbell, M.J., Dong, H., Steinmetz, L., Sapinoso, L., Hampton, G., Elledge, S.J., Davis, R.W., and Lockhart, D.J. (2001). Transcriptional regulation and function during the human cell cycle. Nature genetics *27*, 48-54.

Ciosk, R., Zachariae, W., Michaelis, C., Shevchenko, A., Mann, M., and Nasmyth, K. (1998). An ESP1/PDS1 complex regulates loss of sister chromatid cohesion at the metaphase to anaphase transition in yeast. Cell *93*, 1067-1076.

Cline, M.S., Smoot, M., Cerami, E., Kuchinsky, A., Landys, N., Workman, C., Christmas, R., Avila-Campilo, I., Creech, M., Gross, B., *et al.* (2007). Integration of biological networks and gene expression data using Cytoscape. Nat Protoc *2*, 2366-2382.

Cocker, J.H., Piatti, S., Santocanale, C., Nasmyth, K., and Diffley, J.F. (1996). An essential role for the Cdc6 protein in forming the pre-replicative complexes of budding yeast. Nature *379*, 180-182.

Cohen, S.M. (1993). Imaginal Disc Development. In "The Development of *Drosophila* melanogaster". (ed. M. Bate and A. Martinez Arias). *2*, 747-841.

Coleman, T.R., Carpenter, P.B., and Dunphy, W.G. (1996). The Xenopus Cdc6 protein is essential for the initiation of a single round of DNA replication in cell-free extracts. Cell *87*, 53-63.

Courtois, A., Schuh, M., Ellenberg, J., and Hiiragi, T. (2012). The transition from meiotic to mitotic spindle assembly is gradual during early mammalian development. The Journal of cell biology *198*, 357-370.

Cox, D.N., Chao, A., and Lin, H. (2000). piwi encodes a nucleoplasmic factor whose activity modulates the number and division rate of germline stem cells. Development *127*, 503-514.

Cramer, L.P., and Mitchison, T.J. (1997). Investigation of the mechanism of retraction of the cell margin and rearward flow of nodules during mitotic cell rounding. Mol Biol Cell *8*, 109-119.

Cronin, S.J., Nehme, N.T., Limmer, S., Liegeois, S., Pospisilik, J.A., Schramek, D., Leibbrandt, A., Simoes Rde, M., Gruber, S., Puc, U., *et al.* (2009). Genome-wide RNAi

screen identifies genes involved in intestinal pathogenic bacterial infection. Science *325*, 340-343.

Cruz, C., Glavic, A., Casado, M., and de Celis, J.F. (2009). A gain-of-function screen identifying genes required for growth and pattern formation of the *Drosophila* melanogaster wing. Genetics *183*, 1005-1026.

Cubas, P., de Celis, J.F., Campuzano, S., and Modolell, J. (1991). Proneural clusters of achaete-scute expression and the generation of sensory organs in the *Drosophila* imaginal wing disc. Genes Dev *5*, 996-1008.

Dahmann, C., Diffley, J.F., and Nasmyth, K.A. (1995). S-phase-promoting cyclin-dependent kinases prevent re-replication by inhibiting the transition of replication origins to a pre-replicative state. Curr Biol *5*, 1257-1269.

Danis, E., Brodolin, K., Menut, S., Maiorano, D., Girard-Reydet, C., and Mechali, M. (2004). Specification of a DNA replication origin by a transcription complex. Nat Cell Biol *6*, 721-730.

Datar, S.A., Jacobs, H.W., de la Cruz, A.F., Lehner, C.F., and Edgar, B.A. (2000). The *Drosophila* cyclin D-Cdk4 complex promotes cellular growth. EMBO J *19*, 4543-4554.

Davidson, G., Shen, J., Huang, Y.L., Su, Y., Karaulanov, E., Bartscherer, K., Hassler, C., Stannek, P., Boutros, M., and Niehrs, C. (2009). Cell cycle control of wnt receptor activation. Developmental cell *17*, 788-799.

de Lichtenberg, U., Jensen, L.J., Brunak, S., and Bork, P. (2005). Dynamic complex formation during the yeast cell cycle. Science *307*, 724-727.

DeFalco, T.J., Verney, G., Jenkins, A.B., McCaffery, J.M., Russell, S., and Van Doren, M. (2003). Sex-specific apoptosis regulates sexual dimorphism in the *Drosophila* embryonic gonad. Developmental cell *5*, 205-216.

Del Bene, F., Wehman, A.M., Link, B.A., and Baier, H. (2008). Regulation of neurogenesis by interkinetic nuclear migration through an apical-basal notch gradient. Cell *134*, 1055-1065.

Delon, I., Chanut-Delalande, H., and Payre, F. (2003). The Ovo/Shavenbaby transcription factor specifies actin remodelling during epidermal differentiation in *Drosophila*. Mechanisms of development *120*, 747-758.

Diaz-Benjumea, F.J., and Cohen, S.M. (1995). Serrate signals through Notch to establish a Wingless-dependent organizer at the dorsal/ventral compartment boundary of the *Drosophila* wing. Development *121*, 4215-4225.

Dietzl, G., Chen, D., Schnorrer, F., Su, K.C., Barinova, Y., Fellner, M., Gasser, B., Kinsey, K., Oppel, S., Scheiblauer, S., *et al.* (2007). A genome-wide transgenic RNAi library for conditional gene inactivation in *Drosophila*. Nature *448*, 151-156.

Dimova, D.K., Stevaux, O., Frolov, M.V., and Dyson, N.J. (2003). Cell cycle-dependent and cell cycle-independent control of transcription by the *Drosophila* E2F/RB pathway. Genes & development *17*, 2308-2320.

Dogterom, M., and Yurke, B. (1997). Measurement of the force-velocity relation for growing microtubules. Science *278*, 856-860.

Donovan, S., Harwood, J., Drury, L.S., and Diffley, J.F. (1997). Cdc6p-dependent loading of Mcm proteins onto pre-replicative chromatin in budding yeast. Proc Natl Acad Sci U S A *94*, 5611-5616.

Dumont, S., and Mitchison, T.J. (2009). Force and length in the mitotic spindle. Curr Biol *19*, R749-761.

Duronio, R.J., and O'Farrell, P.H. (1995). Developmental control of the G1 to S transition in *Drosophila*: cyclin Eis a limiting downstream target of E2F. Genes Dev *9*, 1456-1468.

Duronio, R.J., and Xiong, Y. (2013). Signaling pathways that control cell proliferation. Cold Spring Harbor perspectives in biology *5*, a008904.

Dyson, N. (1998). The regulation of E2F by pRB-family proteins. Genes & development *12*, 2245-2262.

Edgar, B.A., and O'Farrell, P.H. (1989). Genetic control of cell division patterns in the *Drosophila* embryo. Cell *57*, 177-187.

Ellefson, M.L., and McNally, F.J. (2009). Kinesin-1 and cytoplasmic dynein act sequentially to move the meiotic spindle to the oocyte cortex in Caenorhabditis elegans. Mol Biol Cell *20*, 2722-2730.

Emori, Y., and Saigo, K. (1993). Distinct expression of two *Drosophila* homologs of fibroblast growth factor receptors in imaginai discs. FEBS Letters *332*, 111-114.

Feger, G. (1999). Identification and complete cDNA sequence of the missing *Drosophila* MCMs: DmMCM3, DmMCM6 and DmMCM7. Gene *227*, 149-155.

Foe, V.E. (1989). Mitotic domains reveal early commitment of cells in *Drosophila* embryos. Development *107*, 1-22.

Freeman, M. (1996). Reiterative use of the EGF receptor triggers differentiation of all cell types in the *Drosophila* eye. Cell *87*, 651-660.

Funabiki, H., Kumada, K., and Yanagida, M. (1996). Fission yeast Cut1 and Cut2 are essential for sister chromatid separation, concentrate along the metaphase spindle and form large complexes. EMBO J *15*, 6617-6628.

Gambello, M.J., Darling, D.L., Yingling, J., Tanaka, T., Gleeson, J.G., and Wynshaw-Boris, A. (2003). Multiple dose-dependent effects of Lis1 on cerebral cortical development. J Neurosci *23*, 1719-1729.

Gao, G., Walser, J.C., Beaucher, M.L., Morciano, P., Wesolowska, N., Chen, J., and Rong, Y.S. (2010). HipHop interacts with HOAP and HP1 to protect *Drosophila* telomeres in a sequence-independent manner. EMBO J *29*, 819-829.

Garcia-Bellido, A., and Merriam, J.R. (1971). Parameters of the wing imaginal disc development of *Drosophila* melanogaster. Developmental biology *24*, 61-87.

Garcia-Bellido, A., Ripoll, P., and Morata, G. (1976). Developmental compartmentalization in the dorsal mesothoracic disc of *Drosophila*. Dev Biol *48*, 132-147.

Garfinkel, M.D., Lohe, A.R., and Mahowald, A.P. (1992). Molecular genetics of the *Drosophila* melanogaster ovo locus, a gene required for sex determination of germline cells. Genetics *130*, 791-803.

Gassmann, R., Carvalho, A., Henzing, A.J., Ruchaud, S., Hudson, D.F., Honda, R., Nigg, E.A., Gerloff, D.L., and Earnshaw, W.C. (2004). Borealin: a novel chromosomal passenger required for stability of the bipolar mitotic spindle. J Cell Biol *166*, 179-191.

Gavet, O., and Pines, J. (2010a). Activation of cyclin B1-Cdk1 synchronizes events in the nucleus and the cytoplasm at mitosis. The Journal of cell biology *189*, 247-259.

Gavet, O., and Pines, J. (2010b). Progressive activation of CyclinB1-Cdk1 coordinates entry to mitosis. Dev Cell *18*, 533-543.

Geng, Y., Eaton, E.N., Picon, M., Roberts, J.M., Lundberg, A.S., Gifford, A., Sardet, C., and Weinberg, R.A. (1996). Regulation of cyclin E transcription by E2Fs and retinoblastoma protein. Oncogene *12*, 1173-1180.

Gilbert, S.F. (2010). Developmental biology, 9th edn (Sunderland, Mass.: Sinauer Associates).

Gilsdorf, M., Horn, T., Arziman, Z., Pelz, O., Kiner, E., and Boutros, M. (2010). GenomeRNAi: a database for cell-based RNAi phenotypes. 2009 update. Nucleic Acids Res *38*, D448-452.

Goshima, G., and Scholey, J.M. (2010). Control of mitotic spindle length. Annual review of cell and developmental biology *26*, 21-57.

Goshima, G., and Vale, R.D. (2003). The roles of microtubule-based motor proteins in mitosis: comprehensive RNAi analysis in the *Drosophila* S2 cell line. The Journal of cell biology *162*, 1003-1016.

Goshima, G., Wollman, R., Goodwin, S.S., Zhang, N., Scholey, J.M., Vale, R.D., and Stuurman, N. (2007). Genes required for mitotic spindle assembly in *Drosophila* S2 cells. Science *316*, 417-421.

Gossen, M., Pak, D.T., Hansen, S.K., Acharya, J.K., and Botchan, M.R. (1995). A *Drosophila* homolog of the yeast origin recognition complex. Science *270*, 1674-1677.

Greenan, G., Brangwynne, C.P., Jaensch, S., Gharakhani, J., Julicher, F., and Hyman, A.A. (2010). Centrosome size sets mitotic spindle length in Caenorhabditis elegans embryos. Curr Biol *20*, 353-358.

Guernsey, D.L., Matsuoka, M., Jiang, H., Evans, S., Macgillivray, C., Nightingale, M., Perry, S., Ferguson, M., LeBlanc, M., Paquette, J., *et al.* (2011). Mutations in origin recognition complex gene ORC4 cause Meier-Gorlin syndrome. Nature genetics *43*, 360-364.

Gulyas, B.J. (1973). Cytokinesis in the rabbit zygote: fine-structural study of the contractile ring and the mid-body. The Anatomical record *177*, 195-207.

Gupta, S., Stamatoyannopoulos, J.A., Bailey, T.L., and Noble, W.S. (2007). Quantifying similarity between motifs. Genome biology *8*, R24.

Gurley, L.R., D'Anna, J.A., Barham, S.S., Deaven, L.L., and Tobey, R.A. (1978). Histone phosphorylation and chromatin structure during mitosis in Chinese hamster cells. European journal of biochemistry / FEBS *84*, 1-15.

Hamaratoglu, F., de Lachapelle, A.M., Pyrowolakis, G., Bergmann, S., and Affolter, M. (2011). Dpp signaling activity requires Pentagone to scale with tissue size in the growing *Drosophila* wing imaginal disc. PLoS Biol *9*, e1001182.

Hans, F., and Dimitrov, S. (2001). Histone H3 phosphorylation and cell division. Oncogene *20*, 3021-3027.

Hara, Y., and Kimura, A. (2009). Cell-size-dependent spindle elongation in the Caenorhabditis elegans early embryo. Current biology : CB *19*, 1549-1554.

Hartwell, L.H., and Weinert, T.A. (1989). Checkpoints: controls that ensure the order of cell cycle events. Science *246*, 629-634.

Hendzel, M.J., Wei, Y., Mancini, M.A., Van Hooser, A., Ranalli, T., Brinkley, B.R., Bazett-Jones, D.P., and Allis, C.D. (1997). Mitosis-specific phosphorylation of histone H3 initiates primarily within pericentromeric heterochromatin during G2 and spreads in an ordered fashion coincident with mitotic chromosome condensation. Chromosoma *106*, 348-360.

Hu, D.J., Baffet, A.D., Nayak, T., Akhmanova, A., Doye, V., and Vallee, R.B. (2013). Dynein recruitment to nuclear pores activates apical nuclear migration and mitotic entry in brain progenitor cells. Cell *154*, 1300-1313.

Hung, T., Wang, Y., Lin, M.F., Koegel, A.K., Kotake, Y., Grant, G.D., Horlings, H.M., Shah, N., Umbricht, C., Wang, P., *et al.* (2011). Extensive and coordinated transcription of noncoding RNAs within cell-cycle promoters. Nat Genet *43*, 621-629.

Ibrahim, D.M., Biehs, B., Kornberg, T.B., and Klebes, A. (2013). Microarray comparison of anterior and posterior *Drosophila* wing imaginal disc cells identifies novel wing genes. G3 *3*, 1353-1362.

Inoue, S., and Salmon, E.D. (1995). Force generation by microtubule assembly/disassembly in mitosis and related movements. Mol Biol Cell *6*, 1619-1640.

Irizarry, R.A., Hobbs, B., Collin, F., Beazer-Barclay, Y.D., Antonellis, K.J., Scherf, U., and Speed, T.P. (2003). Exploration, normalization, and summaries of high density oligonucleotide array probe level data. Biostatistics *4*, 249-264.

Jensen, L.J., Jensen, T.S., de Lichtenberg, U., Brunak, S., and Bork, P. (2006). Co-evolution of transcriptional and post-translational cell-cycle regulation. Nature *443*, 594-597.

Johnson, D.G., Schwarz, J.K., Cress, W.D., and Nevins, J.R. (1993). Expression of transcription factor E2F1 induces quiescent cells to enter S phase. Nature *365*, 349-352.

Johnston, L.A., and Edgar, B.A. (1998). Wingless and Notch regulate cell-cycle arrest in the developing *Drosophila* wing. Nature *394*, 82-84.

Kastan, M.B., and Bartek, J. (2004). Cell-cycle checkpoints and cancer. Nature *432*, 316-323.

Khodjakov, A., and Pines, J. (2010). Centromere tension: a divisive issue. Nat Cell Biol *12*, 919-923.

Kondo, T., and Hayashi, S. (2013). Mitotic cell rounding accelerates epithelial invagination. Nature *494*, 125-129.

Kosodo, Y., Suetsugu, T., Suda, M., Mimori-Kiyosue, Y., Toida, K., Baba, S.A., Kimura, A., and Matsuzaki, F. (2011). Regulation of interkinetic nuclear migration by cell cycle-coupled active and passive mechanisms in the developing brain. EMBO J *30*, 1690-1704.

Kroeger, P.T., Jr., Shoue, D.A., Mezzacappa, F.M., Gerlach, G.F., Wingert, R.A., and Schulz, R.A. (2013). Knockdown of SCF(Skp2) function causes double-parked accumulation in the nucleus and DNA re-replication in *Drosophila* plasmatocytes. PloS one *8*, e79019.

Lancaster, O.M., Le Berre, M., Dimitracopoulos, A., Bonazzi, D., Zlotek-Zlotkiewicz, E., Picone, R., Duke, T., Piel, M., and Baum, B. (2013). Mitotic rounding alters cell geometry to ensure efficient bipolar spindle formation. Dev Cell *25*, 270-283.

Lander, A.D., Nie, Q., Vargas, B., and Wan, F.Y. (2011). Size-normalized Robustness of Dpp Gradient in *Drosophila* Wing Imaginal Disc. Journal of mechanics of materials and structures *6*, 321-350.

Langman, J., Guerrant, R.L., and Freeman, B.G. (1966). Behavior of neuro-epithelial cells during closure of the neural tube. J Comp Neurol *127*, 399-411.

Laub, M.T., McAdams, H.H., Feldblyum, T., Fraser, C.M., and Shapiro, L. (2000). Global analysis of the genetic network controlling a bacterial cell cycle. Science *290*, 2144-2148.

Lawrence, P.A., and Morata, G. (1976). Compartments in the wing of *Drosophila*: a study of the engrailed gene. Dev Biol *50*, 321-337.

Leatherwood, J. (1998). Emerging mechanisms of eukaryotic DNA replication initiation. Curr Opin Cell Biol *10*, 742-748.

Lens, S.M., Vader, G., and Medema, R.H. (2006). The case for Survivin as mitotic regulator. Current opinion in cell biology *18*, 616-622.

Li, F., Ackermann, E.J., Bennett, C.F., Rothermel, A.L., Plescia, J., Tognin, S., Villa, A., Marchisio, P.C., and Altieri, D.C. (1999). Pleiotropic cell-division defects and apoptosis induced by interference with survivin function. Nature cell biology *1*, 461-466.

Li, F., Ambrosini, G., Chu, E.Y., Plescia, J., Tognin, S., Marchisio, P.C., and Altieri, D.C. (1998). Control of apoptosis and mitotic spindle checkpoint by survivin. Nature *396*, 580-584.

Li, X., and Nicklas, R.B. (1995). Mitotic forces control a cell-cycle checkpoint. Nature *373*, 630-632.

Lindsley, D.L., and Zimm, G.G. (1992). The genome of *Drosophila* melanogaster (San Diego: Academic Press).

Loupart, M.L., Krause, S.A., and Heck, M.S. (2000). Aberrant replication timing induces defective chromosome condensation in *Drosophila* ORC2 mutants. Current biology : CB *10*, 1547-1556.

Lyko, F., Ramsahoye, B.H., Kashevsky, H., Tudor, M., Mastrangelo, M.A., Orr-Weaver, T.L., and Jaenisch, R. (1999). Mammalian (cytosine-5) methyltransferases cause genomic DNA methylation and lethality in *Drosophila*. Nat Genet *23*, 363-366.

Maddox, A.S., and Burridge, K. (2003). RhoA is required for cortical retraction and rigidity during mitotic cell rounding. J Cell Biol *160*, 255-265.

Martin-Castellanos, C., and Edgar, B.A. (2002). A characterization of the effects of Dpp signaling on cell growth and proliferation in the *Drosophila* wing. Development *129*, 1003-1013.

Masumoto, H., Muramatsu, S., Kamimura, Y., and Araki, H. (2002). S-Cdk-dependent phosphorylation of Sld2 essential for chromosomal DNA replication in budding yeast. Nature *415*, 651-655.

Mata, J., Curado, S., Ephrussi, A., and Rorth, P. (2000). Tribbles coordinates mitosis and morphogenesis in *Drosophila* by regulating string/CDC25 proteolysis. Cell *101*, 511-522.

Menges, M., Hennig, L., Gruissem, W., and Murray, J.A. (2003). Genome-wide gene expression in an Arabidopsis cell suspension. Plant Mol Biol *53*, 423-442.

Messier, P.E., and Auclair, C. (1974). Effect of cytochalasin B on interkinetic nuclear migration in the chick embryo. Dev Biol *36*, 218-223.

Mevel-Ninio, M., Terracol, R., and Kafatos, F.C. (1991). The ovo gene of *Drosophila* encodes a zinc finger protein required for female germ line development. EMBO J *10*, 2259-2266.

Meyer, E.J., Ikmi, A., and Gibson, M.C. (2011). Interkinetic nuclear migration is a broadly conserved feature of cell division in pseudostratified epithelia. Curr Biol *21*, 485-491.

Milan, M., Campuzano, S., and Garcia-Bellido, A. (1997). Developmental parameters of cell death in the wing disc of *Drosophila*. Proc Natl Acad Sci U S A *94*, 5691-5696.

Mogilner, A., and Oster, G. (2003). Polymer motors: pushing out the front and pulling up the back. Curr Biol *13*, R721-733.

Moreno, E., Basler, K., and Morata, G. (2002). Cells compete for decapentaplegic survival factor to prevent apoptosis in *Drosophila* wing development. Nature *416*, 755-759.

Morgan, D.O. (2006). Cell Cycle: Principles of Control (New Science Press: London.).

Motzny, C.K., and Holmgren, R. (1995). The *Drosophila* cubitus interruptus protein and its role in the wingless and hedgehog signal transduction pathways. Mechanisms of development *52*, 137-150.

Moutinho-Pereira, S., Stuurman, N., Afonso, O., Hornsveld, M., Aguiar, P., Goshima, G., Vale, R.D., and Maiato, H. (2013). Genes involved in centrosome-independent mitotic spindle assembly in *Drosophila* S2 cells. Proc Natl Acad Sci U S A *110*, 19808-19813.

Moyer, S.E., Lewis, P.W., and Botchan, M.R. (2006). Isolation of the Cdc45/Mcm2-7/GINS (CMG) complex, a candidate for the eukaryotic DNA replication fork helicase. Proc Natl Acad Sci U S A *103*, 10236-10241.

Mummery-Widmer, J.L., Yamazaki, M., Stoeger, T., Novatchkova, M., Bhalerao, S., Chen, D., Dietzl, G., Dickson, B.J., and Knoblich, J.A. (2009). Genome-wide analysis of Notch signalling in *Drosophila* by transgenic RNAi. Nature *458*, 987-992.

Murciano, A., Zamora, J., Lopez-Sanchez, J., and Frade, J.M. (2002). Interkinetic nuclear movement may provide spatial clues to the regulation of neurogenesis. Mol Cell Neurosci *21*, 285-300.

Musacchio, A., and Salmon, E.D. (2007). The spindle-assembly checkpoint in space and time. Nat Rev Mol Cell Biol *8*, 379-393.

Nakajima, Y., Meyer, E.J., Kroesen, A., McKinney, S.A., and Gibson, M.C. (2013). Epithelial junctions maintain tissue architecture by directing planar spindle orientation. Nature *500*, 359-362.

Narayan, N., Massimi, P., and Banks, L. (2009). CDK phosphorylation of the discs large tumour suppressor controls its localisation and stability. J Cell Sci *122*, 65-74.

Neufeld, T.P., de la Cruz, A.F., Johnston, L.A., and Edgar, B.A. (1998). Coordination of growth and cell division in the *Drosophila* wing. Cell *93*, 1183-1193.

Neumuller, R.A., Richter, C., Fischer, A., Novatchkova, M., Neumuller, K.G., and Knoblich, J.A. (2011). Genome-wide analysis of self-renewal in *Drosophila* neural stem cells by transgenic RNAi. Cell stem cell *8*, 580-593.

Neurohr, G., Naegeli, A., Titos, I., Theler, D., Greber, B., Diez, J., Gabaldon, T., Mendoza, M., and Barral, Y. (2011). A midzone-based ruler adjusts chromosome compaction to anaphase spindle length. Science *332*, 465-468.

Ni, J.Q., Liu, L.P., Binari, R., Hardy, R., Shim, H.S., Cavallaro, A., Booker, M., Pfeiffer, B.D., Markstein, M., Wang, H., *et al.* (2009). A *Drosophila* resource of transgenic RNAi lines for neurogenetics. Genetics *182*, 1089-1100.

Norden, C., Young, S., Link, B.A., and Harris, W.A. (2009). Actomyosin is the main driver of interkinetic nuclear migration in the retina. Cell *138*, 1195-1208.

Nusslein-Volhard, C., and Wieschaus, E. (1980). Mutations affecting segment number and polarity in *Drosophila*. Nature *287*, 795-801.

Nyberg, K.A., Michelson, R.J., Putnam, C.W., and Weinert, T.A. (2002). Toward maintaining the genome: DNA damage and replication checkpoints. Annu Rev Genet *36*, 617-656.

O'Brochta, D.A., and Bryant, P.J. (1985). A zone of non-proliferating cells at a lineage restriction boundary in *Drosophila*. Nature *313*, 138-141.

Ohtani, K., DeGregori, J., and Nevins, J.R. (1995). Regulation of the cyclin E gene by transcription factor E2F1. Proc Natl Acad Sci U S A *92*, 12146-12150.

Ohtsubo, M., and Roberts, J.M. (1993). Cyclin-dependent regulation of G1 in mammalian fibroblasts. Science *259*, 1908-1912.

Oliva, A., Rosebrock, A., Ferrezuelo, F., Pyne, S., Chen, H., Skiena, S., Futcher, B., and Leatherwood, J. (2005). The cell cycle-regulated genes of Schizosaccharomyces pombe. PLoS Biol *3*, e225.

Oliver, B., Pauli, D., and Mahowald, A.P. (1990). Genetic evidence that the ovo locus is involved in *Drosophila* germ line sex determination. Genetics *125*, 535-550.

Oliver, B., Perrimon, N., and Mahowald, A.P. (1987). The ovo locus is required for sex-specific germ line maintenance in *Drosophila*. Genes Dev *1*, 913-923.

Pardo, M., and Nurse, P. (2003). Equatorial retention of the contractile actin ring by microtubules during cytokinesis. Science *300*, 1569-1574.

Pearson, R.A., Dale, N., Llaudet, E., and Mobbs, P. (2005). ATP released via gap junction hemichannels from the pigment epithelium regulates neural retinal progenitor proliferation. Neuron *46*, 731-744.

Pelham, R.J., and Chang, F. (2002). Actin dynamics in the contractile ring during cytokinesis in fission yeast. Nature *419*, 82-86.

Pflumm, M.F., and Botchan, M.R. (2001). Orc mutants arrest in metaphase with abnormally condensed chromosomes. Development *128*, 1697-1707.

Pomerening, J.R., Sontag, E.D., and Ferrell, J.E., Jr. (2003). Building a cell cycle oscillator: hysteresis and bistability in the activation of Cdc2. Nat Cell Biol *5*, 346-351.

Pospisilik, J.A., Schramek, D., Schnidar, H., Cronin, S.J., Nehme, N.T., Zhang, X., Knauf, C., Cani, P.D., Aumayr, K., Todoric, J., *et al.* (2010). *Drosophila* genome-wide obesity screen reveals hedgehog as a determinant of brown versus white adipose cell fate. Cell *140*, 148-160.

Rebeiz, M., Reeves, N.L., and Posakony, J.W. (2002). SCORE: A computational approach to the identification of cis-regulatory modules and target genes in whole-genome sequence data. Proceedings of the National Academy of Sciences *99*, 9888-9893.

Resino, J., and Garcia-Bellido, A. (2004). *Drosophila* genetic variants that change cell size and rate of proliferation affect cell communication and hence patterning. Mechanisms of development *121*, 351-364.

Resnitzky, D., Gossen, M., Bujard, H., and Reed, S.I. (1994). Acceleration of the G1/S phase transition by expression of cyclins D1 and E with an inducible system. Molecular and cellular biology *14*, 1669-1679.

Rhind, N., and Russell, P. (2012). Signaling pathways that regulate cell division. Cold Spring Harb Perspect Biol *4*.

Rieder, C.L., Cole, R.W., Khodjakov, A., and Sluder, G. (1995). The checkpoint delaying anaphase in response to chromosome monoorientation is mediated by an inhibitory signal produced by unattached kinetochores. J Cell Biol *130*, 941-948.

Rinn, J.L., and Chang, H.Y. (2012). Genome regulation by long noncoding RNAs. Annual review of biochemistry *81*, 145-166.

Robinson, M.D., McCarthy, D.J., and Smyth, G.K. (2010). edgeR: a Bioconductor package for differential expression analysis of digital gene expression data. Bioinformatics *26*, 139-140.

Rogers, S.L., and Rogers, G.C. (2008). Culture of *Drosophila* S2 cells and their use for RNAi-mediated loss-of-function studies and immunofluorescence microscopy. Nat Protoc *3*, 606-611.

Roy, S., Ernst, J., Kharchenko, P.V., Kheradpour, P., Negre, N., Eaton, M.L., Landolin, J.M., Bristow, C.A., Ma, L., Lin, M.F., *et al.* (2010). Identification of functional elements and regulatory circuits by *Drosophila* modENCODE. Science *330*, 1787-1797.

Rustici, G., Mata, J., Kivinen, K., Lio, P., Penkett, C.J., Burns, G., Hayles, J., Brazma, A., Nurse, P., and Bahler, J. (2004). Periodic gene expression program of the fission yeast cell cycle. Nature genetics *36*, 809-817.

Saeed, A.I., Bhagabati, N.K., Braisted, J.C., Liang, W., Sharov, V., Howe, E.A., Li, J., Thiagarajan, M., White, J.A., and Quackenbush, J. (2006). TM4 microarray software suite. Methods Enzymol *411*, 134-193.

Saj, A., Arziman, Z., Stempfle, D., van Belle, W., Sauder, U., Horn, T., Durrenberger, M., Paro, R., Boutros, M., and Merdes, G. (2010). A combined ex vivo and *in vivo* RNAi screen for notch regulators in *Drosophila* reveals an extensive notch interaction network. Dev Cell *18*, 862-876.

Sauer, F.C. (1935). Mitosis in the neural tube. The Journal of comparative neurology *62*, 377-405.

Sauer, M.E., and Chittenden, A.C. (1959). Deoxyribonucleic acid content of cell nuclei in the neural tube of the chick embryo: evidence for intermitotic migration of nuclei. Experimental cell research *16*, 1-6.

Sauer, M.E., and Walker, B.E. (1959). Radioautographic study of interkinetic nuclear migration in the neural tube. Proceedings of the Society for Experimental Biology and Medicine Society for Experimental Biology and Medicine *101*, 557-560.

Schenk, J., Wilsch-Brauninger, M., Calegari, F., and Huttner, W.B. (2009). Myosin II is required for interkinetic nuclear migration of neural progenitors. Proc Natl Acad Sci U S A *106*, 16487-16492.

Schneider, C.A., Rasband, W.S., and Eliceiri, K.W. (2012). NIH Image to ImageJ: 25 years of image analysis. Nature methods *9*, 671-675.

Schwank, G., and Basler, K. (2010). Regulation of Organ Growth by Morphogen Gradients. Cold Spring Harbor Perspectives in Biology *2*.

Schwank, G., Yang, S.F., Restrepo, S., and Basler, K. (2012). Comment on "Dynamics of dpp signaling and proliferation control". Science *335*, 401; author reply 401.

Sclafani, R.A., and Holzen, T.M. (2007). Cell cycle regulation of DNA replication. Annual review of genetics *41*, 237-280.

Seher, T.C., and Leptin, M. (2000). Tribbles, a cell-cycle brake that coordinates proliferation and morphogenesis during *Drosophila* gastrulation. Curr Biol *10*, 623-629.

Serrano, N., and O'Farrell, P.H. (1997). Limb morphogenesis: connections between patterning and growth. Curr Biol *7*, R186-195.

Shareef, M.M., King, C., Damaj, M., Badagu, R., Huang, D.W., and Kellum, R. (2001). *Drosophila* heterochromatin protein 1 (HP1)/origin recognition complex (ORC) protein is associated with HP1 and ORC and functions in heterochromatin-induced silencing. Mol Biol Cell *12*, 1671-1685.

Shedden, K., and Cooper, S. (2002). Analysis of cell-cycle-specific gene expression in human cells as determined by microarrays and double-thymidine block synchronization. Proceedings of the National Academy of Sciences of the United States of America *99*, 4379-4384.

Sherr, C.J., and McCormick, F. (2002). The RB and p53 pathways in cancer. Cancer cell *2*, 103-112.

Shibutani, S.T., de la Cruz, A.F., Tran, V., Turbyfill, W.J., 3rd, Reis, T., Edgar, B.A., and Duronio, R.J. (2008). Intrinsic negative cell cycle regulation provided by PIP box- and Cul4Cdt2-mediated destruction of E2f1 during S phase. Developmental cell *15*, 890-900.

Shishido, E., Higashijima, S., Emori, Y., and Saigo, K. (1993). Two FGF-receptor homologues of *Drosophila*: one is expressed in mesodermal primordium in early embryos. Development *117*, 751-761.

Sideridou, M., Zakopoulou, R., Evangelou, K., Liontos, M., Kotsinas, A., Rampakakis, E., Gagos, S., Kahata, K., Grabusic, K., Gkouskou, K., *et al.* (2011). Cdc6 expression represses E-cadherin transcription and activates adjacent replication origins. J Cell Biol *195*, 1123-1140.

Siller, K.H., and Doe, C.Q. (2009). Spindle orientation during asymmetric cell division. Nat Cell Biol *11*, 365-374.

Skeath, J.B., and Carroll, S.B. (1991). Regulation of achaete-scute gene expression and sensory organ pattern formation in the *Drosophila* wing. Genes Dev *5*, 984-995.

Smith, A.P., Henze, M., Lee, J.A., Osborn, K.G., Keck, J.M., Tedesco, D., Bortner, D.M., Rosenberg, M.P., and Reed, S.I. (2006). Deregulated cyclin E promotes p53 loss of heterozygosity and tumorigenesis in the mouse mammary gland. Oncogene *25*, 7245-7259.

Smyth, G.K. (2004). Linear models and empirical bayes methods for assessing differential expression in microarray experiments. Stat Appl Genet Mol Biol *3*, Article3.

Spear, P.C., and Erickson, C.A. (2012). Apical movement during interkinetic nuclear migration is a two-step process. Developmental biology *370*, 33-41.

Spellman, P.T., Sherlock, G., Zhang, M.Q., Iyer, V.R., Anders, K., Eisen, M.B., Brown, P.O., Botstein, D., and Futcher, B. (1998). Comprehensive identification of cell cycle-regulated genes of the yeast Saccharomyces cerevisiae by microarray hybridization. Mol Biol Cell *9*, 3273-3297.

St Johnston, D., and Sanson, B. (2011). Epithelial polarity and morphogenesis. Curr Opin Cell Biol *23*, 540-546.

Stewart, M.P., Helenius, J., Toyoda, Y., Ramanathan, S.P., Muller, D.J., and Hyman, A.A. (2011). Hydrostatic pressure and the actomyosin cortex drive mitotic cell rounding. Nature *469*, 226-230.

Sturgill, E.G., and Ohi, R. (2013). Kinesin-12 differentially affects spindle assembly depending on its microtubule substrate. Curr Biol *23*, 1280-1290.

Sullivan, W., and Theurkauf, W.E. (1995). The cytoskeleton and morphogenesis of the early *Drosophila* embryo. Curr Opin Cell Biol *7*, 18-22.

Szafer-Glusman, E., Fuller, M.T., and Giansanti, M.G. (2011). Role of Survivin in cytokinesis revealed by a separation-of-function allele. Molecular biology of the cell *22*, 3779-3790.

Tamai, H., Shinohara, H., Miyata, T., Saito, K., Nishizawa, Y., Nomura, T., and Osumi, N. (2007). Pax6 transcription factor is required for the interkinetic nuclear movement of neuroepithelial cells. Genes Cells *12*, 983-996.

Tanaka, S., Umemori, T., Hirai, K., Muramatsu, S., Kamimura, Y., and Araki, H. (2007). CDK-dependent phosphorylation of Sld2 and Sld3 initiates DNA replication in budding yeast. Nature *445*, 328-332.

Tanaka, T., Knapp, D., and Nasmyth, K. (1997). Loading of an Mcm protein onto DNA replication origins is regulated by Cdc6p and CDKs. Cell *90*, 649-660.

Thery, M., and Bornens, M. (2008). Get round and stiff for mitosis. HFSP journal *2*, 65-71.

Thompson, B.J. (2010). Developmental control of cell growth and division in *Drosophila*. Curr Opin Cell Biol *22*, 788-794.

Toth, A., Ciosk, R., Uhlmann, F., Galova, M., Schleiffer, A., and Nasmyth, K. (1999). Yeast cohesin complex requires a conserved protein, Eco1p(Ctf7), to establish cohesion between sister chromatids during DNA replication. Genes Dev *13*, 320-333.

Tripathi, V., Shen, Z., Chakraborty, A., Giri, S., Freier, S.M., Wu, X., Zhang, Y., Gorospe, M., Prasanth, S.G., Lal, A., *et al.* (2013). Long noncoding RNA MALAT1 controls cell cycle progression by regulating the expression of oncogenic transcription factor B-MYB. PLoS Genet *9*, e1003368.

Tsai, J.W., Bremner, K.H., and Vallee, R.B. (2007). Dual subcellular roles for LIS1 and dynein in radial neuronal migration in live brain tissue. Nat Neurosci *10*, 970-979.

Tsai, J.W., Lian, W.N., Kemal, S., Kriegstein, A.R., and Vallee, R.B. (2010). Kinesin 3 and cytoplasmic dynein mediate interkinetic nuclear migration in neural stem cells. Nat Neurosci *13*, 1463-1471.

Ueno, M., Katayama, K., Yamauchi, H., Nakayama, H., and Doi, K. (2006). Cell cycle progression is required for nuclear migration of neural progenitor cells. Brain Res *1088*, 57-67.

Wang, T.C., Cardiff, R.D., Zukerberg, L., Lees, E., Arnold, A., and Schmidt, E.V. (1994). Mammary hyperplasia and carcinoma in MMTV-cyclin D1 transgenic mice. Nature *369*, 669-671.

Warde-Farley, D., Donaldson, S.L., Comes, O., Zuberi, K., Badrawi, R., Chao, P., Franz, M., Grouios, C., Kazi, F., Lopes, C.T., *et al.* (2010). The GeneMANIA prediction server: biological network integration for gene prioritization and predicting gene function. Nucleic acids research *38*, W214-220.

Wartlick, O., Mumcu, P., Julicher, F., and Gonzalez-Gaitan, M. (2011a). Understanding morphogenetic growth control -- lessons from flies. Nat Rev Mol Cell Biol *12*, 594-604.

Wartlick, O., Mumcu, P., Kicheva, A., Bittig, T., Seum, C., Julicher, F., and Gonzalez-Gaitan, M. (2011b). Dynamics of Dpp signaling and proliferation control. Science *331*, 1154-1159.

Webster, W., and Langman, J. (1978). The effect of cytochalasin B on the neuroepithelial cells of the mouse embryo. The American journal of anatomy *152*, 209-221.

Weinert, T.A., and Hartwell, L.H. (1988). The RAD9 gene controls the cell cycle response to DNA damage in Saccharomyces cerevisiae. Science *241*, 317-322.

Weinert, T.A., Kiser, G.L., and Hartwell, L.H. (1994). Mitotic checkpoint genes in budding yeast and the dependence of mitosis on DNA replication and repair. Genes Dev *8*, 652-665.

Weiszmann, R., Hammonds, A.S., and Celniker, S.E. (2009). Determination of gene expression patterns using high-throughput RNA in situ hybridization to whole-mount *Drosophila* embryos. Nat Protoc *4*, 605-618.

Whitfield, M.L., Sherlock, G., Saldanha, A.J., Murray, J.I., Ball, C.A., Alexander, K.E., Matese, J.C., Perou, C.M., Hurt, M.M., Brown, P.O., *et al.* (2002). Identification of genes periodically expressed in the human cell cycle and their expression in tumors. Molecular biology of the cell *13*, 1977-2000.

Whittle, J.R. (1990). Pattern formation in imaginal discs. Seminars in cell biology *1*, 241-252.

Willer, G.B., Lee, V.M., Gregg, R.G., and Link, B.A. (2005). Analysis of the Zebrafish perplexed mutation reveals tissue-specific roles for de novo pyrimidine synthesis during development. Genetics *170*, 1827-1837.

Winey, M., Yarar, D., Giddings, T.H., Jr., and Mastronarde, D.N. (1997). Nuclear pore complex number and distribution throughout the Saccharomyces cerevisiae cell cycle by three-dimensional reconstruction from electron micrographs of nuclear envelopes. Mol Biol Cell *8*, 2119-2132.

Wohlschlegel, J.A., Dhar, S.K., Prokhorova, T.A., Dutta, A., and Walter, J.C. (2002). Xenopus Mcm10 binds to origins of DNA replication after Mcm2-7 and stimulates origin binding of Cdc45. Mol Cell *9*, 233-240.

Wohlschlegel, J.A., Dwyer, B.T., Dhar, S.K., Cvetic, C., Walter, J.C., and Dutta, A. (2000). Inhibition of eukaryotic DNA replication by geminin binding to Cdt1. Science *290*, 2309-2312.

Woods, D.F., and Bryant, P.J. (1991). The discs-large tumor suppressor gene of *Drosophila* encodes a guanylate kinase homolog localized at septate junctions. Cell *66*, 451-464.

Wuhr, M., Chen, Y., Dumont, S., Groen, A.C., Needleman, D.J., Salic, A., and Mitchison, T.J. (2008). Evidence for an upper limit to mitotic spindle length. Curr Biol *18*, 1256-1261.

Xie, Z., Moy, L.Y., Sanada, K., Zhou, Y., Buchman, J.J., and Tsai, L.H. (2007). Cep120 and TACCs control interkinetic nuclear migration and the neural progenitor pool. Neuron *56*, 79-93.

Xiong, B., and Gerton, J.L. (2010). Regulators of the cohesin network. Annu Rev Biochem *79*, 131-153.

Xu, T., and Rubin, G.M. (1993). Analysis of genetic mosaics in developing and adult *Drosophila* tissues. Development *117*, 1223-1237.

Yabuuchi, H., Yamada, Y., Uchida, T., Sunathvanichkul, T., Nakagawa, T., and Masukata, H. (2006). Ordered assembly of Sld3, GINS and Cdc45 is distinctly regulated by DDK and CDK for activation of replication origins. EMBO J *25*, 4663-4674.

Zegerman, P., and Diffley, J.F. (2007). Phosphorylation of Sld2 and Sld3 by cyclin-dependent kinases promotes DNA replication in budding yeast. Nature *445*, 281-285.

Zhang, X., Luo, D., Pflugfelder, G.O., and Shen, J. (2013). Dpp signaling inhibits proliferation in the *Drosophila* wing by Omb-dependent regional control of bantam. Development *140*, 2917-2922.

Zhou, C., and Jong, A. (1990). CDC6 mRNA fluctuates periodically in the yeast cell cycle. The Journal of biological chemistry *265*, 19904-19909.

Zou, L., and Stillman, B. (1998). Formation of a preinitiation complex by S-phase cyclin CDK-dependent loading of Cdc45p onto chromatin. Science *280*, 593-596.